Deanship of Graduate Studies

AL-Quds University

Combined Photoacoustic and Photopyroelectric Detection

Atef Jibreen Abdel Muneam Al-Jamal

M. Sc. Thesis

Jerusalem-Palestine

1428 / 2007

Combined Photoacoustic and Photopyroelectric Detection

BY

Atef Jibreen Abdel Muneam Al-Jamal

B.Sc. Physics, Jordan University

Supervisor: Dr. Mohammad Abu -Taha
Co-Supervisor: Dr. Hatem Eadeh

"Thesis Submitted to the Faculty of Science, Al-Quds University in Partial Fulfillment of the Requirements for the Degree of Master of Science in Physics"

Abu-Dies, Jerusalem

Palestine

1428 / 2007

Master Physics Program

Deanship of graduate studies

Combined Photoacoustic and Photopyroelectric Detection

Presented By:

Student Name: Atef Jibreen Al-Jamal

Registration No 20320007

Supervisor: Dr Mohammad Abu- Taha
Co-Supervisor: Dr Hatem Eadeh

Master thesis submitted for examination at 12 /5/2007 and accepted by the examining committee members as follows

Committee Member		Signature
1- Dr. Mohammad Abu-Taha	Head of Committee	_____
2- Dr. Mousa Abu Tair	Internal Examiner	_____
3- Dr. Zaki M. Saleh	External Examiner	_____
4- Dr. Hatem Eadeh	Member of the committee	_____

Al-Quds University

1428/2007

DEDICATION

To my mother

To my father

To my wife

To my sons

Declaration:

I certify that this thesis submitted for the degree of Master is the result of my own research, except where otherwise acknowledged, and that this thesis (or any part of the same) has not been submitted for a higher degree to any other university or institution.

Signed:…….

Name: Atef Jibreen Abdel Muneam Al- Jammal

Date:

Acknowledgements:

Great thanks and prayer to my Allah, who granted me the capability to finish this work.

I am grateful to my advisor Dr. Mohammad Abu-Taha for his kindness, assistance and patience during the research and Dr Hatem Eadeh the second advisor for his help in the part related to DNA study. Many thanks also go to Dr. M. Abutair for his experimental assistance in the FTIR part.

My deep thanks to my real lover my mother, father, my wife and sons; Ahmad, Mohammad, Heba, Malak, for their support and encouragement.

Special thanks to my colleagues at work, Mr Mohammad Imran the director of education in Hebron and to the staff colleagues in my section at work.

Abstract:

The well known photopyroelectric (PPE) technique is used mainly for liquid sample studies using polyvinylidene difloried film (PVDF) as a sensor. Conversly, photoacoustic (PA) effect is a sensitive detection scheme for trace gases as low as ppb employing a sensitive microphone for detection. The later is also used for studying liquid as well as solid samples. The present work concerned with the study of DNA samples using the photopyroelectric technique to distinguish different DNA samples for it's biological value, which is a simple, inexpensive and easy to perform. The Fourier transform infrared spectroscopy (FTIRS) was used to authenticate DNA samples results obtained by the PPE method in the Mid Infrared region (4000-400 cm^{-1}), where the experiment proved the ability of PPE method to distinguish different DNA sample assuming band absorption of IR radiation in the region ~ 2-10μm. The second part of this work is concerned with the use of photoacoustic and photopyroelectric detection simultaneously in a combined photopyroelectric-photoacoustic chamber, abbreviated (CPPC), to use Methanol and Ethanol as testing examples for both PA and PPE technique to authenticate the use of PVDF as a sensor for trace gas detection, in which the PVDF method have proved very successful in studying trace gas detection in the combined cell. Finally the CPPC design were used to study three different essential oils and their part of the plant used to produce them, i.e. flowers or leaves of jasmine, rose and mint; using different percentage of purity for each oil for comparison. The PA and PPE signals detected have the same origin, although there is some differences that affect the value of the signals detected by both techniques, specially the dependence of the PA signal on cavity volume pressure and temperature.

The results obtained have shown that the PPE and the CPPC methods are suitable, sensitive and low-cost techniques than usual methods used for DNA typing and laser beam systems.

ملخص:

إن الطريقة المعروفة والمسماة الفوتوبايروالكتريك (التأثير الكهربائي الناتج عن الحرارة) PPE تستخدم كوسيلة قياس في دراسة المواد في الحالة السائلة، بينما طريقة الفوتواكوستك (الصوت الناتج عن الضوء) PA تستخدم كطريفة حساسة جدا في حالة الغازات حتى لو كان جزء بالمليون وذلك باستخدام

الميكروفون الحساس كوسيلة قياس. ويمكن استخدام هذه الظاهرة أيضا في الحالة التي تكون فيها المدة صلبة أو سائلة.

إن العمل الذي سوف نقوم به يعنى بدراسة مادة أل DNA باستخدام طريقة التأثير الكهربائي الناتج عن الحرارة الممتصة من قبل مادة أل DNA و قدرة هذه الطريقة للتفريق بين عينات مختلفة منها وذلك لأهمية هذه المادة بيولوجيا والتي يمكن اعتبارها طريقة سهلة وقليلة الثمن بالمقارنة مع الطرق التي تستخدم. ولقد تم بالإضافة إلى ذلك استخدام جهاز FTIR وهو جهاز متقدم وحديث من اجل التأكيد على النتائج التي تم الحصول عليها بالطريقة السابقة الذكر.

أما الجزء الثاني من هذا العمل فقد تم باستخدام طريقتي التأثير الصوتي والتأثير الكهربائي لامتصاص الضوء معا في خلية واحدة اختصرت بالرمز CPPC من اجل استخدام مادتي الميثانول والايثانول كأمثلة لمقارنة الإشارة الصوتية والإشارة الكهربائية الناتجة من اجل التأكيد على أن التأثير الكهربائي لامتصاص الضوء يمكن قياسه باستخدام فلم حساس يدعى "بولي فيني ليدي ن" دفلورايد فلم PVDF. وبعد هذا التأكيد تم استخدام الجهاز الجديد CPPC لدراسة بعض الزيوت المتطايرة وكذلك أجزاء من النباتات التي تستخدم لاستخراجها وهي الياسمين والورد ألجوري والنعنا ع وقد تم استخدام تراكيز مختلفة من زيوت هذه النباتات من اجل المقارنة أيضا.

إن النتائج التي تم الحصول عليها تؤكد أن الطريقتين PPE و CPPC هي طرق حساسة وقليلة التكلفة ومناسبة لاستخدامها في القياسات.

Table of Contents:

List of Tables:

List of Figures:

List of abbreviations:

Symbol	**Abbreviation representation**
PPE	Phptopyroelectric
PAS	Photoacoustic spectroscopy
PA	Photoacoustic
IR	Infrared radiation
BPPE	Back photopyroelectric
FPPE	Forward photopyroelectric
DNA	Dexo nuclear acid
PVDF	Polyvinylyene difluoride film
PVD	Polyvinylyene difluoride
UV/V	ultaviolet/visible

A	Adenine
G	Guanine
C	Cytosine
T	Thymine
RFLP	Retraction fragment length polymorphisms
VNTRs	Variable number tandem repeats
PCR	Polymaries chain reaction
FTIRS	Fourier transform infrared spectroscopy
CPPC	Combined photoacoustic- photopyroelectric chamber
ppb	Part per billion
ppm	Part per million

Chapter one

Historical background

1.1 Introduction

This thesis is concerned with photoacoustic and photopyroelectric detection for liquids and gases. The introduction chapter, will briefly introduce all topics related to detection schemes and used samples. Photoacoustic effect is defined as the production of sound wave when illuminating an absorpant gas with modulated light beam (Bult, Horwitz, Malkins, Cahen,, 1981, 1982). It was discovered by Bell in the year 1880, and then investigated by Tynall and Rontgen later in 1881 (Viengerov, 1938). With the introduction of lasers the photoacoustic methods have been the subject of a number of studies using laser techniques (Malkin and Cahen 1979; Cahen et al. 1980; Malkin et al. 1981; Buschmann et al.1984; Braslavsky 1986; Tam 1986; Peters and Snyder 1988; Buschmann 1989; Buschmann and Prehn 1990; Braslavsky and Heibel 1992; Fork and Herbert 1993; Malkin and Canaani 1994; McClean et al. 1998).

This study also deals with the photopyroelectric detection, which is referred back to 300 years ago, but only in the last 20 years theoretical and experimental studies have been established. The phenomenon is manifestations of spontaneous polarization following temperature increase of certain isotropic solids. The pyroelectric material become electrically polarized when there is a temperature difference between the two surfaces of the material and hence a voltage difference arises across. In 1981, Zemel *et al* reported the first pyroelectric chemical sensor (Pd-$LiTaO_3$). Many efforts followed to attain a simple, sensitive, fast, and purely

photopyroelectric chemical detector based on polyvinylidene fluoride film (PVDF) (Constantinos, Andreas, 1990).

Photoacoustic spectroscopy (PAS) is a useful technique for direct measurements of nonradiative states in semiconductors (Hiroshi, Nobuo, Fumiya, 2001). The photothemal and photoacoustic spectroscopic methods have the sensitivity which enable it to be used in many applications. For example, the photoacoustic method offers unique capabilities for photosynthesis studies including the storage of energy by electron transport, oxygen evolution by leaf tissue at microsecond time resolution, and the conformational changes of photosystems caused by charge separation (Stephen, Tao, Thomas, 2000). Photoacoustics monitor of phytoplankton populations and the use of photoacoustics to study protein dynamics are also possible. Measurements of optical absorption coefficient help to obtain structural information of biological tissues (Stephen, Tao, Thomas, 2000). The characterization of biological tissues can be done by using optical properties, such as absorption and scattering (Cheong, Prahl, Welch, Trrans, 1990; Tuchin 2000). The detected photoacoustic signals can be used to reconstruct the optical energy deposition, which is related to the absorption coefficient distribution of the tissue (Chao, Pai, 2006). The need for high-quality images for internal human body has motivated research on photoacoustic imaging. A new imaging technique, which combines the high contrast of optical methods with the spatial resolution of ultrasound imaging distinguishes different absorbers such as oxygenated or deoxygenated hemoglobin, water or melanin, according to their spectrum (Joel, Michael, Robert, Peter, Martin, 2005). The spectroscopic detection and monitoring of pollutant gases in view of increased awareness of environmental problems, utilizes the photoacoustic method in conjunction with a high resolution laser technique (Andras, Miklos, 1996). The photoacoustic response of the material, compared to the luminescence spectrum, can be used to determine the macroscopic coefficient which describes the two photon up-conversion (Eugenio, Roberto, Jorge, Fernando,

2001). The several applications of photoacoustic spectroscopy include the conversion of light energy into heat energy and then into sound energy that is detectable by a microphone.

Direct measurements of heat energy transfer from a modulated radiation using pyroelectric polyvinylidene fluoride film (PVDF) were used by Coufal in 1984. The technique was used for thermal characterization of oil, and many other fields of industry (Frandas, Bicanic, 1999). This technique will be used to study DNA, an important material that contains the basic elements of genetic information transfer. It is believed that since the discovery of DNA structure in 1953 by James Watson and Francis Crick, knowledge of the composition and organization of the genetic material has accumulated at an astonishing pace. By the early 1980s, it had become clear that most genomes DNA show very little variation from one species to another. The small percentage that does vary presents enormous potential for fruitful study (Watson, Crick, 1953). A lot of development and understanding of DNA as an important carrier for genetic information from generation to another have been performed. DNA sequencing which is the determination of nucleotide order for a given DNA fragment, considered the gold standard typing technique, but the technique is highly demanding which makes it less feasible at this time (Jeffreys, Wilson, Thein, 1985).

Further advances in sequencing technology give the ability to compare genomes with each other quickly and cheaply. While this comparison between different long stretches of DNA - one million bases or more - should yield an enormous amount of information about the role of inheritance in disease susceptibility, response to environmental influences and even evolution ("http://en.wikipedia.org/ wiki/DNA_sequencing, October, 2006, October 2006").

For the above reason it is suggested to study DNA in a simple technique using the pyroelectric effect to differentiate between different organisms based on the difference of their DNA sequences.

A combination of the optoacoustic and photopyroelectric techniques will be used to study essential oils which is an odorous substances used for their therapeutic properties for thousands of years depending on the type and properties of the essential oil. The majority of essential oils are composed of volatile compounds and the oil produced in one part of a plant is different from that produced in another. They have a biological activity including antimicrobial, antioxidant, antibacterial and antifungal properties. Several constituents of these oils have been studied using different analytical techniques (Carson, Riley, 1995). In this study, mint, jasmine, and rose oils are investigated along with the corresponding part of plant from which the oil is extracted.

Mint oil extracted from the mint plant which is a one meter high with perennial herb and has slightly hairy serrated leaves with pinkish-mauve flowers arranged in a long conical shape, propagated by underground roots and cultivated all over the world. The oldest evidence of use was found in Egypt in a tomb dating back to 1000 BC (Corliss, 1992). The industry of volatile oil dated back to 5000 years ago by the Egyptians. It was described to the scientific world in 1696 by John Ray (Siegel, Maier, 1998). The first cosmetic chemists were done by the ancient Greeks, with the creation of both soap and lotion (Hay, Waterman, 1993).

Damask rose oil extracted from rose flower that reaches up to seven feet high with rich pink and white flowers (Rhea, 2005), grown in rootstocks and cuttings, and picked as early as

possible when it reaches full bloom (Mana, 2001). The Egyptian artifacts date to 1500 B.C, and the first documantations dated to 5000 B.C by the Sumerians. The plant were planted in Western Asia since the Bronze Age, and then spread out all over the word (Gernot, 2003).

Jasmine oil extracted from the jasmine flower which is an evergreen, fragile, climbing shrub, reaches a height of 10 meters, and has dark green leaves and small, white, star-shaped flowers. The aroma is most intense at night, with finer quality for higher altitude flowers (Simon, Chadwick, Craker, 1984). It is an old plant used by the Chinese, Arabs and Indians for medical purposes, as well as for an aphrodisiac and for other ceremonial purposes (Julia, 1995).

In this study the traces of the three evaporated essential oils are used as examples to authenticate the use of the photopyroelectric detection in combination with photoacoustic method.

Methanol and Ethanol are used to dilute these oils prior to investigation. Methanol (Methyl alcohol) CH_3OH was first used by Egyptians in their embalming process, but the first pure methanol, was isolated in 1661 by Robert Boyle. The German chemist Matthias Pier in 1923 prepared methanol by chemical reactions of carbon oxide and hydrogen ("http://en.wikipedia. org/wiki/Methanol, October, 2006").

Ethanol (Ethyl alcohol) C_2H_6O was used in alcoholic beverages since prehistory. It was used by Neolithic peoples in northen China 9000-year-ago. Pure ethanol was obtained 1796, and its structural formula was published in 1858. The first preperation of ethanol from ethelene by

the acid-catalysed hydration of ethylene was done in 1928 ("http://en.wikipedia.org/wiki/Ethanol, October, 2006").

1.2 Statement of the problem

The importance of PA and PPE methods in spectroscopic detection of trace gases or vapors has been shown. PVDF is specially used in liquid detection, while the PA method is used for detection in all phases of matter (Chirtoc, Mihailescu, 1989). Normally both methods are used in conjunction with laser as a source of radiation. The present work has new specific goals:

1- Use the PVDF as a sensor to study DNA, as a distinguishing technique for organisms based on their different DNA sequences.

2-Develop a new detection scheme in which both PA and PPE are combined in one cell measured simultaneously.

3-In both of the above cases a broadband-pulsed IR source is used as a light source instead of laser beam, allowing portable detection system to be constructed.

4- Use FTIR spectroscopy to authenticate this technique

Studies are aimed at enhancing the use of both PA and PVDF methods, and provide deeper understanding of the PA and PPE signals. Fourier transformed infrared spectroscopy was also used to confirm our results.

1.3 Brief review of chapters:

Chapter two of this thesis deals with the theoretical aspects of PPE and PA effects, and a brief discussion of infrared spectroscopy. The techniques involve the use of pyroelectric polyvinylidene difluoride (PVD) thin film detector and a sensitive microphone, which will be discussed further in chapter two. In chapter three a description of the apparatus used in this study including the experimental setup, experimental procedure and problems under investigation are given. The experimental results will be presented in chapter four, and are discussed in chapter five. Finally, conclusions, and suggested further work are given in chapter six, which is followed by a list of references.

Chapter two

Theoretical background

2.1 Introduction.

In this chapter, the theoretical background of the main topics necessary for the subjects discussed in this thesis is presented. The PVD film as the basic sensor in the experiment will be briefly reviewed. This is followed by an introduction to the branch of spectroscopy employing the PVD film as a thermal sensor for material characterization. An introduction to the photoacoustic spectroscopy and gas trace detection using a microphone is introduced in view of the use of Helmholtz cell and its frequency resonance. The relevant information of the samples used in this study are discussed.

2.2 Spectroscopic Methods.

Many types of spectroscopic methods are used and each method depends on a physical quantity measured usually an amount or intensity of some parameter (Agarwal, 1995). Examples include, measuring the intensity of emitted electromagnetic radiation (Aklonis, 1981) and the electron energy loss in Auger electron spectroscopy. There are different measurement processes depending on the type of spectroscopic method used. In absorption spectroscopy, the range of electromagnetic spectra depends on the absorbing substance (Benz, William, Euler, 2002). For example in atomic absorption spectroscopy, the light of a particular frequency passes through the vapor of atomized sample, can be used to measure concentrations of ions such as sodium and calcium in blood, in the ultraviolet/visible (UV/V) range, the absorption spectroscopy is most often performed on liquid samples to detect molecular content and the infrared spectroscopy is performed on liquid, semi-liquid (paste or grease), dried, or solid samples to determine molecular and structural information (Bianchi, Catalano, 1996). Emission spectroscopy depends on the range of electromagnetic spectra for which the substance radiates. In this process the substance absorb energy and become in an excited state, then it radiates energy as light by different means such as collision either due to high temperatures or due to chemical reactions (Bower, Maddams, 1992). Scattering spectroscopy depends on some physical properties of the substance by measuring the amount of light that is scattered at certain wavelengths, incident angles, and polarization angles (Bower, Maddams, 1992).

In fluorescence spectroscopy, high energetic photons excite the sample, which in turn emits photons with lower energy (Boyer, 1974). In X-ray spectroscopy, if the energy of X-rays is sufficient to excite the inner shell electrons to outer empty orbitals, or remove them

completely, an empty level in the inner shell "hole" is formed but will be filled by a transition from an outer orbital electron. In this de-excitation process, energy will be emitted as radiation (fluorescence) or other less-bound electron from the atom is removed (Auger effect). The absorption or emission frequencies are characteristic of the specific atom (Bret, Ludwig, Marek, Urban, 1996). A variation in frequency occurs for some specific atom according to the characteristic of the chemical bonding. These characteristic X-ray frequencies or Auger electron energies can be measured and used in chemistry and material sciences to determine elemental composition and chemical bonding (Bret, Ludwig, Marek, Urban, 1996). In X-rays crystallography, a crystalline material scatters X-ray photons at well-defined angles. It can be used to calculate the distances between planes of atoms within the crystal (Burns, Ciurczak, 1992).

2.3 Photoacoustic spectroscopy (PAS)

Photoacoustic spectroscopy is based on the photoacoustic effect, discovered by Alexander Graham Bell in 1880 when sunlight passing through a sample was rapidly interrupted with a rotating slotted disk. The idea was that the absorbed energy from the sunlight is transformed into kinetic energy of the sample by energy exchange processes creating a local heating and thus a pressure wave or sound (Chirtoc, Bicanic, Dadarlat, 1985). After that, materials exposed to the non-visible portions of the solar spectrum can also produce sound waves. Using different wavelengths, one can use the photoacoustic spectrum of the sample to identify the absorbing components in it. The photoacoustic effect can be used to study solids, liquids, and gases (Chirtoc, Mihailescu, 1989).

Photoacoustic spectroscopy is a powerful technique to study concentration of gases at the part per billion (ppb) or even part per trillion levels. This is enhanced by using the intense lasers beams because the intensity of the generated sound is proportional to the light intensity (Colthup, 1990). Sensitive microphones and lock-in amplifiers (Frandas, Paris, Bissieux, Chirtoc, Antoniow, Egee, 2000), can greatly contribute to signal-to-noise improvement. Enclosing the gaseous sample in a cylindrical chamber, and modulating the frequency of the absorbed radiation to an acoustic resonance will amplify the sound signal (Frandas, Paris, Bissieux, Chirtoc, Antoniow, Egee, 2000). Patel and co-workers did an example that illustrates the potential of the photoacoustic technique in 1970 when they measured the temporal variation of the concentration of nitric oxide in the stratosphere at an altitude of 28 km using a balloon-borne photoacoustic detector (Fried, 1995). A very low cost instrument for the control of carbon dioxide concentration have been developed and commercialized in the last twenty years (Fried, 1995). Using low-cost thermal sources, which are modulated electronically, and low cost microphones and proprietary signal processing with digital signal processors decrease the costs of these systems (Harrick, 1995).

When investigating solid and semisolid materials, the sample is placed in a closed chamber filled with a gas such as air and illuminated with monochromatic radiation of any desired wavelength, with intensity modulated at some suitable acoustic frequency; absorption of radiation results in a periodic heat flow from the sample, which generates sound that is detected by a sensitive microphone attached to the chamber (Hollas, 1996).

The absorption of optical radiation when transmitted through the sample whether it is gas, liquid, or solid, can be measured by several techniques. The straightforward detection technique requires a measurement of the optical radiation level with and without the sample in

the optical path, with transmitted power P_{out}, and the incident power P_{in}, are related through the equation $P_{out} = P_{in}\, e^{\alpha \mu}$, where α is the absorption coefficient and μ is the length of the absorber (Hollas, 1996).

In photoacoustic detection, no direct detection of optical radiation is carried out. In stead, a measurement is made of the power absorbed by the medium from the incident radiation so it is a calorimetric method. Since the photoacoustic signal is proportional to the incident power and the absorption-length product $\alpha\ \mu$, therefore, for given sources of noise from the detection transducers, the signal-to-noise ratio improves, as the incident energy is increased (Ivanov, Migunova, Mikhailov, 1988).

The modulated-amplitude of the optical radiation at an audio frequency will be absorbed by a gaseous medium confined in a cell with appropriate optical windows for the entrance and exit of the radiation. Nonradiative relaxation of the medium will cause a periodic variation in the temperature of the column of the irradiated gas, and this will cause a corresponding periodic variation in the gas pressure at the audio frequency, and the fluctuations in the pressure. Sound is efficiently detected using a sensitive gas-phase microphone (Ivanov, Migunova, Mikhailov, 1988).

Since the measurement of extremely small absorption coefficients and hence small concentrations of the absorption gases is possible, many applications can be done, including high-resolution spectroscopy of isotopically substituted gases, excited states of molecules and forbidden transitions, and pollution detection. The photoacoustic spectroscopy technique in conjunction with tunable lasers can be routinely used for detection of undesirable gaseous constituents at sub-parts-per-billion levels (Ivanov, Migunova, Mikhailov, 1988).

For weak absorption in liquids and solids, a very sensitive calorimetric spectroscopic technique has been developed, where a pulsed tunable laser for excitation and a submerged piezoelectric transducer for liquids, or a contacted piezoelectric* transducer for solids have been used for the detection of the ultrasonic signal generated by the absorption of the radiation and its subsequent conversion into a transient ultrasonic signal. Monitoring water pollution, impurity detection in thin semiconductor wafers, transmission studies of ultra pure glasses used in optical fibers have used this technique.

2.3.1: Photoacoustic theory

PAS is a process that transforms the light energy into sound waves when a modulated light is absorbed by the sample located in a sealed cell, the non-radiative decay of this absorbed light produces a modulated transfer of heat to the surface of the sample. This will produce pressure waves in the gas inside the cell that can be detected by the attached microphone (Laine, Al-Jourani, Carpenter, Sedgbeer, 1997). The microphone signal obtained as a function of wavelength, will give a spectrum proportional to the absorption spectrum of the sample. PAS gives information about the depth in sample absorption, so the amount of the sample contributing to the PA signal is proportional to the thermal diffusion depth μ, which is

---

*Piezoelectric effect is the generation of an electrical field when putting a piezoelectric material under mechanical stress, in which a shift of the positive and negative charge centers of the elementary units in the material takes place, the effect is proportional to the deformation and is reversible, hence the effect describes the relation between mechanical stress and electrical voltage (http://en.wikipedia.org/wiki/ Piezoelectricity, May 2007).

inversely proportional to the modulation frequency f. For example, when a typical organic polymer is exposed to light with high modulation frequency, the depth is small (f = 1 KHz; m ~ 4 mm,), but when the modulation frequency is lower, a much thicker layer is probed (f = 100 Hz; m ~ 16 mm) (Laine, Al-Jourani, Carpenter, Sedgbeer, 1997).

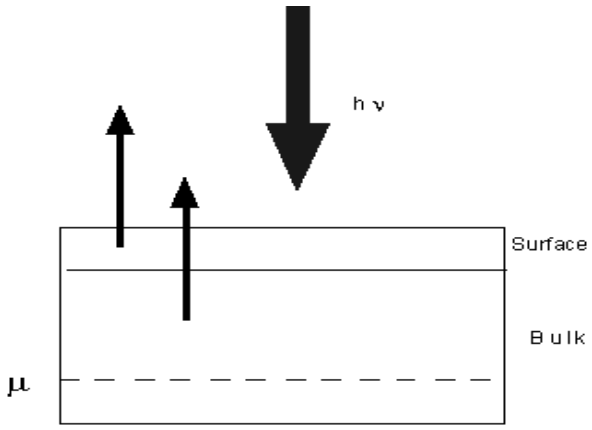

Fig 2.1 Photoacoustic Signal Generation

After: (Laine, Al-Jourani, Carpenter, Sedgbeer, 1997).

Figure 2.1 describes the PA signal generation and its relation to depth. The model shows a thermally thin surface layer on a bulk substrate. After that, the heat diffused from the point of absorption to the surface of the sample to be detected. A phase lag between the time of absorption and the thermal signal occurs because thermal diffusion is a slow process relative to light absorption and non- radiative decay. Therefore, the surface absorption have no phase lag because the heat does not have to travel far to generate a pressure change in the transfer gas that can be detected (Laine, Al-Jourani, Carpenter, Sedgbeer, 1997).

2.3.2: Absorption of light:

The first step in the generation of acoustic signal is the absorption of energy from a modulated light beam. Because the absorbed heat proportional to the intensity of the light beam, the relation between them is given by:

$$H = \alpha I \qquad 2.1$$

Where $I\left(\vec{r},t\right)$: the intensity of the light beam measured in $erg.cm^{-2}.\sec^{-1}$

$\vec{r}$: is the position in (cm)

t: is the time in (sec)

$\alpha\left(in\ cm^{-1}\right)$ is the absorbance. Not that $H\left(\vec{r},t\right)$: (the absorbed heat) has the dimensions of $erg.cm^{-3}.\sec^{-1}$.

So far, two conditions are necessary to make the relation linear, firstly the intensity is sufficiently small so as there is no saturation in the absorbing transition, secondly time variation of I is much slower than the rate of transfer of the absorbed energy. Then

$$\alpha = N\frac{S\tau}{\pi\Delta\upsilon\tau_c} \qquad 2.2$$

Where

$$\tau^{-1} = \tau_R^{-1} + \tau_C^{-1} \qquad 2.3$$

N: density of absorbing molecules

$\Delta\upsilon$: Line width of transition

S: line strength of transition

τ_R: Radiative lifetime

τ_c: Collisional decay time of the upper state

Which represent the conversion of light energy into heat energy (Kreuzer, 1971)

2.3.3: Excitation of sound

The second step is the excitation of sound i.e. the generation of photoacoustic signal. The generation of sound is caused by the change of pressure i.e. the difference between the total pressure P and the average value P_0, therefore the pressure p that causes the sound is given by:

$$p = P - P_0 \qquad 2.4$$

The absorbed heat $H\left(\vec{r},t\right)$ that leads to the generation of the acoustic signal, as reported by Morse and Ingard 1961 is given by the partial differential equation:

$$\nabla^2 p - \frac{1}{c_0^2}\frac{\partial^2 p}{\partial t^2} = -\left[\frac{\gamma - 1}{c_0^2}\right]\frac{\partial H}{\partial t} \qquad 2.5$$

Where

c_0 : Velocity of sound

$\gamma = \frac{C_p}{C_v}$: Ratio of specific heat of the gas

C_p : Specific heat at constant pressure

C_v : Specific heat at constant volume

In this equation, we have neglected the effect of acoustic loss from heat conduction and viscosity, which will be considered later as perturbation of loss-free solution. To solve equation 2.5 we use the Fourier transform method for both sides expressing the solution of p as an infinite series expansion of normal modes, p_j Rosencwaig (1980):

$$\left(\nabla^2 + \frac{\omega^2}{c_0^2}\right) p\left(\vec{r},\omega\right) = \left[\frac{\gamma - 1}{c_0^2}\right] i\omega H\left(\vec{r},\omega\right) \qquad 2.6$$

Where

$$p\left(\vec{r},t\right) = \int p\left(\vec{r},\omega\right) e^{-i\omega t}\, d\omega \qquad 2.7$$

$$H\left(\vec{r},t\right)=\int H\left(\vec{r},\omega\right)e^{-i\omega t}\,d\omega \qquad 2.8$$

Appling the boundary conditions to determine the normal mode solution for the homogeneous wave equation. Since the walls of the container are rigid then the normal component of the acoustic velocity is vanished. Because the acoustic velocity $\vec{u}\left(\vec{r},t\right)$ is a fluid velocity of the gas, it is related to the gradient of p as:

$$\vec{u}\left(\vec{r},\omega\right)=\left(i\omega\,p_0\right)^{-1}\vec{\nabla}.p\left(\vec{r},\omega\right) \qquad 2.9$$

The normal mode solution p_j of the homogeneous wave equation since the gradient of p normal modes at the boundary vanishs then the homogeneous wave equation is given by:

$$\left(\nabla^2+K_j^2\right)p_j(r)=0 \qquad 2.10$$

Where

$$K=\frac{\omega}{c_0} \qquad 2.11$$

Since the modes are orthogonal they may be normalized with the normalization condition given by:

$$\int p_i^{*}\,p_j\,dV=V_c\,\delta_{ij} \qquad 2.12$$

where the volume integral is over the volume V_c of the gas container.

For a cylindrical cell of length (l*)* and radius (a) equation 2.10 in cylindrical coordinates becomes:

$$r^{-1}\frac{\partial}{\partial r}\left(r\frac{\partial p_j}{\partial r}\right)+r^{-2}\frac{\partial^2 p_j}{\partial\Phi^2}+\frac{\partial^2 p_j}{\partial z^2}+\frac{\omega}{c_0^2}p_j=0 \qquad 2.13$$

The solution as given by Morse (1961):

$$p_j=\begin{matrix}\cos\\ \sin\end{matrix}\left(m\Phi\right)\left\{AJ_m\left(k_r\,r\right)+BN_m\left(k_r\,r\right)\right\}\left\{C\sin\left(k_z\,z\right)+D\cos\left(k_z\,z\right)\right\} \qquad 2.14$$

Where:

J_m: Bessel function of the first kind

N_m: Bessel function of the second kind

As r approaches zero, N_m becomes infinite and hence B = 0, considering one end at z = 0 then the other end is at z= *l* therefore the gradient of p normal to the wall must vanish which means that C = 0 and the allowed value of k_z given by:

$$k_z = \left(\frac{\pi}{l}\right) n_z \qquad n_z = 1, 2, 3 \ldots. \qquad 2.15$$

Applying the boundary conditions at r = a therefore:

$$\frac{d\, J_m k_r r}{d\, r}\Big|_{r=a} = 0 \qquad 2.16$$

Which is equivalent to:

$$\frac{d\, J_m(\pi\alpha)}{d\alpha}\Big|_{\alpha=\alpha_{mn}} \qquad 2.17$$

$$k_r = \frac{\pi\alpha_{mn}}{a} \qquad 2.18$$

Where α_{mn} represent the nth root of the equation involving mth order of Bessel function has been tabulated (Morse, 1948), and equation 2.14 becomes:

$$p_j = \begin{matrix}\cos \\ \sin\end{matrix}(m\Phi)\left[A J_m(k_r r)\right]\left[D\cos(k_z z)\right] \qquad 2.19$$

Taking the integral values of m, then p is continuous and the resonant frequency can be obtained when substituting equation 2.19 into equation 2.13 and the resonant frequency is given by:

$$\omega_j = c_0 \sqrt{k_z^2 + k_r^2} \qquad 2.20$$

which means that the modes are pure longitudinal and pure radial. The acoustic pressure p is the sum over all normal modes with the mode amplitude A_j and is given by the following relation:

$$p\left(\vec{r},\omega\right)=\sum_j A_j\left(\omega\right)p_j\left(\vec{r}\right) \qquad 2.21$$

Substituting this equation in equation 2.5 and using 2.10 and 2.13 and considering the orthogonality of p_j then the mode amplitude is given by:

$$A_j\left(\omega\right)=-\frac{\left(\gamma-1\right)/V_c}{\left(1-\omega^2/\omega_j^2\right)}\frac{i\omega}{\omega_j^2}\int p_j^* H dV \qquad 2.22$$

In this equation the integral represent the coupling between the heat source H and the normal mode p_j, the dominator is the mod resonance and A_j become infinite when ω approaches natural resonant frequency. Including the loss effect from viscosity and conduction by including the quality factor Q_j then equation 2.22 becomes:

$$A_j=\frac{-i\omega}{\omega_j^2}\left[\frac{\left(\left(\gamma-1\right)/V_c\right)\int p_j^* H dV}{1-\left(\frac{\omega}{\omega_j}\right)^2-i\left(\frac{\omega}{\omega_j Q_j}\right)}\right] \qquad 2.23$$

Where

$$Q_j=\omega_j\frac{energy\ stored\ in\ \mathrm{mode}\ j}{rate\ of\ loss\ of\ energy\ from\ \mathrm{mode}\ j}$$

$$Q_j=\omega_j\frac{E_j}{L_s+L_v} \qquad 2.24$$

L_s: Surface loss of energy L_v volume loss of energy

Using equation 2.1 and 2.23 to find the relation between acoustic signal and intensity so:

$$A_j = -\frac{i\omega}{\omega_j^2}\frac{\alpha\left[(\gamma-1)/V_c\right]\int p_j^* I dV}{\left[1-\left(\frac{\omega}{\omega_j}\right)^2-\left(\frac{i\omega}{\omega_j Q_j}\right)\right]} \qquad 2.25$$

Considering two special cases first assume that I is constant throughout the volume of the container that is:

$$I\left(\vec{r},\omega\right)=I(\omega) \qquad 2.26$$

Then

$$\int p_j^* I\, dV = 0 \qquad \text{for j} \neq 0 \qquad 2.27$$

and the lowest order mode p_0 has resonance frequency ω_0 and present a constant pressure in the container which is independent on the position and this means that I and p_0 are proportional to each other therefore:

$$A_0(\omega)=\frac{i\alpha(\gamma-1)I}{\omega(1+(i/\omega\tau_0))} \qquad 2.28$$

τ_0 : damping time result from heat conduction to the walls

Considering a cylindrical container with cross sectional area A_c and length l and volume V_c then the total light beam power:

$$W = \frac{IV_c}{l} \qquad 2.29$$

And equation 2.28 becomes:

$$A_0 = \frac{i\alpha(\gamma-1)Wl}{\omega(1+i/\omega\tau_0)V_c} \qquad 2.30$$

A second special case where only the first order mode is excited then equation 2.25 become:

$$A_1(\omega) = -\frac{i\omega}{\omega_1^2}\frac{\alpha(\gamma-1)Wl}{\left[1-\left(\frac{\omega}{\omega_1}\right)^2-i\left(\frac{\omega}{\omega_1 Q_1}\right)\right]V_c} \qquad 2.31$$

and because it is not possible to adjust I so that only the first order mode is excited then we considered equation 2.31 as the upper limit on mode amplitude and the ratio between zero resonance and first order resonance we have:

$$\frac{A_1(\omega_1)}{A_0(0)} = Q_1/\omega_1\tau_0 \qquad 2.32$$

and this equation shows that when the ratio is great then the first order mode can be made larger than the zero mode and the value of the ratio is depending on mode damping (Yoh, Han, 1977).

2.4 Helmholtz resonator

The resonance means that the frequency of the driving system is the same as the natural frequency of the system, i.e. it is a special case of forced vibration.

A Helmholtz resonator or Helmholtz oscillator is a container of gas (usually air) with an open port. A volume of air in and near the open hole vibrates because of the 'springiness' of the air inside. A common example is an empty bottle, the air inside vibrates when you blow across the top, as shown in Fig. 2.2 (McLennan, 2003). Consider a column of air at the neck of the bottle. The air jet can force this column of air a little way down the neck, thereby compressing the air inside. That pressure drives the column of air out but, when it gets to its original position, its momentum takes it on outside the body a small distance. This rarifies the air inside the body, which then sucks the column of air back in. It can thus vibrate like a mass on a spring. The jet of air from your lips is capable of deflecting alternately into the bottle and outside, and that provides the power to keep the oscillations going (Winstanley, Inst, 1955).

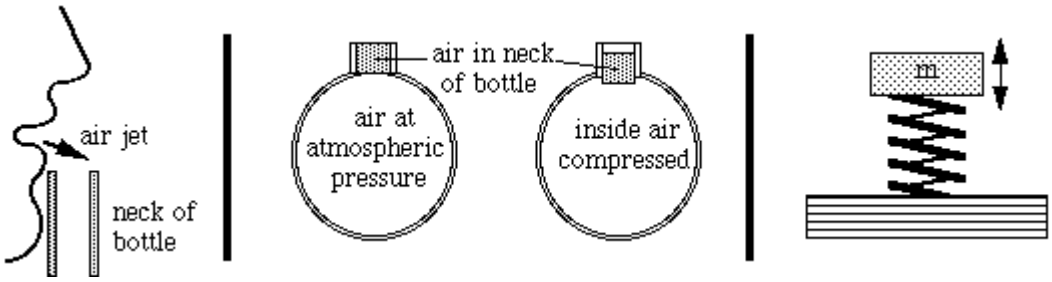

Fig. 2.2 A scheme for the air vibration inside the bottle
(After: www.phys.unsw.edu.au/~jw/guitarintro.html, October 2006)

Derivation of the Helmholtz resonance frequency:

Because the sound produced has a wavelength of a few meters, so it is fair to assume that the wavelength of sound produced is much longer than the dimensions of the resonator for a typical bottle (McLennan, 2003), but it is worth checking whenever you start to describe something as a Helmholtz oscillator. The consequence of this approximation is the ability to neglect pressure variations inside the volume of the container i.e. the pressure oscillation will have the same phase everywhere inside the container. Let the air in the neck have an effective length L and cross sectional area S. Its mass is then SL times the density of air □ . If this 'plug' of air descends a small distance x into the bottle, it compresses the air in the container so that the air that previously occupied volume V now has volume V-Sx. Consequently, the pressure of that air rises from atmospheric pressure P_A to a higher value P_A +p see Fig 2.3.

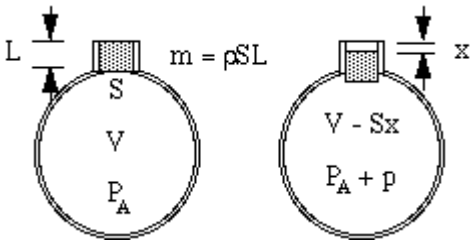

Fig 2.3 Variation of pressure in the container
(After:www.phys.unsw.edu.au/~jw/guitarintro.html, October 2006)

Now you might think that the pressure increase would just be proportional to the volume decrease. That would be the case if the compression happened so slowly that the temperature did not change. In vibrations that give rise to sound, however, the changes are fast and so the temperature rises on compression, giving a larger change in pressure. Technically, they are adiabatic, meaning that heat has no time to move, and the resulting equation involves a constant γ, the ratio of specific heats. As a result, the pressure change p produced by a small volume change ΔV is just:

$$\frac{p}{P_A} = -\gamma \frac{\Delta V}{V} = -\gamma \frac{Sx}{V} \qquad 2.33$$

Where

$\gamma = \frac{(dp/dV)}{(P_A/V)}$ is the heat capacity ratio

Now the mass m is moved by the difference in pressure between the top and bottom of the neck, i.e. a net force pS, so we write Newton's law for the acceleration as:

$$F = ma$$
$$or \qquad 2.34$$
$$\frac{d^2x}{dt^2} = \frac{F}{m}$$

Substituting for F, m, and the value of p from 2.33 gives:

$$\frac{d^2x}{dt^2} = \frac{pS}{\rho SL} = \frac{-\gamma SP_A}{\rho VL}\, x \qquad 2.35$$

So the restoring force is proportional to the displacement. This is the condition for Simple Harmonic Motion, and it has a frequency, which is $1/2\pi$ times the square root of the constant of proportionality, so:

$$f = \frac{1}{2\pi}\sqrt{\frac{\gamma SP_A}{\rho VL}} \qquad 2.36$$

Now the density, the pressure and ratio of specific heats determine the speed c of sound in air, so the frequency can be written:

$$f = \frac{c}{2\pi}\sqrt{\frac{S}{VL}} \qquad 2.37$$

$$c = \sqrt{\frac{\gamma P_A}{\rho}} \text{ (The speed of sound)} \qquad 2.38$$

and if we include the damping factor then the frequency is given by:

$$f = \frac{c}{2\pi}\sqrt{\frac{S}{Vl}}\sqrt{1-\frac{k^4 SV}{8\pi^2 l}} \qquad 2.39$$

Experiments show that the natural frequency of vibration doesn't depend on the shape of the cavity (Robert, Randall, 1951).

2.5 Microphone

In this work a microphone was used as a sensor to the PA signal. In the following a brief description of it's main basic types.

The condenser microphone is usually made of a thin metal producing a large radial tension and operates with suitable bias voltage to produce an electrical signal when a pressure wave

impinges on the diaphragm; it pushes the diaphragm closer to an affixed metal plate increasing the capacitance between these two surfaces. The capacitance change leads to signal voltage V_s that increases with the bias voltage V_B and diaphragm area A_m. The applied force on the diaphragm is of two parts resulting from the sound pressure and the bias voltage. Condenser microphones usually have a frequency up to 15 KHz with low distortion, sensitive to mechanical vibration, response well to pressure impulses (krenzer, Lioyd, 1977).

The electrets microphone is composed of a solid material of high dielectric constant and electrically polarized. One face is metallized and the other is placed on an affixed back plate. When a sound wave impinges on the metallized side, it leads to a small change in the electric polarization characteristics of the electric material and this will produce a small voltage between the two surfaces of the microphone. An advantage of this type is that it needs no bias voltage.

2.6 Photopyroelectric spectroscopy

The photopyroelectric (PPE) method, which describes the thermo-optic characterization of materials, depends on the increase in temperature when materials absorb radiation. A pyroelectric transducer in thermal contact with a sample (Mandelis, 1984) can detect it. The incident radiation is modulated within two reasons: continues radiation will increase the sample temperature until it is evaporated, secondly the intrinsic property of pyroelectric sensor responds only to discreet temperature variations (Frandas, Paris, Bissieux, Chirtoc, Antoniow, Egee, 2000). Different configurations are possible for the PPE method (Mandelis, Zver, 1985). The main two configurations are the back configuration (BPPE) and the front configuration (FPPE). Figure 2.4 shows the (BPPE) configuration used in the PPE

detection with (m) representing the partially transparent sample with absorption coefficient β and thickness L_m, and (p) representing the opaque sensor with thickness x and absorption coefficient σ.

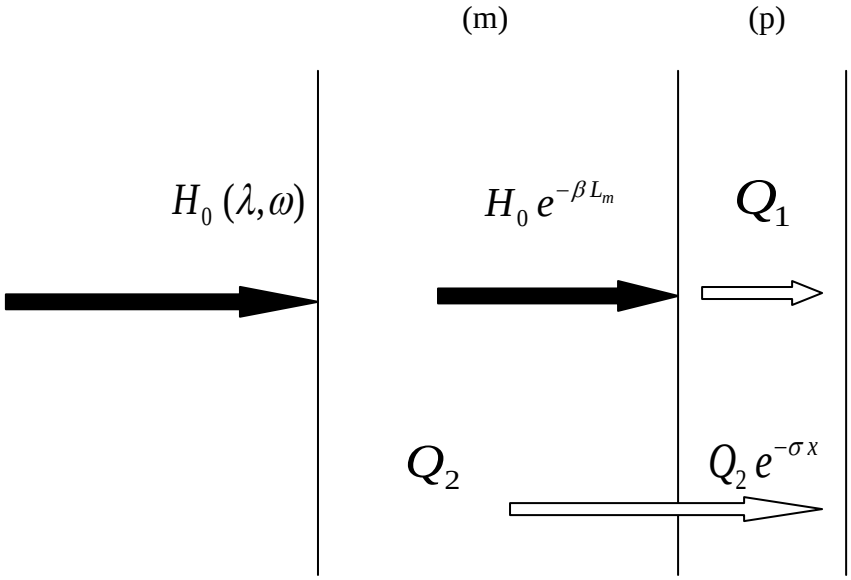

Fig.2.4. Schematic illustrating of the Back-detection BPPE
(Redrawn after Frandas et al, 2000)

The optical flux of the incident radiation H_0, and the heat generated in the pyroelectric sensor Q_1, generate an amount of heat Q_2 in the sample. The photopyroelectric effect, therefore, links the amount of heat generated in a sample, and detected by the sensor, to the absorption profile of the sample to a given radiation (Frandas, Paris, Bissieux, Chirtoc, Antoniow, Egee, 2000). Information about the optical transmission and absorption at the same depth can be obtained. The heat generated in the sample will produce a thermal wave that is detected by the pyroelectric sensor (Chirtoc, Bentefour, Gloriex, Thoen, 2001). Therefore, it is possible to perform spectroscopy for transmission and absorption modes, or to measure the samples parameters by suitable adjustment for the experiment (Frandas, Paris, Bissieux, Chirtoc, Antoniow, Egee, 2000). For thermo physical properties, the front

detection (FPPE) is used with opaque sample in which the sensor is facing the impinging radiation as seen in Fig.2.5.

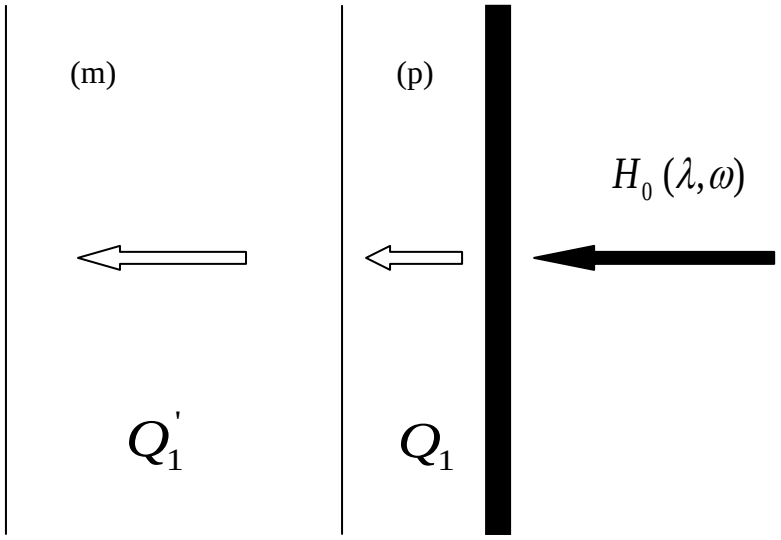

Fig.2.5. Schematic illustrating of the front detection FPPE.
(Redrawn after Frandas et al, 2000)

In the FPPE approach, the sensor absorbed an amount of heat Q_1 from the incident radiation. The amount of heat Q_1' exchanged to the sample depends on many of its physical properties and the sample act as a heat sink (Frandas, Paris, Bissieux, Chirtoc, Antoniow, Egee, 2000).

When a periodic modulation of angular frequency ω (ω = 2πf, where f is the modulation frequency) and for a monochromatic radiation (wavelength λ= constant) is given, then PPE voltage response *V* (ω, t) is given by (Chirtoc, Mihailescu 1989):

$$V(\omega,t)=v_0(\omega,t)\Gamma(\omega)\exp(i\omega t) \qquad 2.40$$

$v_0(\omega,t)$: Factor for current modulation

$\Gamma(\omega)$: signal amplitude

For a signal processing by an inverting current preamplifier with a feed – back resistor R_f, the factor ν_0 for current modulation operation has the form:

$$V_0 = \frac{PH_0SR_f}{2L_pC_p} \qquad 2.41$$

Where:

P: is the pyroelectric coefficient

H_o: is the optical flux of the incident light

S: is the area of the opaque sensor

L_p: is the thickness of opaque sensor

C_p: is the volume specific heat of the pyroelectronic sensor

Heat diffusion in the sensor or the sample is governed by thermal diffusivity (α), with sensor material length (μ) given by:

$$\mu = \sqrt{\frac{2\alpha}{\omega}} \qquad 2.42$$

Where: $\alpha = \frac{K}{C}$ is the thermal diffusivity with K denoting thermal conductivity,

C = ηc is the volume specific heat.

η: is the density, and (c) is the specific heat.

Heat transfer between two media can be characterized by the thermal effusivity $e = (CK)^{\frac{1}{2}}$. For given (α) and (e), C and K are computed from

$$C = k\alpha^{-\frac{1}{2}} \qquad 2.43$$

$$K = e\alpha^{\frac{1}{2}} \qquad 2.44$$

In the BPPE configuration in Fig. 2.4, the sample and the sensor are both thermally thick *i.e.* L_m/μ_m >1, L_p/μ_p >1, and the sample is opaque (Frandas, Paris, Bissieux, Chirtoc, Antoniow, Egee, 2000).

Where

L_m , μ_m are sample thickness and length respectively

L_p , μ_p are sensor thickness and length respectively

The amplitude of the signal $|\Gamma|$ and the phase Φ are reduced as follows:

$$|\Gamma| = 2\exp\left[-\left(\omega/2\alpha_m\right)^{\frac{1}{2}} L_m\right]\left[1+e_m/e_p\right]^{-1} \qquad 2.45$$

Where:

$$\alpha_m = \pi\left(L_m/slope\right)^2 \quad \text{(Thermal diffusivity of the sample)} \qquad 2.46$$

e_m , e_p are thermal effusively for the sample and sensor respectively

For the FPPE configuration shown in Fig. 2.5, If the sample is thermally thick (L_m/μ_m > 1) and the sensor thermally thin (L_p/μ_p < 1), the signal amplitude depends on the samples reciprocal effusivity (e_m):

$$|\Gamma| = \frac{\sqrt{\omega}}{e_m} C_p L_p \qquad 2.47$$

On the other hand if the sample and the sensor are thermally thin, the signal amplitude depends on the samples volume specific heat (Chirtoc, Mihailescu, 1989):

$$|\Gamma| = \frac{1}{1 + (C_m L_m) / C_p L_p} \qquad 2.48$$

C_m , C_p are volume specific heat for the sample and the sensor respectively

In this study the photopyroelectric (PPE) method is proposed as a new technique for thermal characterization of DNA and for gas traces. The (PPE) method is shown to be capable of providing temperature dependence of thermal diffusivity, thermal effusivity, thermal conductivity and volume specific heat (Frandas, Bicanic, 1999). All these quantities depend on the increase in the sample temperature due to the absorption of the radiation. Polyvinylidene difluoride film (PVDF) is the pyroelectric sensor used in this work (Coufal 1984). That characterized by a temperature dependent electrical polarization, generating an electrical charge on its electrodes when heated. The complicated expression for the amplitude (Γ) and the phase (ϕ) of the measured PPE signals give information about the thermal behaviors of the sample. To simplify the mathematical expression, certain experimental conditions are proposed. Using various configurations and detection schemes to obtain values of thermo physical parameters and their temperature dependences have been previously proposed (Dadarlat, Bicanic, Visser, Mercuri, Frandas 1995), the configuration used in this study is shown in Figure 2.6 below.

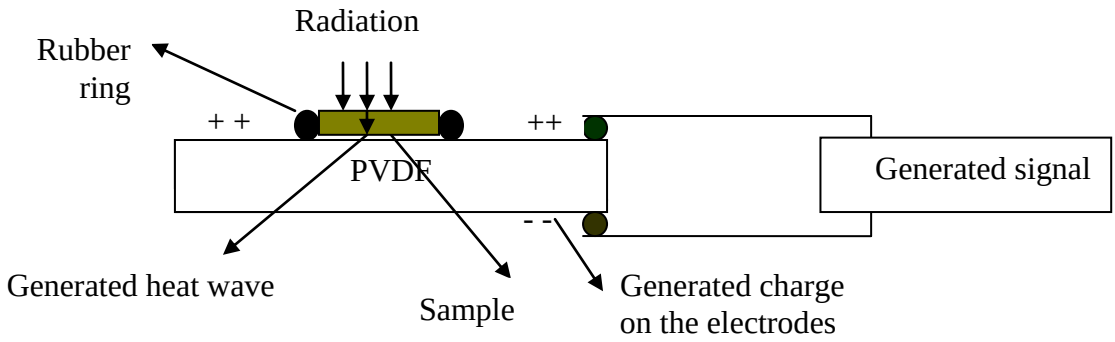

Fig.2.6. PPE method of the measurement of the sample temperature.

For the two configurations used. Back configuration is used with thermally thick samples and thick sensors, while front configuration is used with thermally thin sensor and thermally thick sample. The modulated light is absorbed by the opaque sample in the first one and the simplified expression for a thermally thick sample and sensor for the amplitude (Γ) and phase (ϕ) of the signal are given by the (Marinell 1992):

$$\Gamma = \frac{const}{e_{m+} + e_p} \exp\left(- \sqrt{\frac{\pi f}{\alpha_m}} \right) L_m \qquad 2.49$$

$$\phi = -\sqrt{\frac{\pi f}{\alpha_m}} L_m \qquad 2.50$$

Where e_{m+}: is the thermal effusivity of the material (sample).

e_p: is the thermal effusivity of the pyroelectric sensor.

α_m : is the thermal diffusivity of the sample.

L_m: is the thickness of the sample.

f: is the modulation frequency.

In the second configuration, the modulated light is absorbed directly by the sensors electrode, and the sample acting as heat sink, and the simplified expression when the sensor is thermally thin and the sample is thermally thick for the amplitude is given by (Dadarlat, Frandas 1993):

$$\mathrm{A} = \frac{const}{e_m} \qquad 2.51$$

The constant phase is constants that appear in equation (2.49) and (2.51) depend on the light irradiance, the pyroelectric coefficient of the sensor and the equivalent electrical impendence of the measuring system.

2.6.1: Polyvinylidene difluoride film (PVDF).

The PVDF is a polymer whose long chain molecule is composed of a large number of repeated units of identical structures. Some polymers are natural such as proteins, cellulose, and silk, others are synthetic, such as polystyrene, polyethylene, and nylon (Morawetz 1985).

In this study, a fluoropolymer called polyvinylidene difluoride (PVD) is prepared by a casting method, and extensively studied because it is a Ferro electric polymer. At least three main crystalline modifications exist. These are denoted α, β, γ and a minor phase denoted δ. All the crystals are distinguished by the conformation of the (C –C) bonds along the chain backbone (Marcel, William, Euler 2002). All four types are produced in different ways. α-phase and γ-phase, are obtained from solution deposition. Oriented β-phase is produced by stretching a PVD film. The γ-phase with regularly repeated intervals is obtained by annealing PVD film near melting point. Finally, the δ-phase is obtained by poling in an electrical field (Marcel, et al 2002). The crystal modifications strongly depend on the solvent evaporation rate, temperature and polarity of the solvent. The PVDF undergoes cross-linking polymerization under ionizing radiation (Ivanov, Migunova, Mikhailov, 1988). The morphology of semi crystalline polymers of particular importance is altered by thermal treatment of polymer such as annealing, quenching, super cooling and other treatment. The imperfectly formed crystals is melted in the annealing which is for a semi crystalline polymer near its melting temperature (Bret, Ludwing, Marek, Urban 1996).

The polyvinylidene difluoride film (PVDF), is a photosensitive material with a simple semi crystalline structure prepared by the emulsion free-radical polymerization**.

Unsaturated compounds are usually taken, as a sensitizing additive is reasonable to the effectiveness of the crosslinking because the direct use of radiation is complicated by dehdrofluorination side reaction, which becomes appreciable at increased absorption doses. The PVDF is a good sensor because it is inexpensive, easily handled and readily available in various thicknesses down to (25μm) sandwiched between two aluminum foils and can be easily attached to curved as well as flat surface (Zott, Heusinger 1978), as shown in Fig: 2.7.

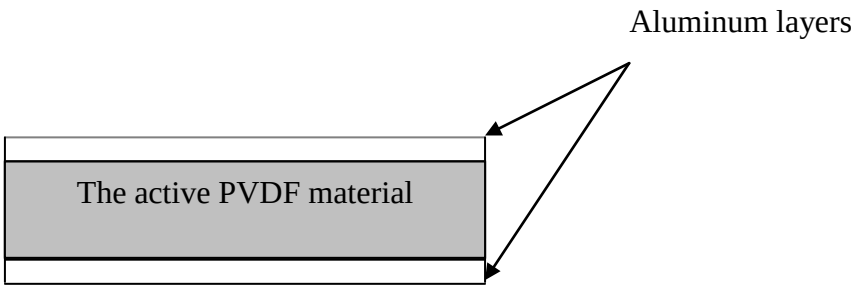

Fig: 2.7.Schematic illustration showing the PVDF.

**which is a useful reaction used to make polymers from small molecules containing carbon-carbon double bonds by using an initiator molecules that have the ability to breakdown the bond and separating a pair of electrons, making two fragments, each have unpaired electron, which will be discontent to be alone, and still want to be paired, for which the carbon-carbon double bond is very easily attached by the free radical (Ludwing, Marek, Urban, 1996).

2.6.2: PPE signal

Since the polarization vector is a function of temperature, changing the temperature will change the charge on the surface depending on dimensional change in the pyroelectric, which creates a potential difference across the opposite surfaces known as pyroelectricity. According to Zemel, the pyroelectric capacitor (Constantinos, Andreas, 1990):

$$Q = -C_p\left(V - V_0\right) + p(T)\left(\langle T\rangle - T_0\right) \qquad 2.52$$

Q : Charge density

$V - V_0$: Potential drop across the pyroelectric capacitor

C_p : Capacitance

p : pyroelectric coefficient

T : Temperature

T_0 : Initial temperature

$\langle T\rangle$ Instantaneous temperature rise averaged over all its thickness

The total pyroelectric current is the integral of the current density over the capacitor surface A as follows:

$$I = \int_A \frac{dQ}{dt}\, dA = \int_A \left(-C_p A \frac{dV}{dt} + p \frac{d\langle T\rangle}{dt} \right) dA \qquad 2.53$$

And the output voltage can be written as:

$$V(t) = \frac{pA \exp\left(-t/\tau\right)}{C} \int_0^t \exp\left(t'/\tau\right) \left\langle \frac{\delta T}{\delta t'} \right\rangle dt' \qquad 2.54$$

where

t : the time

$C = C_p + C_a$ and

C_p : Pyroelectric capacitance

C_a : input preamplifier capacitance

τ : Characteristic circuit time constant and $\tau = RC$

$R_T = \left[\left(1/R_p\right) + \left(1/R_A\right)\right]^{-1}$ and

R_p : Pyroelectric capacitor resistance

R_A : Preamplifier resistance

Now if the temperature varies sinusoidally at a frequency (f) then the pyroelectric voltage is:

$$V(f) = \frac{2\pi\ j\ f\ p\ R_T\ A\langle T\rangle}{1 + 2\pi\ j\ f\ \tau} \qquad 2.55$$

where $j^2 = -1$

To find the temperature distribution across the pyroelectric transducer in the z direction then the use of Fourier heat conduction equation is taken:

$$\frac{\partial T}{\partial t} = D_T\ \frac{\partial^2 T}{\partial\ z^2} \qquad 2.56$$

$D_T = \dfrac{k}{C_v}$: Thermal diffusivity of the pyroelectric detector

k : Thermal conductivity

C_v : Volume heat capacity

Therefore we can show that

$$\left\langle \frac{\partial T}{\partial t} \right\rangle = \frac{k}{C_v} \left\langle \frac{\partial^2 T}{\partial\ t^2} \right\rangle = \frac{1}{C_v\ z_0}\ \Delta H(t) \qquad 2.57$$

Where $\Delta\ H(t) = H(\ 0, t\ ) - H(\ z_0, t)$: the net heat flux into the transducer of thickness z_0 .

Using equation (2.57) and equation (2.54) to get:

$$V(t) = \frac{p\ A \exp(\ -t/\tau\ )}{C\ C_v\ z_0} \int_0^t \Delta H(t'\ ) \exp(\ t'\ /\ \tau)\, dt' \qquad 2.58$$

Evaluating the pyroelectric response at $t = \tau_{th}$ where τ_{th} : thermal time constant that is long compared to RC time constant then equation (2.58) becomes:

$$V(t) = \left(\frac{p\, R_T\, A}{C_v\, z_0} \right) \Delta H(t) \qquad 2.59$$

The pyroelectric material become electrically neutral when a constant temperature environment arise around, and when a harmonic modulation of the absorbed beam intensity arise around, a harmonic change in temperature will appear, which subsequently give rise to voltage.

2.7 Infrared spectroscopy

After understanding the theoretical background of PA and PPE effect, and the monitors used to detect these effects, the intend was to understand how the infrared spectroscopy affect the materials that will be used. The range of wavelength used in electromagnetic radiation used in IR spectroscopy is 700 nm - 200μm (Hollas 1996). The energy may be absorbed or emitted as a result of vibrations within a molecule between the component atoms (Smith 1971). The quality of absorption spectrum depends strongly on the method of sample preparation and the optical interface between the sample and the infrared instrument (Feinstein 1990). The same sample when use with different principles of optical measurement produces variations in the final spectrum, when different sampling accessories used for the same sample. For an absorbed band of IR, the intensity is proportional to the square of the transition moment or infrared active dipole moment, and depends upon the direction of the transition moment i.e. dipole electric field vector and the electric field direction vector of the incident infrared radiation (Harrick 1995).

The instrumental developments increased the use of infrared spectroscopy for both structural diagnostic tool and analytical purposes. The intensity of infrared radiation when passes through a sample of any substance is reduced by the same factor for each equal increase in distance traveled. If the reduction in intensity is due to absorption and not for scattering, then the following equation can be considered,

$$I = I_o \exp(-\alpha x) = I_o \, e^{-\alpha x} \qquad 2.60$$

Where x: is the distance traveled, I_o: is the intensity of incident radiation and α: is the absorption coefficient (Lovell 1991).

Group frequencies are most useful above about 1500cm-^{1}; below this frequency, the absorptions are due to the skeletal vibrations of the molecule. This is the "fingerprint" region, where even similar molecules may have quite different spectra. Far infrared, (approx. 400-10 cm^{-1}), has low energy and may be used for rotational spectroscopy. Mid- infrared (approx. 4000-400 cm^{-1}) may be used to study the fundamental vibrations associated rotational-vibrational modes, while the higher energy near-IR (14000-4000 cm^{-1}) can excite overtone or harmonic vibrations. Infrared spectroscopy is useful because chemical bonds have specific frequencies and corresponding to energy levels at which they vibrate. The vibrational frequencies are determined by the shape of the molecular potential energy surfaces, the masses of the atoms and, eventually by the associated vibronic coupling. In order for a vibrational mode in a molecule to be IR active, it must be associated with changes in the permanent dipole. The resonant frequencies can be related to the strength of the bond, and the mass of the atoms at either end of it. Thus, the frequency of the vibrations can be associated with a particular bond type (http://www.answers. com/topic/infrared-spectyroscopy-correlation-table, October 2006). Infrared radiation causes covalent chemical bonds to vibrate in different

modes. The part of the infrared spectrum molecules absorb depends on the strength of the chemical bond between the atoms, which is influenced by their atomic structure. Therefore molecules with different kinds of bond (e.g. a C-H and a C=O), would expect to yiel at least two different absorption bands. Beer-Lambert law gives how much of this radiation is absorbed which states: the amount of infrared absorbed is proportional to the concentration of the absorbing species and the distance the IR light has to travel through it (Nell, Hons, 2000). The existence of double and triple bonds shifts to the absorption peak at longer wavelengths, and the molar absorptivity (ε) roughly doubles with each new double bond. Hence, the appearance of several absorption peaks is proportional to the high number of double bond and triple bond systems, and is often solvent dependent. Vibrational fine structure is most pronounced in vapor phase spectra, and is increasingly broadened and oftenobscured in solution (http://www. cem.msu. edu/UV-Visible Spectroscopy, Visible and Ultraviolet Spectroscopy).

2.8 DNA structure

DNA is a polymer with monomer units called nucleotides. The polymer is known as a "polynucleotide." Each nucleotide consists of a 5-carbon sugar (deoxyribose), a nitrogen-containing base attached to the sugar, and a phosphate group. There are four different types of nucleotides found in DNA, differing only in the nitrogenous base. The four nucleotides are given one letter abbreviations as shorthand for the four bases (A: for adenine, G: for guanine, C for cytosine, T for thymine) (Richard, Hallick, 1995). The structure of each nucleotide is classified according to the number of rings in each:

Pyrimidines: which have one ring they are cytosine and thymine as shown in Fig. 2.8

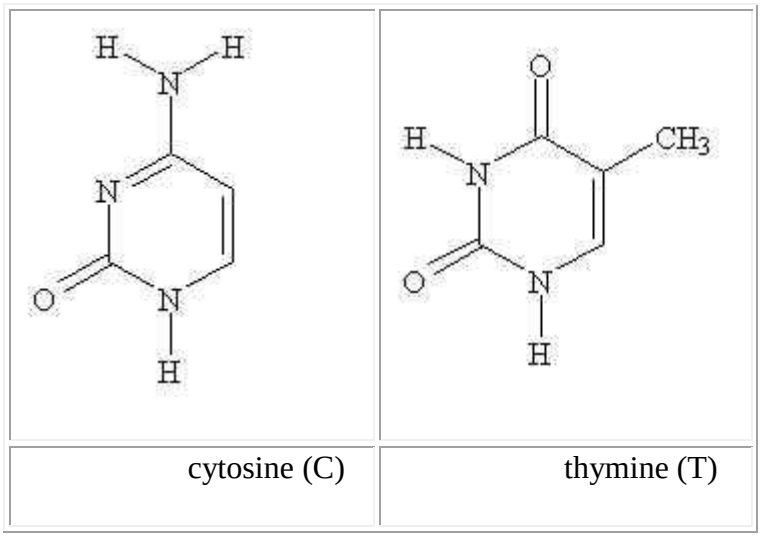

cytosine (C)	thymine (T)

Fig 2.8 Structure of cytosine and thymine
After: http://dl.clackamas.cc.or.us/ch106-09/nucleoti1.htm, October, 2006

Purins: which have tow rings they are adenine and guanine as shown in Fig. 2.9

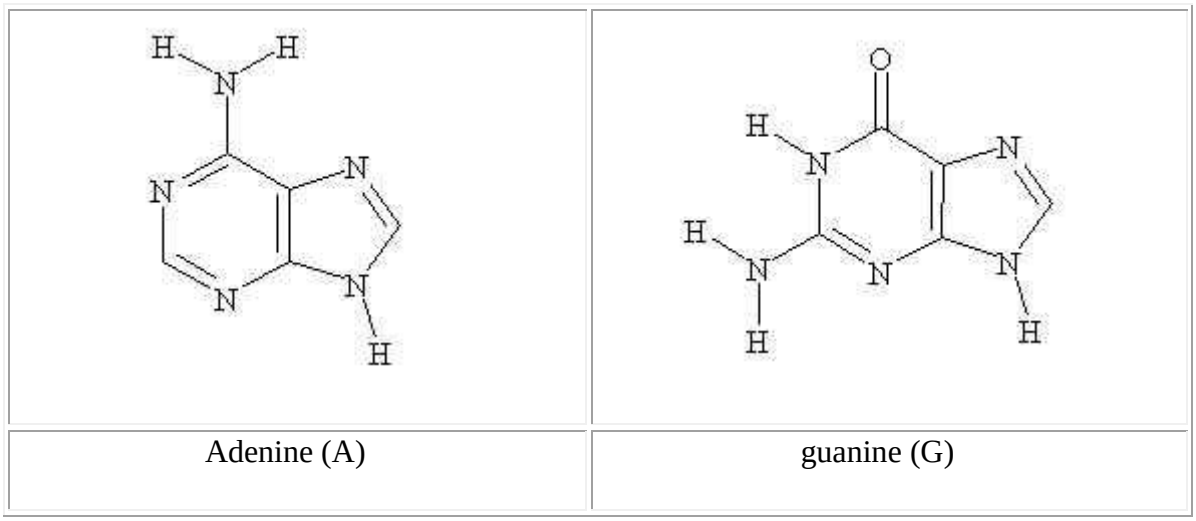

Adenine (A)	guanine (G)

Fig 2.9 Structure of adenine and guanine
After: http://dl.clackamas.cc.or.us/ch106-09/nucleoti1.htm October, 2006

Adenine hybridizes with thymine (A-T) with double bonds and cytosine hybridizes with guanine (C-G) with triple bonds to form double stranded DNA molecule. This is important because the PPE signal depend on the increase in the sample temperature due to the absorption of radiation, which is affected by double and triple bonds. The number of rings

and the number of hydrogen bonding sites as shown in Fig 2.10 and Fig 2.11 (http://dl.clackamas.cc.or.us/ch106-09/linking.htm, October, 2006)

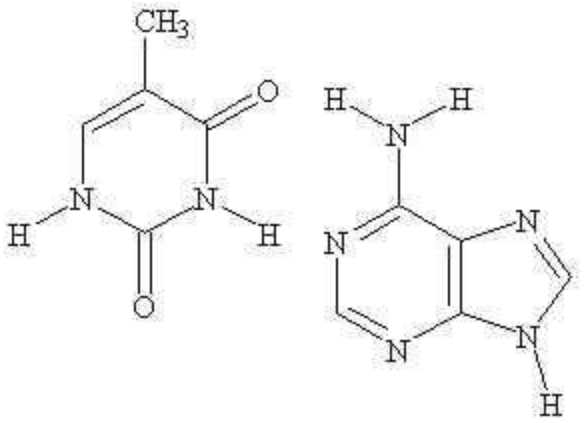

Fig 2.10 Forming double bond between thymine and adenine.
After: http://dl.clackamas.cc.or.us/ch106-09/linking.htm, October, 2006

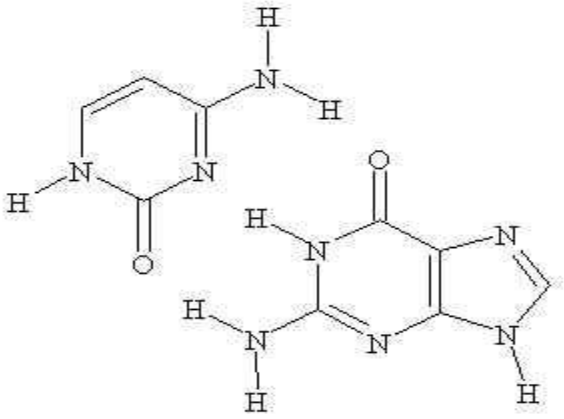

Fig 2.11 Forming triple bond between cytosine and guanine.
After: http://dl.clackamas.cc.or.us/ch106-09/linking.htm, October, 2006

So the number of adenine bases equals the number of thymine bases, and the number of guanine bases equals the number of cytosine bases in DNA structure.

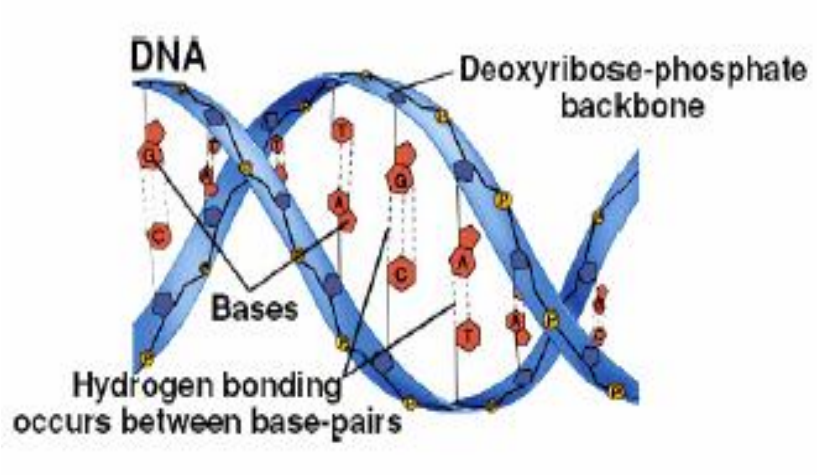

Fig 2.12: Structure of DNA double strand
After: (Jeffreys, Wilson, Thein, 1985)

Genetic fingerprinting: DNA typing are techniques used to distinguish between individuals of the same species using only samples of their DNA (Jeffreys, Wilson, Thein, 1985).

The Basis of DNA Typing

All DNA testing is based on the observation that the genome of each organism is different. The myriad of small and large differences in nucleotide sequence among individuals are known as DNA polymorphisms. Two fundamentally different types of polymorphisms have been widely exploited for DNA typing: tandem repeats and retraction fragment length polymorphisms (RFLP).

Tandemly Repeated DNA

The eukaryotic genome is densely populated with islands of short sequences that are repeated repeatedly in small to large arrays called minisatellites and microsatellites. Another term commonly used to describe these sequences is variable number tandem repeats (VNTRs).

For a given repetitive locus, the number of repeats is highly variable among individuals and heterozygosity is high (i.e. the number of repeats at the locus is usually different on the two pairs of chromosomes of one individual). Analyzing the number of repeats at one or more such loci provides a highly sensitive measure of individual identity.

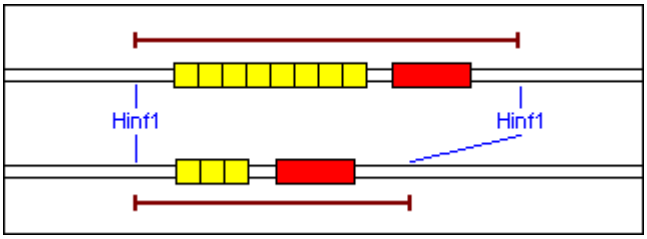

Fig 2.13 Illustration of VNTR process
After: (Watson, Crick, 1953)

Fig 2.13 depicts a VNTR locus with 8 versus 3 repeats. Digestion with the restriction enzyme Hinf1 will yield fragments of two lengths.

Variability in Restriction Sites

Single base changes in DNA often introduce or obliterate a restriction enzyme site. For example, a mutation that changes the sequence AGATCC to GGATCC will introduce a BamH1 site into that segment of DNA. Such sequence variability is exceedingly common, particularly in non-coding regions of DNA, and determining whether a particular group of restriction sites exists in DNA is a very sensitive means of differentiation one individual from many others.

Because polymorphisms in a restriction sites translates into variability in the length of fragments after digestion of DNA with that restriction enzyme, these DNA markers are called restriction fragment length polymorphisms or RFLPs.

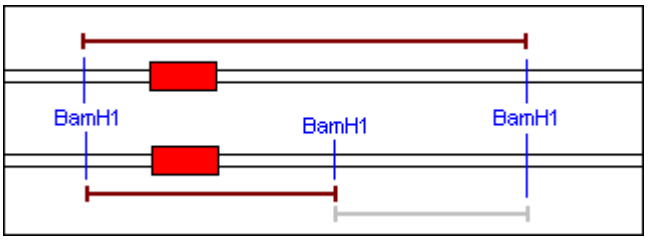

Fig 2.14 Illustration for RFLP process
After: (Watson, Crick, 1953)

The figure depicts a BamH1 RFLP in which the top strand of DNA has only two GGATCC sites while the lower has three. Digestion followed by hybridization with the (red) probe will reveal two fragments of differing length (Watson, Crick, 1953).

DNA sequencing

Although infrequently used at this time, DNA sequencing is considered the gold standard typing technique but the technique is highly demanding which makes it less feasible at this time ("http://en.wikipedia.Org/wiki/DNA_sequencing, October, 2006"). The infrared spectroscopy can be used to investigate DNA samples since the infrared spectra of the nucleotides are in the range (670 to 1443 cm^{-1}). The strong absorptions around 3333 cm^{-1} are probably associated with hydroxyl and amino stretching vibrations, the bands at 1667 cm^{-1} associated with C=C, C==N, and C-0 stretching, and the strong compounds show a band in the region of 1042 to 1087 cm^{-1} (Elkan, Melvin, 1948). The difference between organism can be detected by this methods based on the difference between number of nucleotide, as shown using tandemly repeated technique.

2.9 Essential oils

In the following, a brief introduction to the material side of some essential oils used in the study.

Essential, aromatic, fragrant, ethereal, and steam-volatile oils are materials that are extracted from different plant parts of aromatic crops, and extensively used in fragrance, flavor and pharmaceutical industries and in aromatherapy (Rajeswara, Kaul, Syamasundar, 2003). The activity of the essential oils depends on the type and concentration of the oil, and the collection period of the herb (Carla, Giuseppe, 2000). The essential oils are extracted from plants using steam Distillation methods, in which a pressurized steam passes through the plant material that is placed into a still. The globules of oil in the plant appeared and burst, leaving

the oil to evaporate. After that the essential oil vapor and the steam is cooled and condensed back to liquid, then separated by a centrifuge method. This process produces small amounts of oil. For example, more than 8 million Jasmine flowers are needed to produce just 2 pounds of jasmine oil **(**Potter, 1986**)**. The Cold Pressing method is used to extract the essential oils from citrus rinds that are chopped and pressed. The result is a watery mixture of essential oil and liquid with relatively short shelf life (Potter, 1986). Another method is the solvent extraction method in which a hydrocarbon solvent dissolves the essential oil. The result is a combination of wax and essential oil called the concrete, from which the essential oil can be extracted using pure alcohol. Finally, the high-pressure CO2 extraction method is used, in which carbon dioxide liquefied under pressure used to extract the essential oil from the plant. When the liquid is depressurized, the carbon dioxide returns to a gaseous state, and only pure essential oil remains (http://www.frontierherb.com/aromatherapy/esso.extr.html.1996.Frontier Cooperative Herb,October 2006). The various components of the essential oil provide the PA signal different absorption peaks. Additional peaks mean additional component in the oil. The components of essential oil are complicated and have several double and triple bond in addition to the sugar rings, which increase the number of peaks. Investigation of the absorbed signal for the essential oil needs to investigate each component alone, which is a hard task (Rai, 1992). In this study, three essential oils are used to test our developed technique.

Mint oil is one of the essential oils that have several compounds, which give it some properties such as fresh, sharp, menthol smell, clear to pale yellow in color and watery in viscosity. The most important chemical components of mint oil are menthol and a terpene, menthone (Hay, Waterman 1993). The oil is extracted using steam distillation method (Tassou, Koutsoumanis, Nychas, 2000).

The Damask rose oil has several properties depending on its component which give it a deep, rosy, fresh aroma, the color ranges from clear to a pale yellow or greenish tint, with more than 300 different components. The characteristic components are acyclic monoterpene alcohols, geraniol, citronellol and nerol, while the minor important trace components are β-damascenone, β-damascone and β-ionone. Rose oil and rose water are not identical since 2-phenyl ethanol appears in rose water is lost during steam distillation in rose oil (Gernot, 2003). Because of the volatility of rose oil, the best time for distillation, when the flower opens before the sun rise, producing 10g of the essential oil needs 100kg of fresh rose flowers (Gernot, 2003).

Jasmine oil has several properties such as sweet taste, rich floral smell and non-toxic, although some people do have an allergic reaction to it (Robert, 1995). The oil have more than 100 components, and the main ones are benzyl acetate, linalool, benzyl alcohol, indole, benzyl benzoate, cis-jasmone, geraniol, methyl anthranilate (Australia, 1997). The oil is prepared using solvent extraction method with a volatile solvents namely hexane (Simon, Chadwick, Craker, 1984). Since steam distillation technique induces thermal degradation of many compounds contained (Ernesto, Giovanna, 1994). The expected spectrum of these three essential oils were obtained by the FTIR spectrometer in the range 1000 cm^{-1} – 6000 cm^{-1}, and related to the PPE and PA signals obtained in the range 1000 cm^{-1} – 5000 cm^{-1} using the new technique.

2.10 Methanol and Ethanol

In the following a brief preview of methanol and ethanol structure and absorption spectrum:

2.10.1: Methanol (Methyl alcohol) CH_3OH

It has the shape shown in Fig 2.15

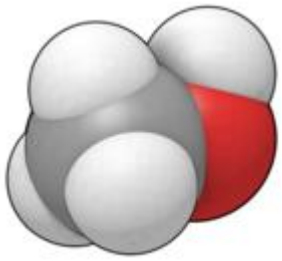

Fig 2.15 structure of methanol

(After "http://en.wikipedia.org/wiki/Methanol" , October 2006)

Methanol (CH_3OH) is the simplest alcohol, and is a light, volatile, colorless, flammable, poisonous liquid with a distinctive odor (http://www.daytonnursery.com/ Encyclopedia /Encyclopedia .htm, October 2006). The photoacoustic spectroscopy shows higher resolution and good S/N ratio (Ronaldo, Viscovini, Artemio, Danil, 2000). Methanol spectra were found to fall between "5000 to 667" cm^{-1}. The bands have been classified in relation to the O —H, C —H, C —O, and C —C vibrations within the molecules. Several weak bands also appear as a result of fundamentals and combinations. Methanol has a broad region of absorption, the intense absorption occurs near 3704, 2941, 1346, 1333 and 1042 cm^{-1}. which are attribute to O - H and C - H stretching, O – H and C - H bending and C —O stretching vibrations, respectively. In the vapor state of methanol there is appreciable absorption in the 1346 cm^{-1} region that has been assigned to the O—H bending frequency. A further general confirmation results in many weak maxima between "1667 to 1000" cm^{-1}. The twisting of the OH with respect to CH_3, gives rise, to a broad absorption centered around 250 cm^{-1}. The first overtone of this band shows a large number of rotational lines in the region from 862 to 380 cm^{-1}. Combinations of the O—H twisting with the C—O stretching and the CH_3 rocking vibrations

might well give rise to the complicated structure between 1515 and 1087 cm^{-1} (Earle, Plyler, 1952).

2.10.2: Ethanol (Ethyl alcohol) C_2H_6O

Ethanol has the structure shown in Fig 2.16

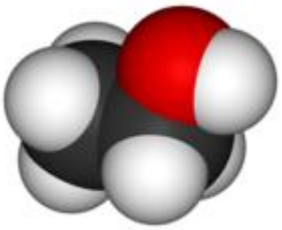

Fig 2.16 structure of ethanol

(After: "http://en.wikipedia.org/wiki/Ethanol , October 2006)

Ethanol is a flammable, colorless, mildly toxic chemical compound with a distinctive perfume-like odor, boiling at 78 ^0C at atmospheric pressure and freezes at -114 ^0C. It is a low molecular weight open chain compound, completely miscible with water (http://w w w .pueblo.gsa.gov/cic_text/health/sun_uv/sun-uv-you.htm, October 2006). Liquid ethanol consists of hydrogen-bonded pairs of ethanol molecules, which makes it more viscous and less volatile than less polar organic compounds of similar molecular weight. When mixed with water, the total volume is less than their individual components, and reduces the surface tension of water (http://en.wikipedia.org/wiki/Ethanol, October 2006). The spectra of ethanol have been measured from 5000 to 250 cm^{-1} in the vapor state and from 5000 to 767 cm^{-1} in solutions. In ethanol, it is more difficult to untangle the C — H vibrations in the 2941 cm^{-1} region because there are stretching vibrations that occur in the CH_2 and CH_3 groups that give rise to five fundamentals. The ethanol spectrum should have nine more fundamentals than

methanol. Three refer to internal vibrations of the CH_2 group. The C—C—O skeletal vibrations give rise to three bands that consist of one bending and two stretching vibrations. The band at 427 cm^{-1} is assigned to this bending vibration, and the two bands observed at 1064 and 877 cm^{-1}, are related to the C—O and C —C stretching vibrations. The two small bands at 379 and 355 cm^{-1} may be part of the first harmonic of the longer wavelength band, but only a few small structures that may be a part of this rotation were observed in the ethanol spectrum. The spectrum from 833 to 385 cm^{-1} is considerably different from that observed for methanol, which has many rotational lines in this region. In the 1250 cm^{-1} region, the ethanol bands are somewhat better defined than those for methanol. There are three intense bands at 1456, 1391 and 1242 cm^{-1}. These are assigned respectively to the asymmetric C—H bending in CH_2 and CH_3, to the O—H bending, and to the bending of the CH_2 hydrogen's symmetrically about the C—C axis (Earle, Plyler, 1952). The above theoretical studies encourage the use of these materials in our study since the infrared source radiate in the range 5000- 1000 cm^{-1}.

Chapter three

Experimental

3.1 Introduction

In this chapter a description of the experimental system used in this study is given. Two arrangement were follow; Firstly the usual arrangement for PVDF (Frandas and Bicanic, 1999). The BPPE method used by (Frandas, Paris, Egee, Bissieux, Chirtoc, Antoniow, 2000), was employed to study DNA samples as shown in Fig 3.1. Secondly, a combined cell containing PVDF and microphone is used for simultaneous detection of both signals. This arrangement as shown in Fig 3.2 is constructed and used for the first time. In the following a full description of both systems are given briefly and followed by preliminary results taken for known samples used to authenticate the system.

3.2 Photopyroelectric cell design.

The photopyroelectric cell used in the present study consists of a square piece of biaxial PVD foil metallised on both sides with aluminum foil to provide for reflecting surfaces and

electrode connections. The foil dimension is 1cm $\times$1cm size, 25 μ m thickness. The aluminum foil is important to make sure that only the heat propagating from the sample is detected and not that generated through direct interaction between radiation and detector. The foil was glued to a block of Perspex glass, which acts as a holder and support for the PVDF. The sample to be used was maintained on the top of the foil using a micro peptide. An aluminum box enclosed the cell, i.e. Perspex block and foil on top, to minimize the ambient electromagnetic interference, prevent the evaporation of the liquid during measurements and reduce air turbulence. The infrared radiation is shone in through a small opening (1cm $\times$ 1cm) size in the aluminum box. Two electrodes are connected to the top and bottom foils with silver paint constitute the PPE signal output. This cell design was used by Al Sarahneh, 2005 in studying olive oil adulteration. The cell shown in Fig 3.1 is connected to the electronic monitoring system for signal processing as shown in Fig 3.6.

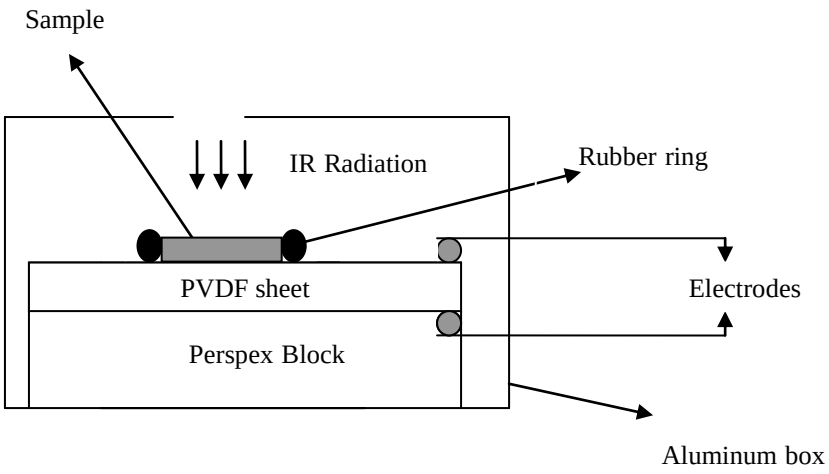

Fig. 3.1. Schematic showing the Photopyroelectric cell used to study DNA samples .

3.3 Combined photoacoustic-photopyroelectric chamber design (CPPC).

This cell was designed to allow simultaneous detection of PPE and PA signals. Fig 3.2 shows a schematic of the combined photoacoustic - phtopyroelectric chamber used in the present study. A square piece of biaxial PVD foil 1cm $\times$1cm size 25 μm thickness, is fixed on the Perspex holder and held against an aluminum pipe constituting the PA cell. The foil was glued to a Perspex glass to support and prevent heat transfer to the out side. The aluminum pipe is isolated from the PVD film by a rubber ring having dimensions of 0.24 cm depth and inner diameter 0.82 cm, used to prevent the heat transfer from the pipe to the PVD so that the measurement reflects heat absorbed from the gas or some radiation falling directly on the PVD. The aluminum pipe is 6.93 cm long having internal and external diameter of 0.79 cm and 0.98 cm respectively. In the middle of the pipe a Helmholtz cell was fitted, which is connected to the aluminum pipe through a small hole. The Helmholtz cell neck is 1.56 cm long and has internal and external diameters of 0.1cm and 0.25cm, respectively. The main Helmholtz volume consists of a cylindrical cup with the dimensions: 0.44 cm long, inner diameter 0.71cm, and outer diameter 0.8cm. A very sensitive microphone used to measure the PA signal is fixed on the top of the cup constituting the main Helmholtz cavity, with a volume = 0.186 cm^3, as shown in Fig 3.3. An additional small hole at the edge of the pipe near the PVD film used to inject the liquid inside the cell. This hole is blocked using a rubber bung after sample is allowed in. The IR radiation source is fixed on the other end of the cylinder using special holder. The source holder is easily demountable to open the cylinder when needed to add samples and allow vapor for previous samples escape out of cell. The cell where the PVD film is maintained enclosed in an aluminum box to minimize the ambient electromagnetic interference. Two electrodes are connected to the top and bottom aluminum foils with silver paint and two other electrodes were connected to the

microphone constituting input for PPE and PA signals respectively to the phase sensitive detector (Fig 3.2, Fig 3.3 and Fig 3.7).

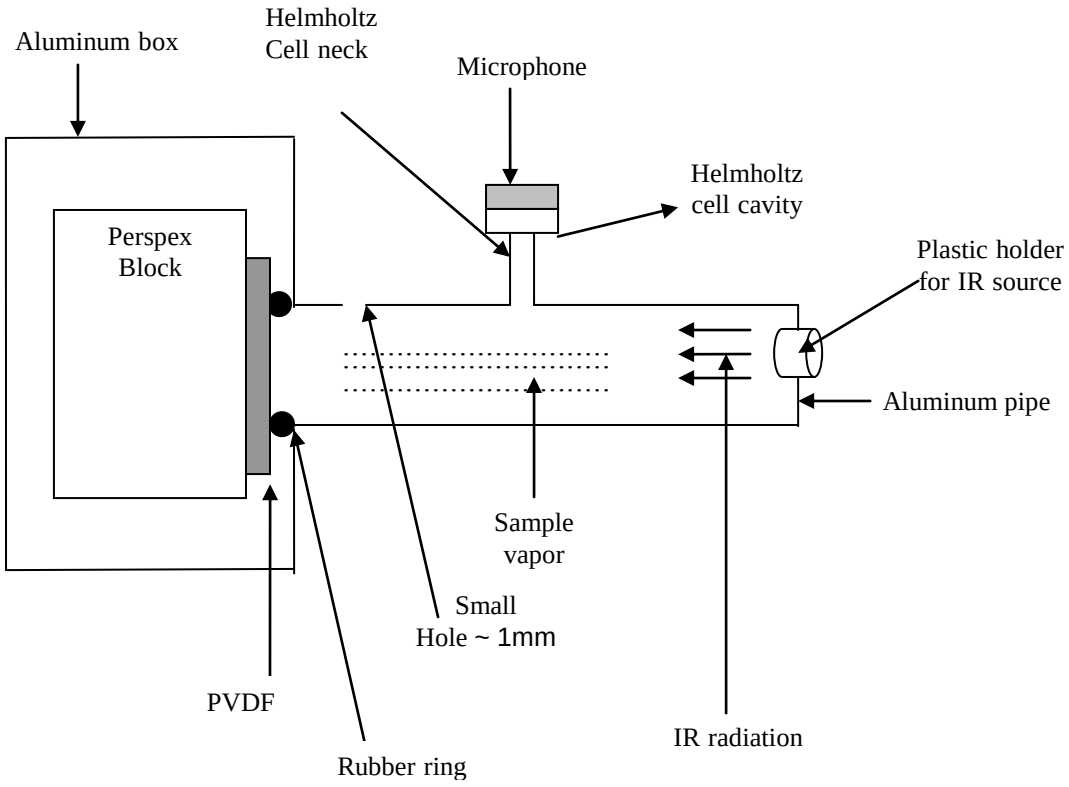

Fig. 3.2. Combined photoacoustic – photopyroelectric chamber assemply

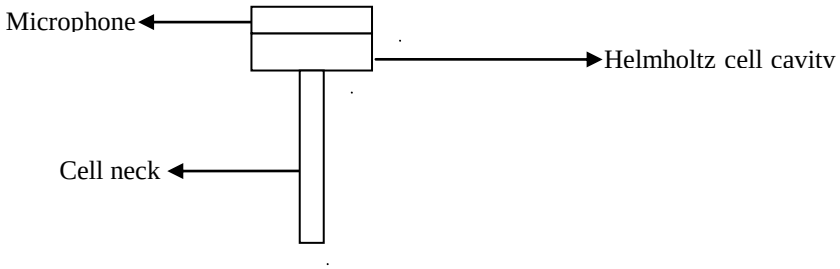

Fig 3.3 Schematic drawing of the Helmholtz cell

3.4 Wide band Infrared (IR) source.

The infrared source used in this study is high-intensity IR emitter normally used in gas sensors and provided by Ion Optics Ltd. It has along term stability and can make a shot-to-shot repeatedly, with high Signal-to-noise ratio. The source is a broadband infrared light source emitting in the range 2 – 9.5 µm, have a pulsed operation at large temperature modulation with an active area $32.7\,mm^2$, rated temperature $850\,^0c$, minimum and maximum resistance 2.8 ohms, 4.5 ohms respectively, the source become dull red at 300 mA, and red at 320 mA, with rated drive power ~ 0.461 watts, as seen in the figure below.

Fig 3.4 Photo of the infrared source used in the present study
(After: http://www.metax.co.uk/infrared_source.htm, October 2006)

The source is an electrically pulsed, high intensity infrared radiates with, low thermal-mass filament tailored for high emissivity in the range (2-5 µm). The low temperature operation reduces the chance of igniting combustible gases, and efficient in the band emission at wavelengths > 8 µm with temperatures several times cooler than tungsten bulbs that gives life span for many years. For a constant current drives, the power delivered increased according to the relation $I^2 R$ since R increased by increasing the heat, and for constant

voltage the power decreased slightly according to the relation V^2 / R for the same reason. The high-efficiency device minimizes drive power, greatly reducing parasitic heating of detectors and optics; also it eliminates the mechanical choppers, permitting a sealed optical path as in the present study. The high emissivity enables it to efficiently and rapidly cool via thermal radiation. Fig 3.5 below shows that the hot filament (left image) nearly cools to background temperature (right image) before the next pulse, thus providing several hundred degrees of temperature modulation. The emissivity is enhanced and controlled by creating random surface texture (micron scale rods/cones). This texture modifies the reflection and absorption spectra relative to that for a flat filament of the same material. For wavelengths small compared to the feature sizes, the surface scatters most incoming light, therefore it has low reflectivity (the filaments appear visibly black), and by Kirchoff's law, it must have high emissivity (>80%). For wavelengths long compared to the feature sizes, the surface still looks like flat metal and it therefore has low emissivity, characteristic of the flat metal.

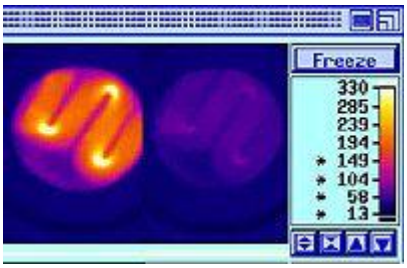

Fig 3.5 Image for cooling and pulsed radiation of IR source
(After: http://www.metax.co.uk/infrared_source.htm, October 2006)

3.5 Equipment:

The equipment used in this study included three main parts, i.e. detection units, electronic signal processing system, and IR source. The detection unit is either the PVD and its corresponding cell, or the combined PVD, microphone cell. Either of the cells is connected to

the electronic signal processing system. The later includes: Phase sensitive detector, power function generator, connecting leads, battery (9v), and oscilloscope. IR radiation is obtained from a miniature pulsed wideband IR source as discussed in see section 3.4. The source is driven by an AC signal from a power function generator, a current of 0.3 Amps is needed to drive the source. Radiation is allowed to fall on certain amount of a sample placed on top of the PVD or in the combined cell. The absorbed radiation consequently generates a PPE and PA signals that can be picked up from either or both detection units, using a phase sensitive detector.

3.6 Experimental set up:

Equipments are arranged such that the electronic processing system has the same setup for all parts of the experiment. For each part the output from either, the combined chamber, or the PVD cell is connected to the input of the electronic monitoring system. Fig 3.6 represents the experimental setup for DNA study, and Fig 3.7 shows a complete setup to detect PA and PPE signal simultaneously, which developed by us and used for the first time.

3.6.1: DNA sample study

IR absorption of DNA samples was indirectly measured with PPE using radiation from the miniature pulsed wideband IR source. The source is driven by an AC signal from a power function generator. Radiation is shone on a single drop sample placed on top of the PVDF film. The radiation absorbed by the sample generates a PPE signal that can be picked up by a phase sensitive detector as seen in Fig. 3.6. For different samples of DNA of known structure one single drop of 10 μ*l* using a micro peptide was placed directly on the PVD film in a region bounded by a rubber ring. The resulting absorption of the IR radiation by the drop of DNA

generates a heat wave that is picked up by the PVD film as PPE signal that can be detected by signal processing system.

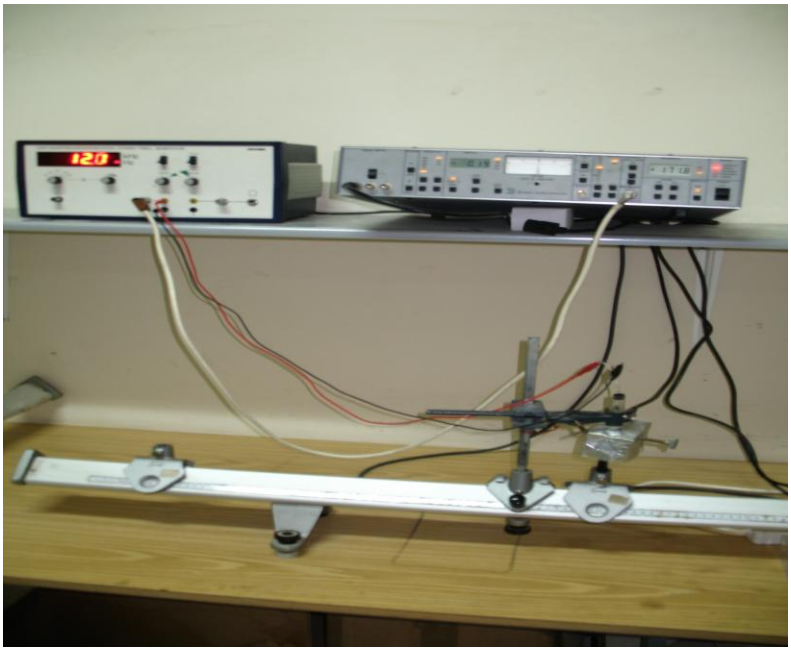

Fig 3.6a Photo for the complete photopyroelectric detection system used for DNA study

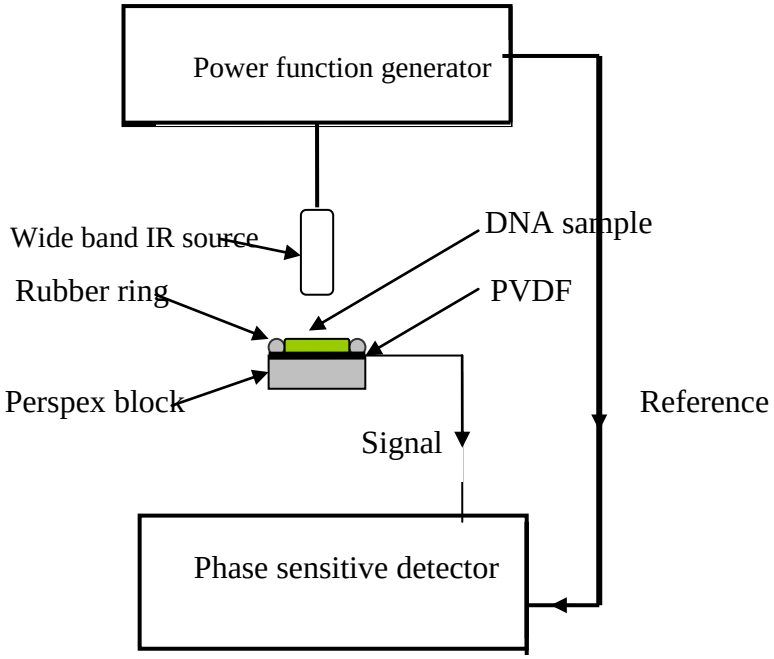

Fig: 3.6b Schematic illustration for the complete photopyroelectric detection system used for DNA study.

3.6.2: Simultaneous PA-PPE signal detection

In this study IR absorption of evaporated essential oil samples was simultaneously measured as a PPE and PA signals using radiation from the miniature pulsed broadband IR source. Radiation is shone along the axis of the aluminum pipe in a region filled with oil vapor. The absorbed radiation generates a PPE and PA signals that can be fed in the electronic processing system shown in Fig. 3.7. The resulting absorption of the IR radiation by evaporated essential oil generates a heat wave and a change in the pressure of the gas inside the Helmholtz cell, hence simultaneous generation of PPE and PA signals respectively.

The direct radiation on the PVD film is sensed directly as radiated from the source, but when the sample is evaporated inside the cell; it will absorb part of the radiation from the source and hence reduce the amount of radiation reaching the PVD film.

Simultaneously, the nonradiatively decaying excited atomic and molecular species in the tube cause a change in the pressure of the gas in the tightly enclosed cell that can be sensed by a sensitive microphone i.e. PA signal that can be detected by the electronic processing system.

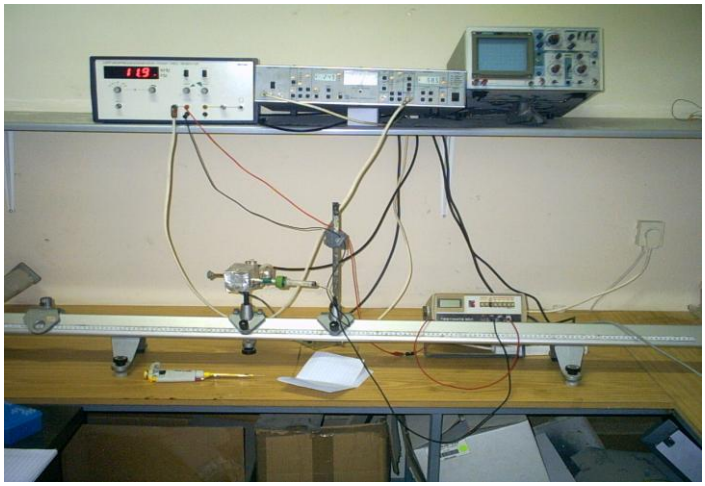

Fig 3.7a Photo for the combined Photoacoustic-Photopyroelectric System used for trace gas detection

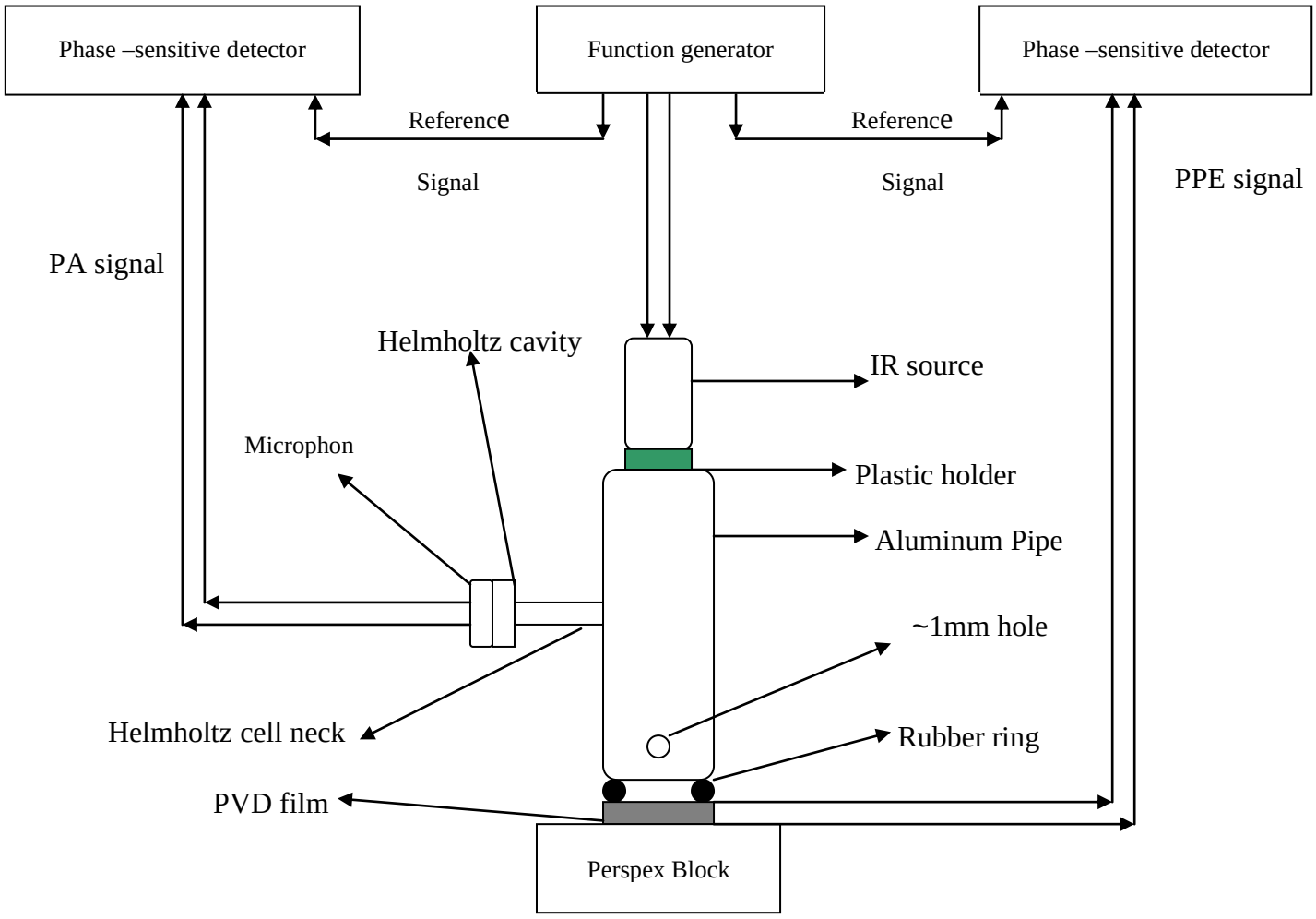

Fig 3.7b Schematic illustration for the combined Photoacoustic-Photopyroelectric System used for trace gas detection

3.7 Experimental samples:

Different samples investigated to study the absorption signal for DNA samples. The unknown DNA samples were brought from the biological lab of the university, without any information about their structure and purity. Three other sets of primers were ordered from (Invitroge Company), each set was complement with each other as shown in the company's instruction sheet. The lyophilized primers were reconstituted with ultra pure water and the final concentration of each primer was of 100 pmols/µ*l*(100 µM). The complement primers were mixed together so that they form double stranded DNA. These primers were of known molecular weight, concentration and AT/CG ratio i.e. ratio between double and triple bonds.

The final DNA samples included in this study were of PCR products of known length and sequences.

In the second part of this study, a set of essential oils, brought from a local shop were investigated and the vapor absorption was detected simultaneously. Their degree of purity is not known. The plant species used to extract these oils were brought from the garden the same day of the experiment. Essential oil samples were introduced into the system on identical pieces of cloth 0.5 cm X 0.5 cm.

3.8Authentication of the experimental system:

A set of known samples was used to examine the experimental setup, to gain enough knowledge and experience and authenticate the system reiability. The PPE cell was investigated by using the unknown DNA samples, which give different signals for different samples, with signal to noise ratio exceed 140 in most applications.

Using the combined PA-PPE assembly, the system was run using standard methanol and ethanol samples. For simultaneous detection of PA and PPE signals, the system was arranged as shown in Fig. 3.7. Preliminary testing was achieved using a single drop of methanol placed in the pipe. The PPE and PA signals were simultaneously detected and compared. The signal to noise ratio calculated was found to exceed 100 and 30 for the PPE and PA signals respectively in most applications. Ethanol C_2H_6O was also used to investigate simultaneous detection for PA and PPE signals against time.

3.9 Cleaning the cell.

Both experimental arrangements were used to test many samples. For the sake of satisfactory results, the sensing units i.e. PVD and PA cell have to be cleaned before introducing new sample.

Cleaning the photopyroelectric film was found to be important in this work, since DNA samples produce films of low vapor pressure. Cleaning the film was achieved by wiping the film with a cotton wool soaked with a cleaning agent such as acetone. To be sure, that the film is clean the system is run and background signal level is proved the same.

For the combined cell it is important, to ensure that there will be no residual molecules in the pipe from previous sample prior to introducing new sample. This is done by leaving the pipe open for 10 minute and using hot air generator evaporate and drive out any residual gases or unevaporated liquids.

3.10 Conclusion:

Two detection systems were assembled and examined using known samples. The results confirmed the reliability of both systems. The combined PPE-PA system proved satisfactory for simultaneous detection of PPE and PA signals. Excellent signal-to-noise ratios about 140, for PVD sensor were achieved. For PA, the signals-to-noise ratio was ≈ 30. The reasons for this lower value will be explained in chapter 5. For further understanding and authenticating of the results, many of the samples were studied using the well-established FTIR technique.

Chapter four

Results

4.1 Introduction

Results of the photopyroelectric wideband study of DNA compounds, and the combined photoacoustic – phototpyroelectric gas trace detection of natural essential oils vapors were utilized. Relevant to the photopyroelectric monitor the study involved different types of DNA samples having different quality (sequences), quantity (number of nucleotides), different molecular weights and CG/AT ratio. The absorbed signal of the unknown DNA samples were taken first, with optimum PPE signal taken at modulation frequency of 12 Hz, and current source 300mA. These are the typical operating conditions for most of the experimental parts to follow. Secondly, the absorbed signals of the synthesized DNA samples detected at a concentration of 100 μ moles, with details of DNA samples ready for testing, shown in table 4.1. The obtained PPE signal for each sample was drawn against the (molecular weight, number of nucleotide, number of double bond, number of triple bond and CG/AT ratio), with optimum PPE signal taken at, (12) Hz, 4 μ L of the sample and 300mA current through the source, to have an indication of their structure in order to relate certain parameter in the DNA structure to the signal. Finally, the DNA of PCR that was produced in the lab with known

length and sequences were investigated against the number of nucleotide. The main purpose of this study is to use the photopyroelectric spectroscopy to monitor DNA samples, and compare different types according to the signal, then compare the result with those taken by Fourier Transform Infrared Spectrometer (FTIR) for the same sample using 5 µl of sample on a zink solenoid transparent plate ZnSe with wave numbers in the range 7000-1000 cm^{-1}.

For the combined PPE–PA chamber the cell centering was on the IR absorption resulting in PA and PPE signals of methanol (CH_3OH), to investigate the system, since it is a known material with absorbed signal in the range 5000 to 667 cm^{-1}. Parameters that optimize the signal amplitude will be fixed for the rest of the experimental result, i.e. 12 Hz modulation frequency and 300 mA driving source current. A comparison between the PA signal and the PPE signal were investigated to authenticate the use of PVD film as a monitor for gas traces. The different parameters i.e. changing the modulation frequency of the source, while leaving the driving source current, and the concentration of molecules inside the pipe constant, or changing the current and leaving frequency and concentration of molecules constant, finally adding volumes of methanol in the cell to change the concentration of molecules inside the pipe, with extra volume added and leaving the current and frequency constant are investigated for methanol. A time of approximately10 minutes is allowed before starting measurement so the added sample evaporates. The investigations in the new cell were performed at optimum parameters: 12 Hz modulation frequency of the IR source, which is driven by 300 mA. A volume of 5 μL from sample used and these parameters kept at these values unless they are changed on purpose. Using IR source emitting in the range 2- 9.5 µm i.e. wave number 5000-1000 cm^{-1} as part of the experimental arrangements of Fig 3.7, the background signal for air alone which was found to be for the PPE signal equal to 7.547 a.u and for the PA signal equal to -1.309 a.u. The true PPE signal were then obtained for the methanol for example, by

subtracting the obtained signal with sample introduced, from the background PPE signal for air alone. The PA signal due to IR absorption is obtained by subtracting the background signal of air in the cell from the signal obtained after adding sample.

The PA and PPE signals were then measured versus time at constant volume, frequency and current for ethyl alcohol (ethanol C_2H_5OH), which will be used to dilute the essential oil samples. The background signal for this and the remaining parts was taken for a small piece of clothes placed in the cell and used to introduce sample in the cell, it was found to be for the PPE signal ~ 8.857a.u and for the PA signal ~ -2.619 a.u. The same procedure was also carried out for some essential oil i.e. Damask rose oil, Jasmine oil and Mint oil, since they are volatile oils. The same experiment was performed for plant leaves, where certain weight of the plant part used to produce the essential oil placed in the cell. For example, 0.03 g of dried and green Mint leaves and 0.03g of jasmine and rose flower were studied and compared. Investigation of the diluted jasmine and rose oils samples by ethyl alcohol, for which the ratio is determined by the purity of the oil calculated by finding the percentage of the volume of essential oil to the total volume i.e. purity = ((volume of essential oil)/(volume of the essential oil + volume of ethanol)) X 100% , where also done, and indicated on the corresponding figures, while the mint oil was investigated without dilution. In all the above application, the combined cell was perfectly closed after adding the material directly. The comparison of the signal at different purities was also investigated.

4.2 Tested samples.

In this section, a description of the investigated samples will be introduced briefly.

4.2.1: The DNA samples.

Different DNA samples were tested at three stages; firstly, the unknown DNA samples investigated for absorption of infrared radiation i.e. PPE signals of each sample. Then perfectly pure synthetic DNA samples obtained from (*Invitroge company*) with known structure were used. Finally, the DNA of PCR products of known length and sequences were used. All samples were tested employing the PPE and FTIR. The three synthetic DNA samples were prepared in the lab; each set of primers is a complement with others as indicated by the manufactures technical sheet. The lyophilized primers were reconstituted with ultra pure water and the final concentration of each primer was 100pmols/µl (100 µM). The complement primers were mixed together so that they form double stranded DNA. These primers were of known molecular weight, number of nucleotide, AT/CG ratio and concentration. The DNA samples prepared prior to experimental test according to the following table:

Table 4.1 Details of different manufacture DNA samples ready for testing.

Chain	Number of nano moles	Volume of water (micromole)
P1	34.2	342
P2	27.1	271
P3	25.6	256
P4	21.0	210
P5	24.8	248
P6	26.9	269

Samples were allowed one day to make sure that all powder is dissolved before the next step of taking a pair of dissolved chains consistent with each other according to its structure in order to form double stranded DNA, where P1 and P2 mixed with each other by taking the same volume from each sample (271µ*l*) to form DNA1, (P3 and P4) at 210 µ*l* from each sample chain to form DNA2 and (P5 and P6) at 248 µ*l* from each chain to form DNA3 indicated in table 4.1.

One single droplet (4µl) from each sample was analyzed using the empirical system shown in Fig.3.6. Then these samples were tested using FTIR. DNA samples were kept at -20 ^{0}C all the time prior to experiment. The experiment is aimed to test the method's ability to distinguish samples of different structure, since DNA is a fingerprint for each organism.

4.2.2: Liquid vapor detection using CPPC.

For the combined PPE-PA arrangement, methanol CH_3OH and ethanol C_2H_5OH vapors are used as known materials to investigate the system reliability. Ethanol was used to dilute the essential oils to give different purities for the purpose of investigating constitute at different concentrations. The mint, jasmine and rose oils, were obtained from local shop, with unknown concentration, and considered undiluted essential oils. Fresh plant tissues used to produce these essential oils are taken from the garden in the same day of investigation. The idea is to test the system ability to detect traces of oil vapor and plant tissue and use the result to distinguish different essential oils at different purities using the combined cell.

4.3 Known materials results

In this part of the experiment methanol and ethanol as known materials were investigated to ensure the detection ability of the newly designed system.

4.3.1: Methanol results

Methanol is a volatile material that causes a gas trace that can be detected using a PA effect. In this study, a new technique will be used to detect the gas trace by simultaneous PPE and PA technique using the empirical system shown in Fig.3.7 at different experimental conditions.

4.3.1.1: Signal versus concentration.

Signal dependence on the concentration of trace gases of the sample component that has been evaporated was investigated by gradually increasing the volume of added sample in the cell. As the volume is increased, it is expected that saturation signal will be reached. For each sample increment, a time of about 10 minutes is allowed for evaporation before measurement started. The direct radiation on the PVD film is shown in Fig 4.1b, indicating the decrease in the PPE signal due to the increase of the evaporated molecules of methanol, where by Fig 4.1a represents the absorption by evaporated methanol molecules calculated by subtracting the PPE signal from the background signal of the air alone.

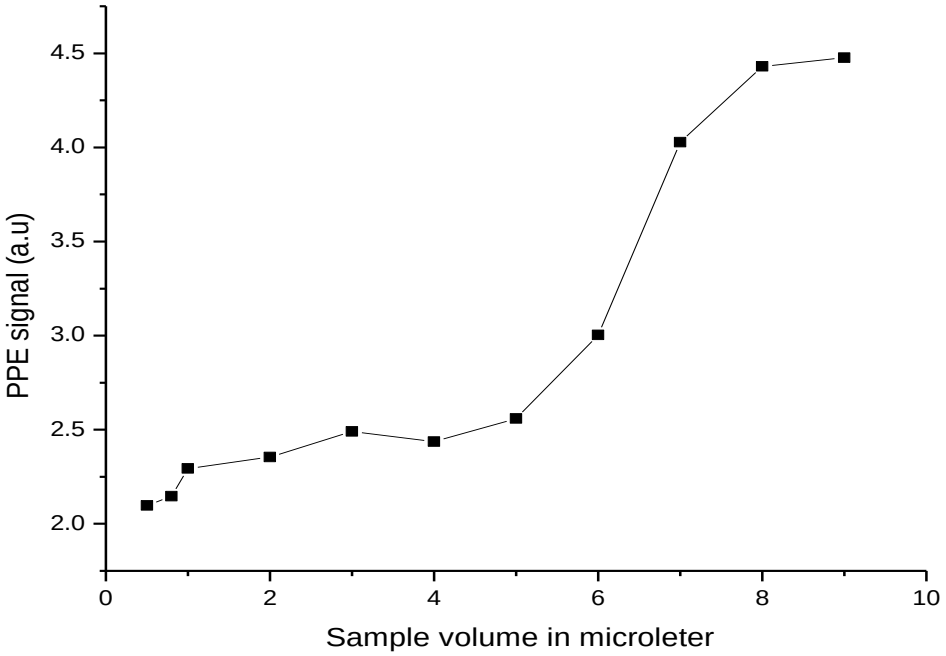

Fig 4.1a Absorption of methanol molecules versus the increase in trace gas concentration

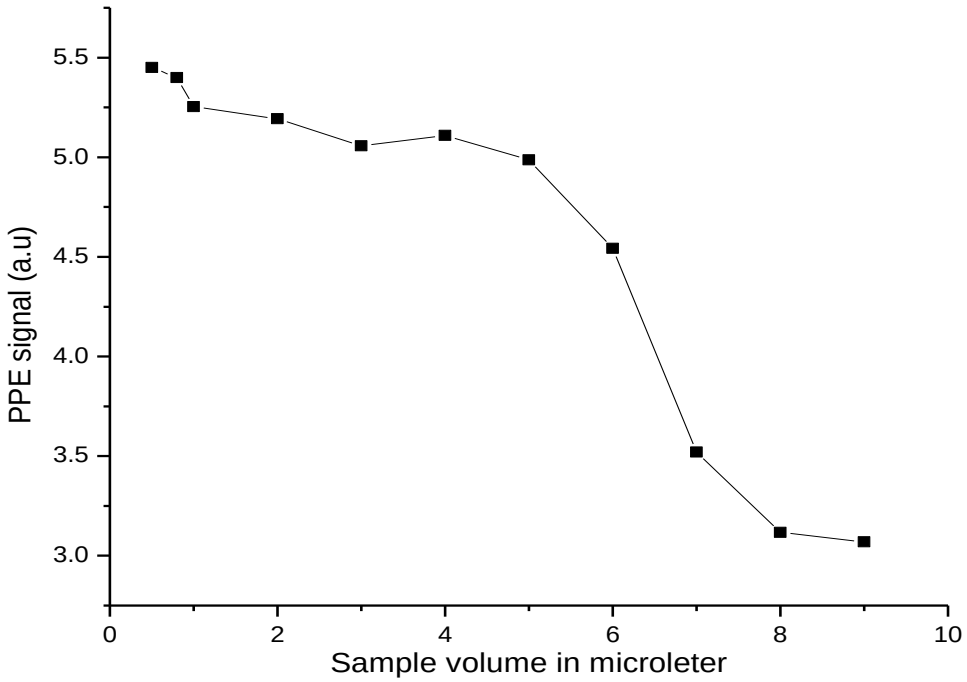

Fig 4.1b PPE signal of direct IR radiation on PVD film versus increase in trace gas concentration of methanol

The PA signal due to IR absorption by methanol molecules is shown in Fig 4.2.

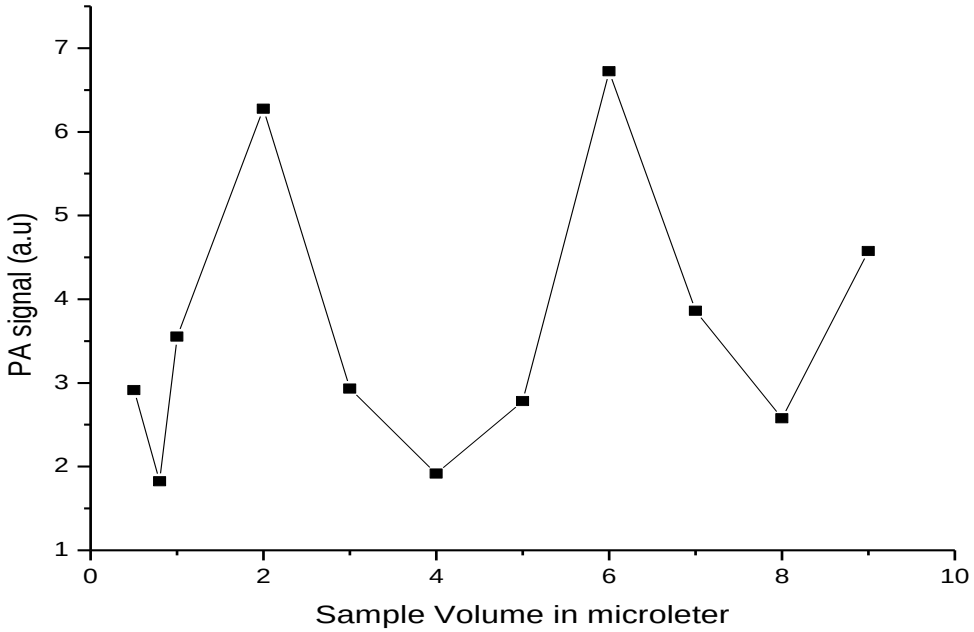

Fig 4.2 Methanol PA signal versus increased in trace gas concentration

4.3.1.2: Signal versus current.

Taking certain volume of methanol i.e. “constant concentration of evaporated molecules of methanol in the pipe”, and leaving the modulation frequency constant at 12 Hz, while changing the driving IR source current. The corresponding PPE and PA signals were shown in Fig 4.3 and 4.4 respectively.

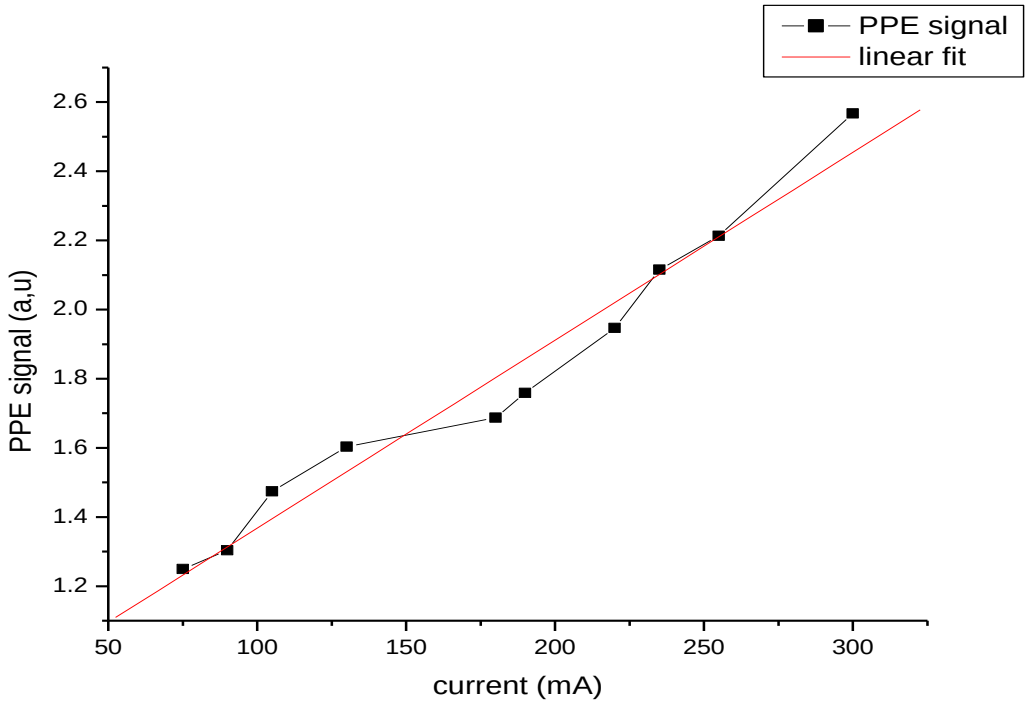

Fig 4.3 Methanol PPE signal versus increased in driving IR source current

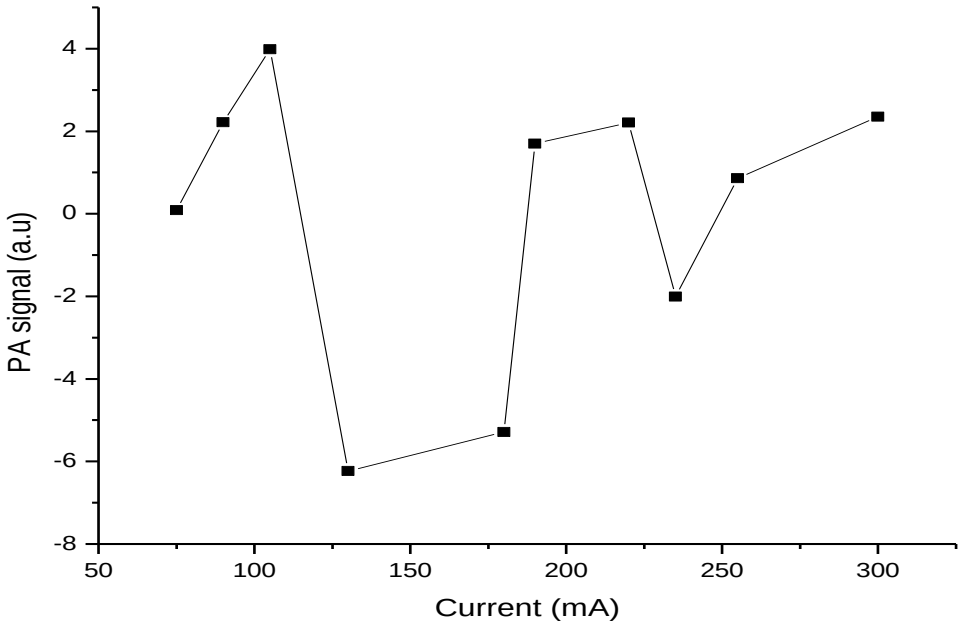

Fig 4.4 Methanol PA signal versus increased in driving IR source current

4.3.1.3: Signal versus frequency

The effect of changing the source modulation frequency was performed leaving other parameters at their optimum values. Using the experimental setup of Fig 3.7, the direct radiation falling on the PVD film is shown in Fig 4.5b, the PPE signal reading from IR absorption by methanol molecules was shown in Fig 4.5a, and the PA signal was shown in Fig 4.6

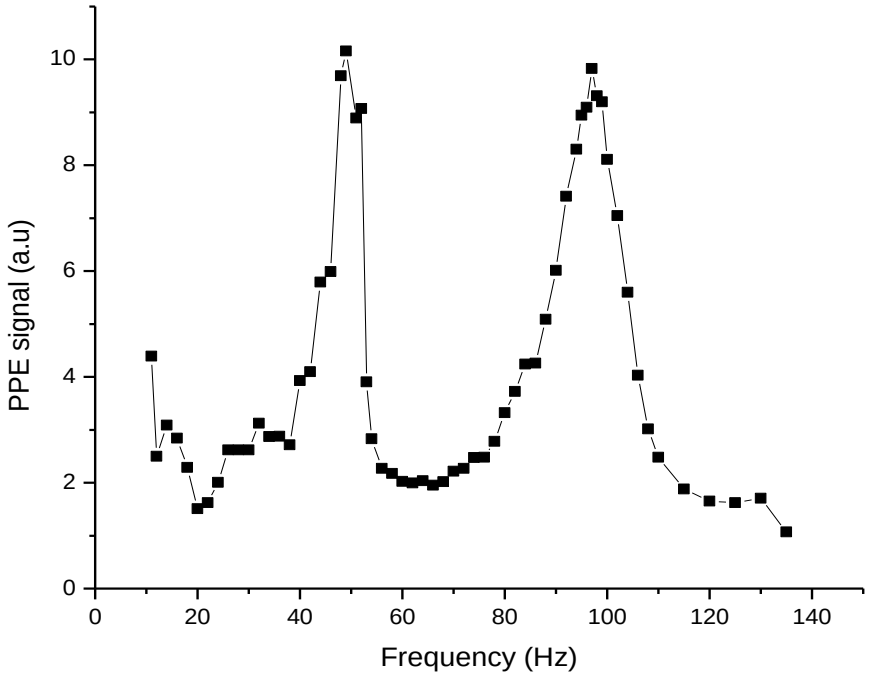

Fig 4.5a Absorption of methanol molecules versus increased in modulation frequency

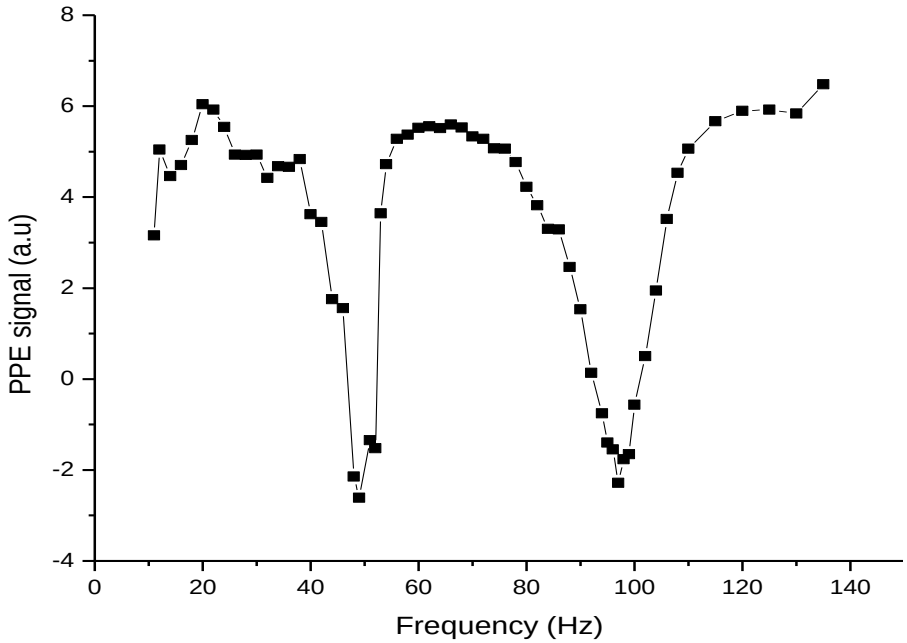

Fig 4.5b Methanol PPE signal of direct IR radiation on PVD film versus increase in modulation frequency

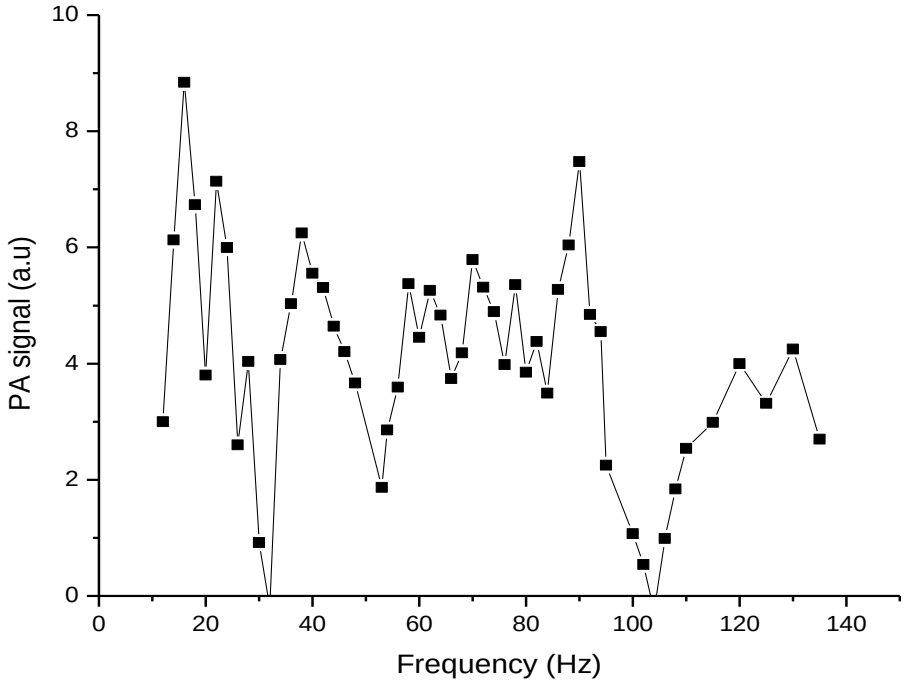

Fig 4.6 Methanol PA signal versus increased modulation frequency

FTIR absorption spectrum of liquid methanol using 5µl of the sample was shown in Fig 4.7.

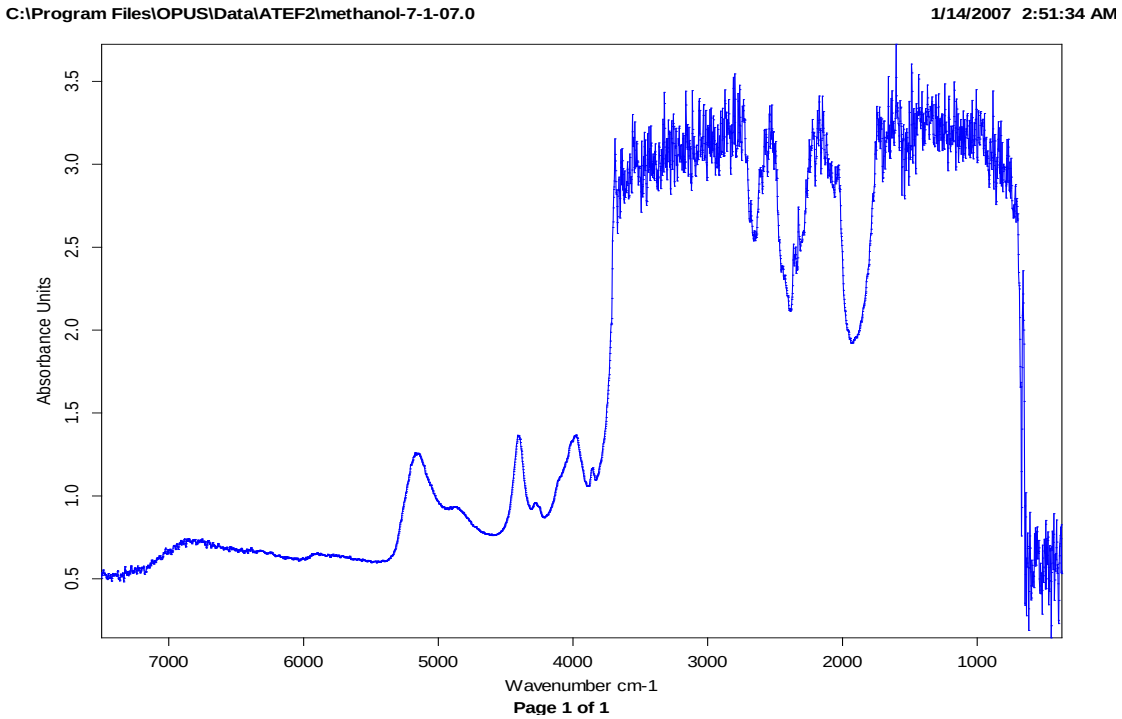

Fig 4.7 FTIR absorption spectrum of liquid methanol

4.3.2: Ethanol result

Ethanol is a volatile material that causes a gas trace that can be detected using PA technique in conjunction with a microphone. Using the new cell design of combined detection shown in Fig.3.7, the PPE and PA signals were obtained as a function of evaporation time as shown in Fig 4.8, and Fig 4.9 respectively. While the absorbed signal obtained by FTIR spectrometer using 5µl from liquid ethanol was shown in Fig 4.10.

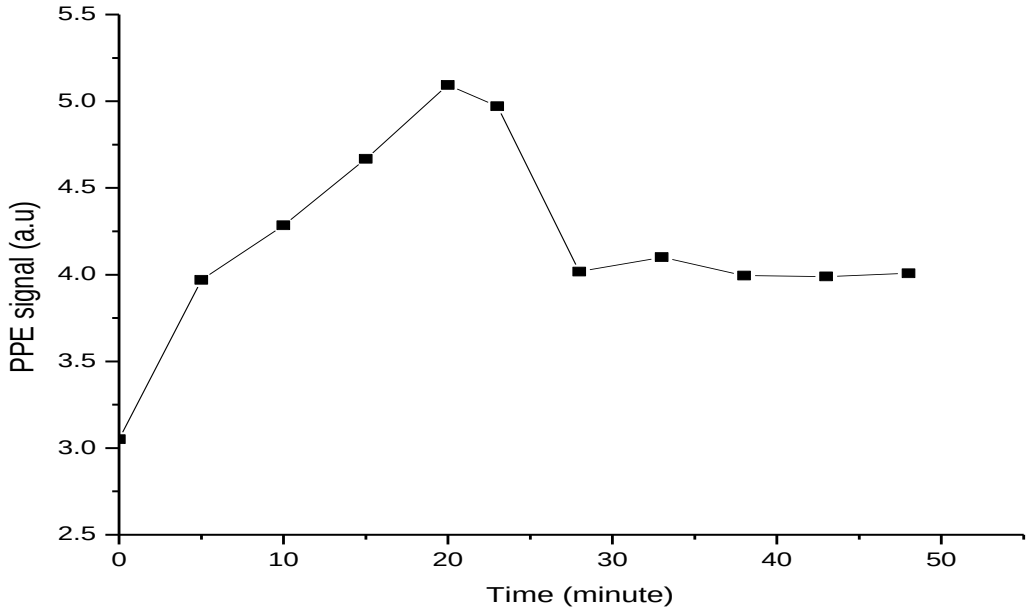

Fig 4.8 Ethanol PPE signal versus evaporation time

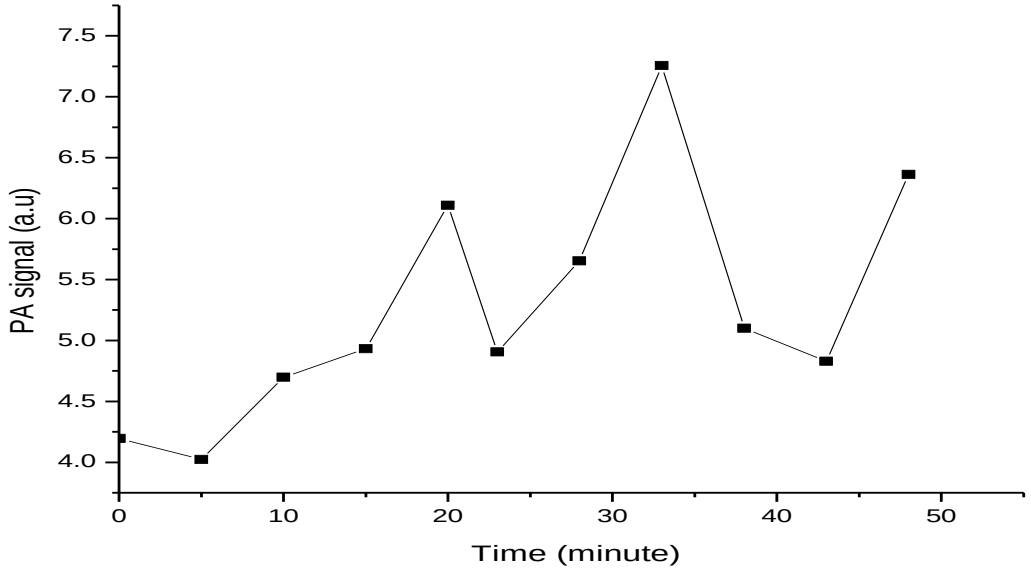

Fig 4.9 Ethanol PA signal versus evaporation time

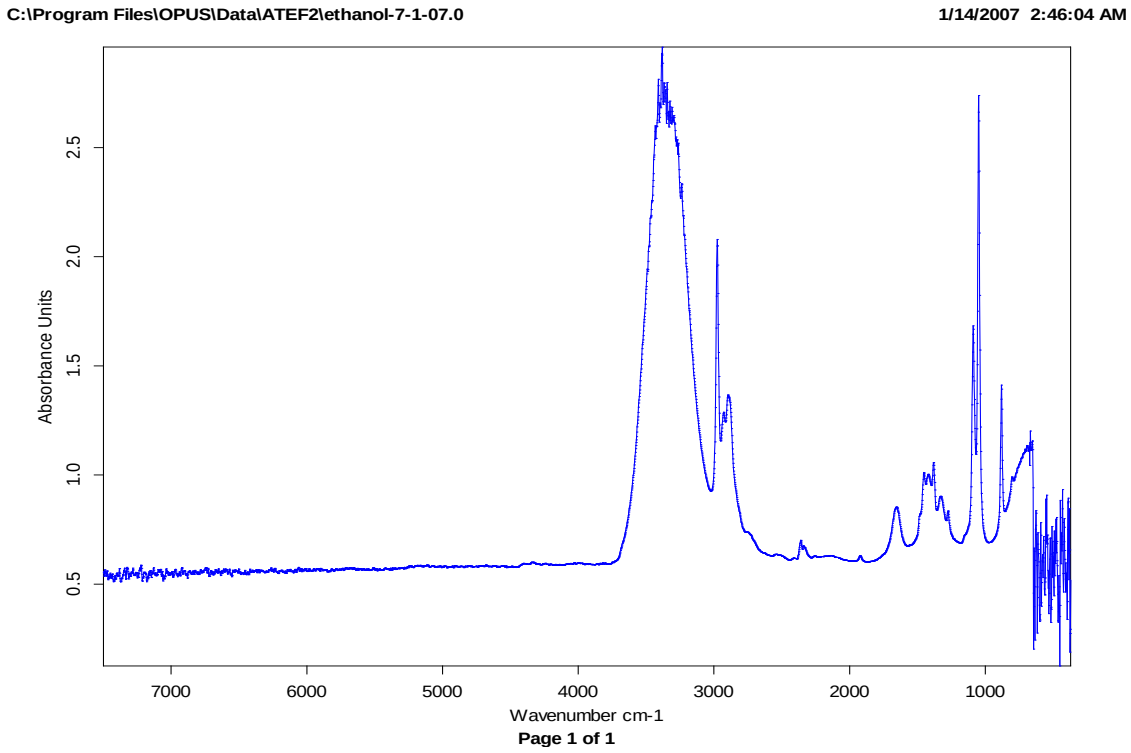

Fig 4.10 FTIR absorption spectrum for liquid ethanol

4.4 DNA data.

DNA is the genetic material that constitutes a fingerprint that helps to distinguish living organism. In this study, a PVD technique is used for the first time to distinguish samples of DNA, employing the experimental setup shown in Fig.3.6 on three stages.

The first stage is to investigate the IR absorption of the unknown DNA samples. The purpose is to test the system shown in Fig.3.6 ability to differentiate between different samples. The result is shown in table 4.2 below, these unknown DNA samples were indicated as UN1 up to UN6 without any further information about their structure.

Table 4.2: PPE signals for the unknown DNA samples

Type of DNA	Signal obtained (a.u)
UN1	3.609
UN2	5.576
UN3	2.298
UN4	0.859
UN5	2.994
UN6	3.639

The second stage was to investigate synthetic DNA samples. In this experiment, the signal is investigated against different parameters i.e. number of nucleotide, molecular weight, number of double bond, number of triple bond and CG ratio (the ratio of triple bond in DNA double strand). The results are shown in the Fig 4.11 - Fig 4.15. The purpose of this experiment is to determine the optimum parameter in DNA structure that affect the signal. The complete information about the synthetic DNA and the PCR samples are indicated in Table A1.

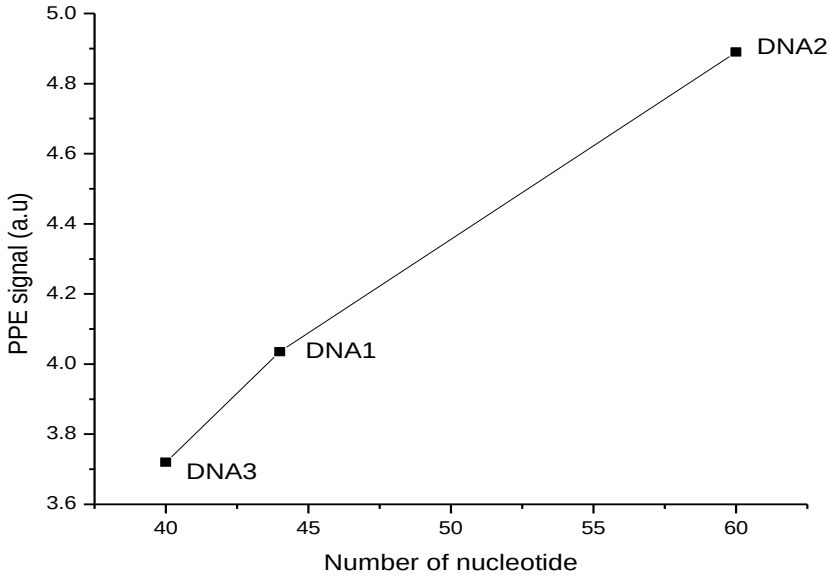

Fig 4.11 PPE signal versus number of nucleotide for three synthetic DNA samples

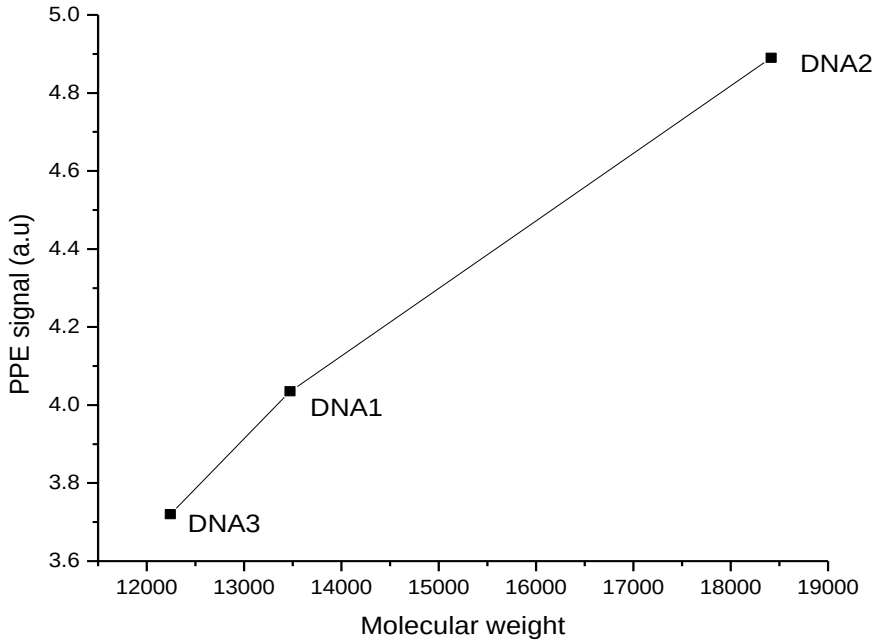

Fig 4.12 PPE signal versus molecular weight for three synthetic DNA samples

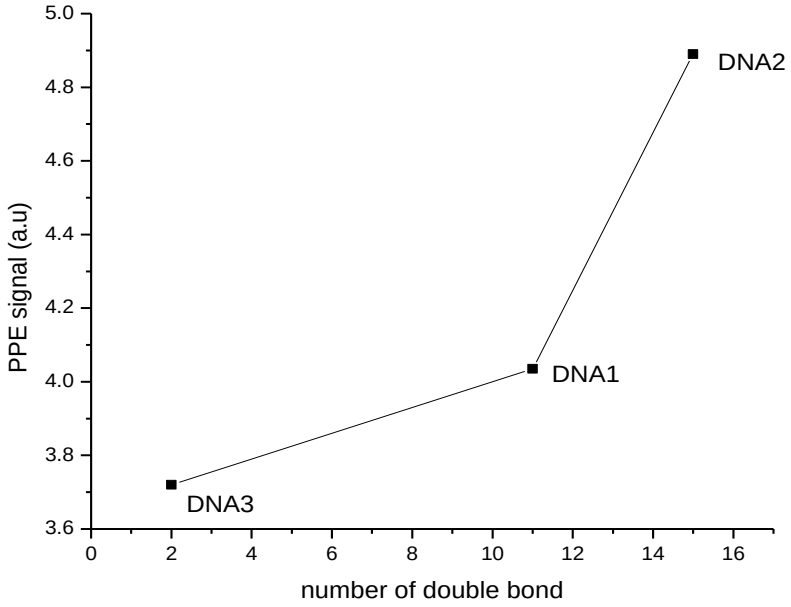

Fig 4.13 PPE signal versus number of double bonds for three synthetic DNA samples

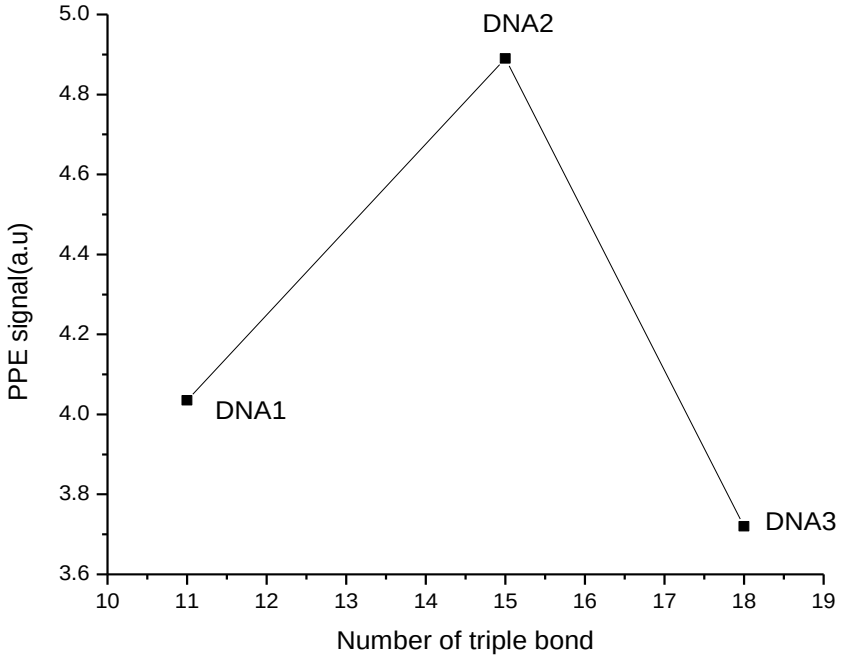

Fig 4.14 PPE signal versus number of triple bonds for the three synthetic DNA samples

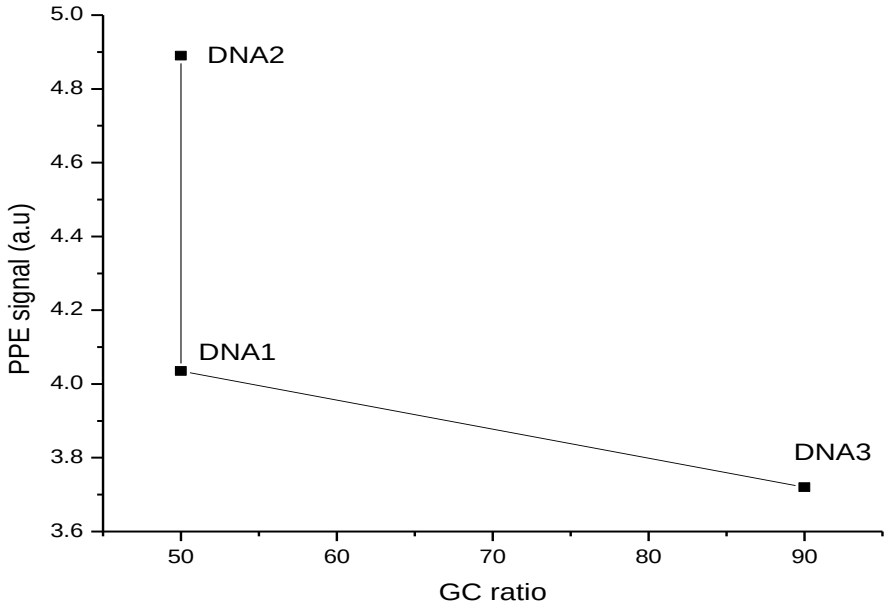

Fig 4.15 PPE signal versus GC ratio for the three synthetic DNA samples

The third stage was to investigate the additional three DNA samples of PCR products, indicated DNA121, DNA216, DNA1036, with known length and sequences (table A1). The

relation between the absorbed PPE signal and the number of nucleotide was plotted for these three DNA samples and the three synthetic ones as shown in Fig 4.16.

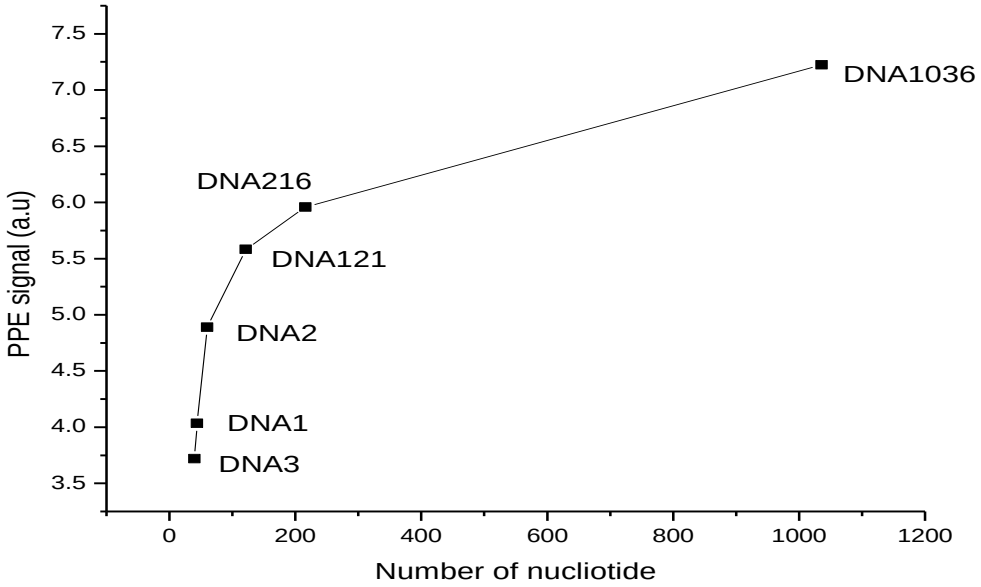

Fig 4.16 PPE signal versus number of nucleotide for the three synthetic DNA samples and the three DNA samples of PCR products (see table C1)

Finally, the DNA samples were investigated using FTIR spectrometer and the results are shown in Fig 4.17 to Fig 4.20.

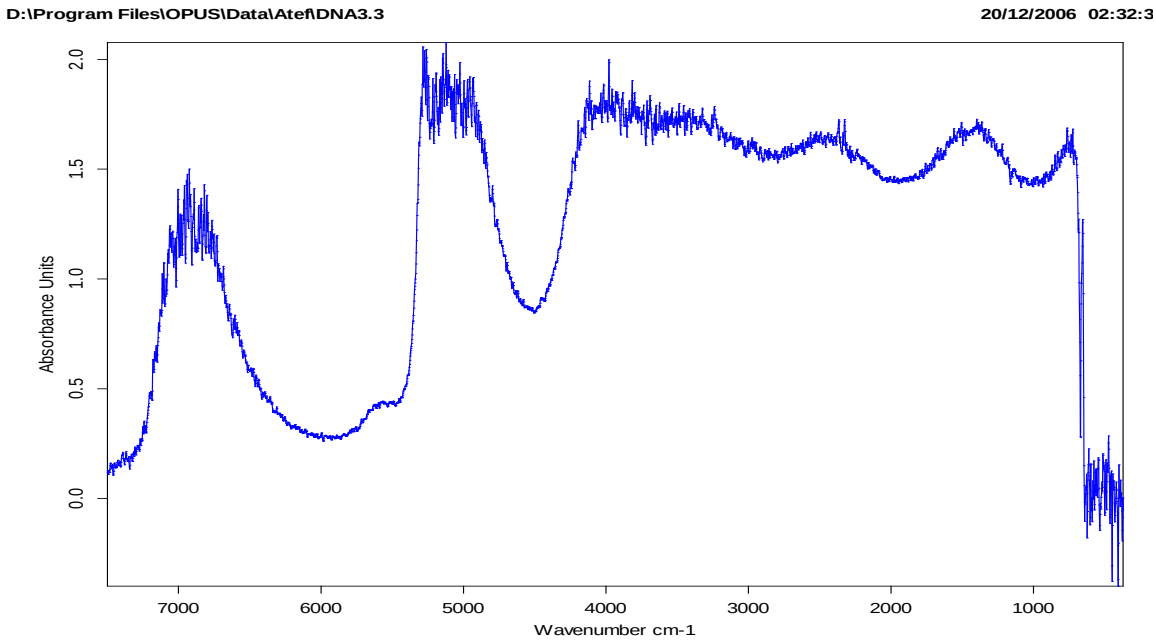

Fig 4.17 FTIR absorption spectrum of DNA1 sample

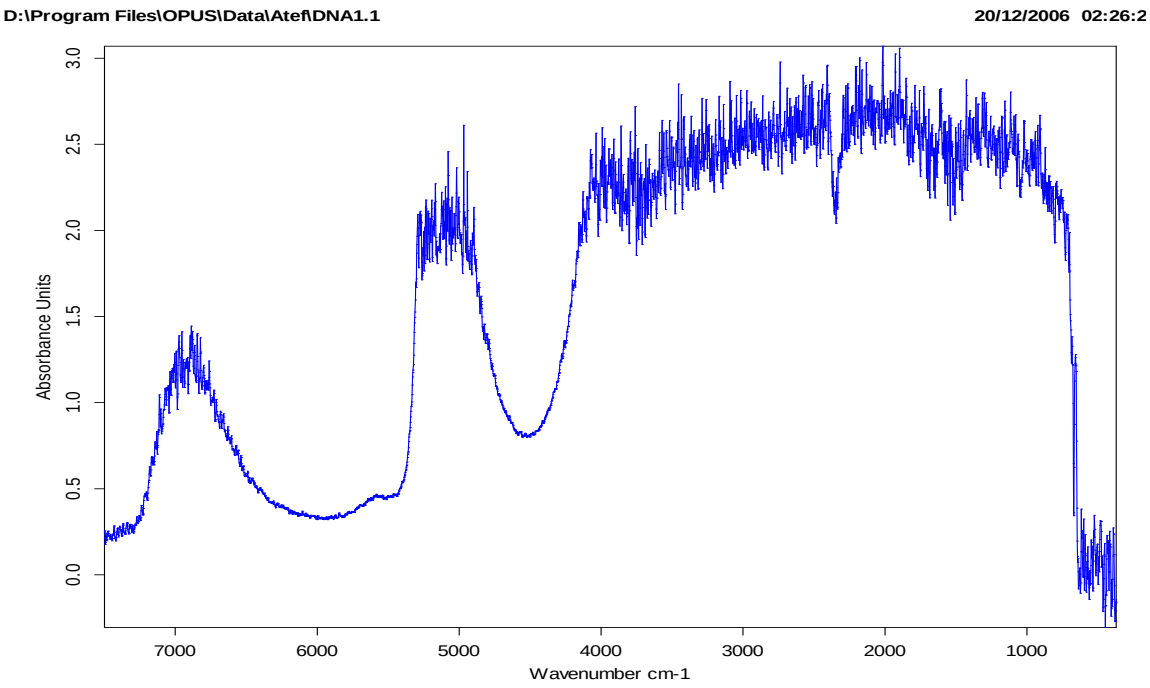

Fig 4.18 FTIR absorption spectrum of DNA2 sample

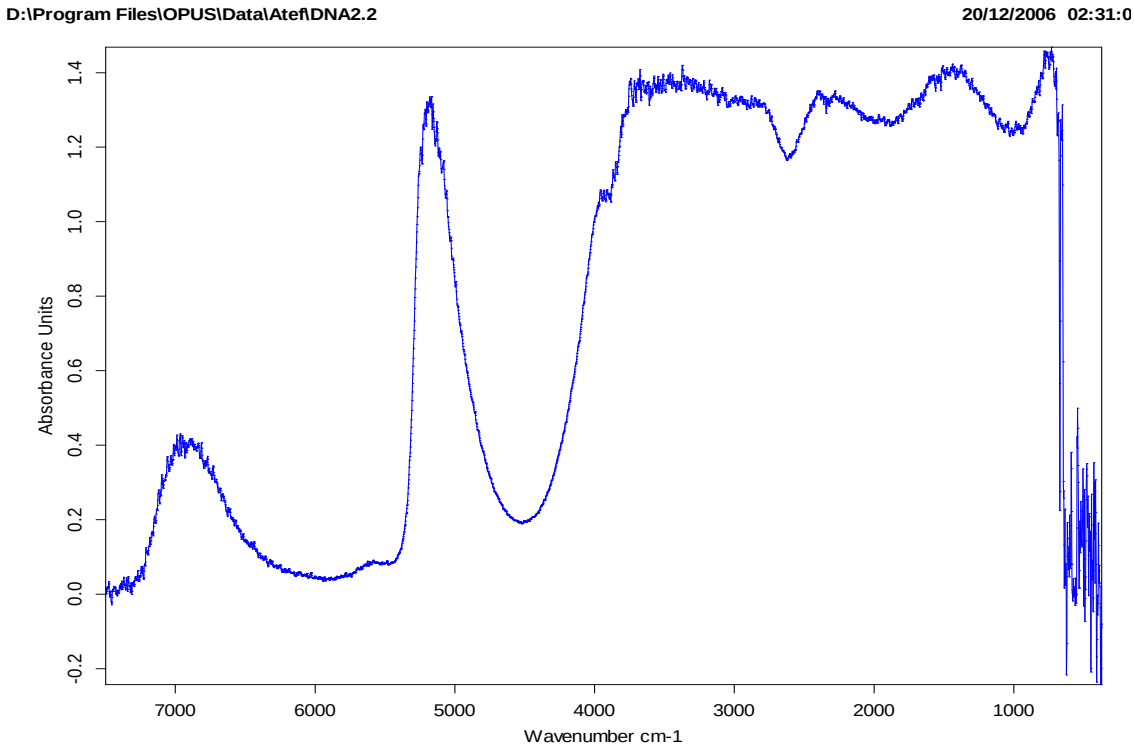

Fig 4.19 FTIR absorption spectrum of DNA3 sample

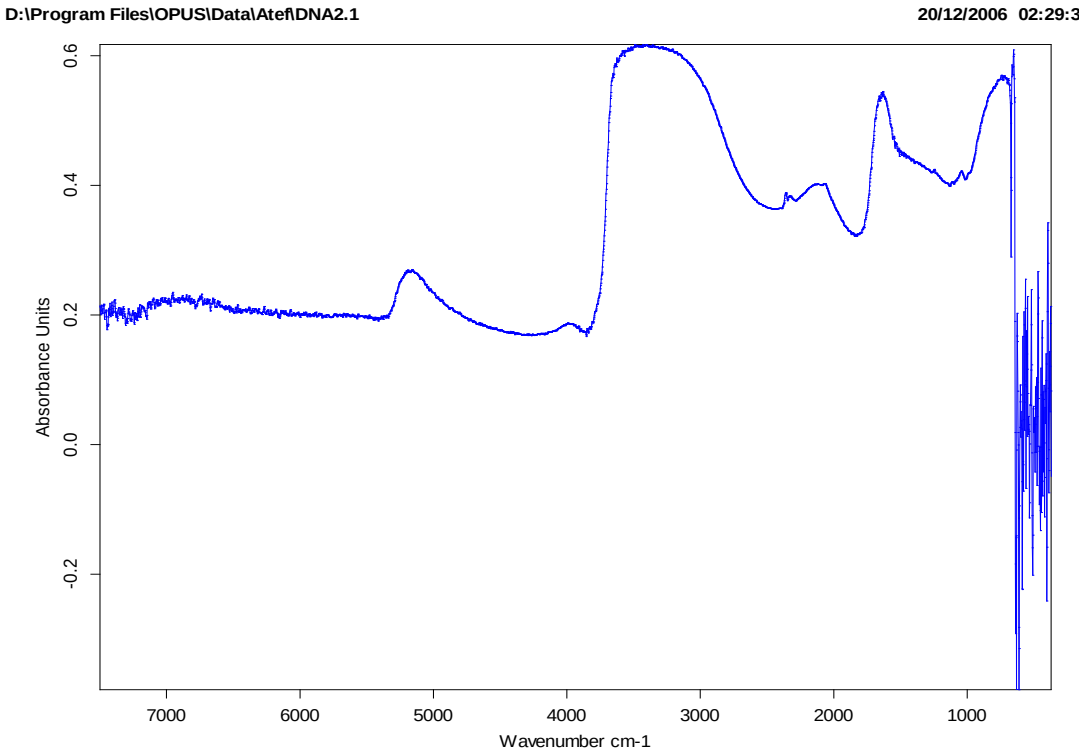

Fig 4.20 FTIR absorption spectrum of DNA121 sample

4.5 Essential oil results

The three essential oils and the plant tissue used to produce them were investigated by the simultaneous PPE and PA technique using the system shown in Fig 3.7. Diluted rose and jasmine oils at different purities are investigated and compared for simultaneous PPE and PA signals.

4.5.1: Results for Jasmine oil and flower

Pure jasmine oil and 0.03 g from jasmine flower are investigated for possible signal correlation. Different purities of jasmine oil were also studied and the results are indicated

for PA and PPE signal on the Fig 4.21 - Fig 4.28. The different experimental conditions are made clear in the figure captions.

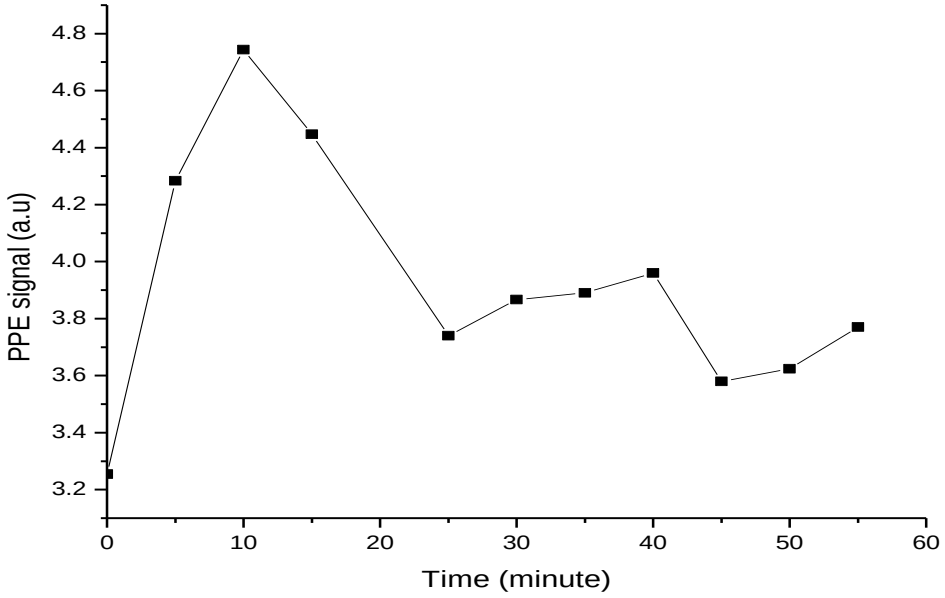

Fig 4.21 PPE signal from 0.03g jasmine flower versus evaporation time

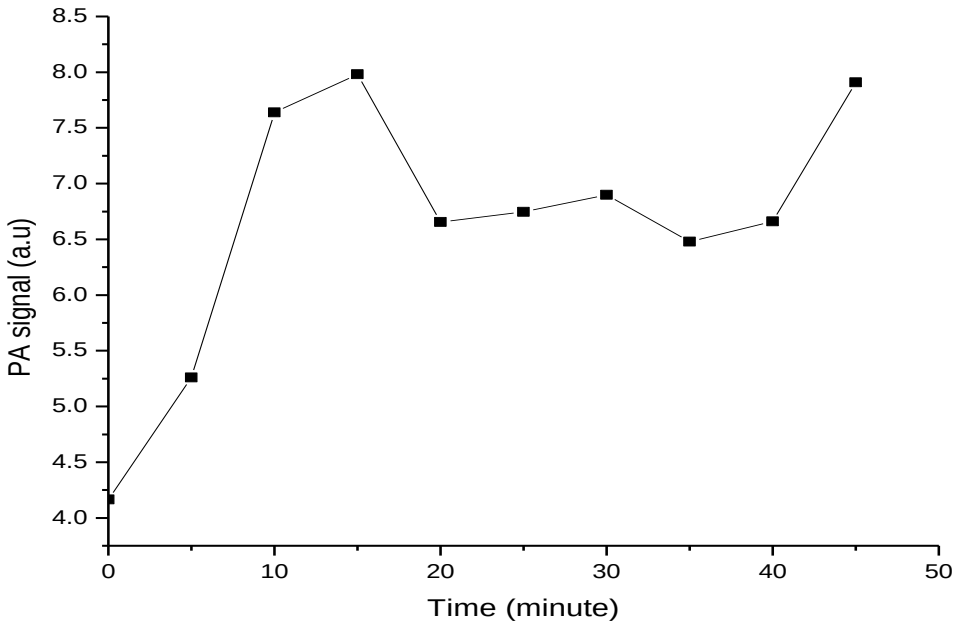

Fig 4.22 PA signal from 0.03g jasmine flower versus evaporation time

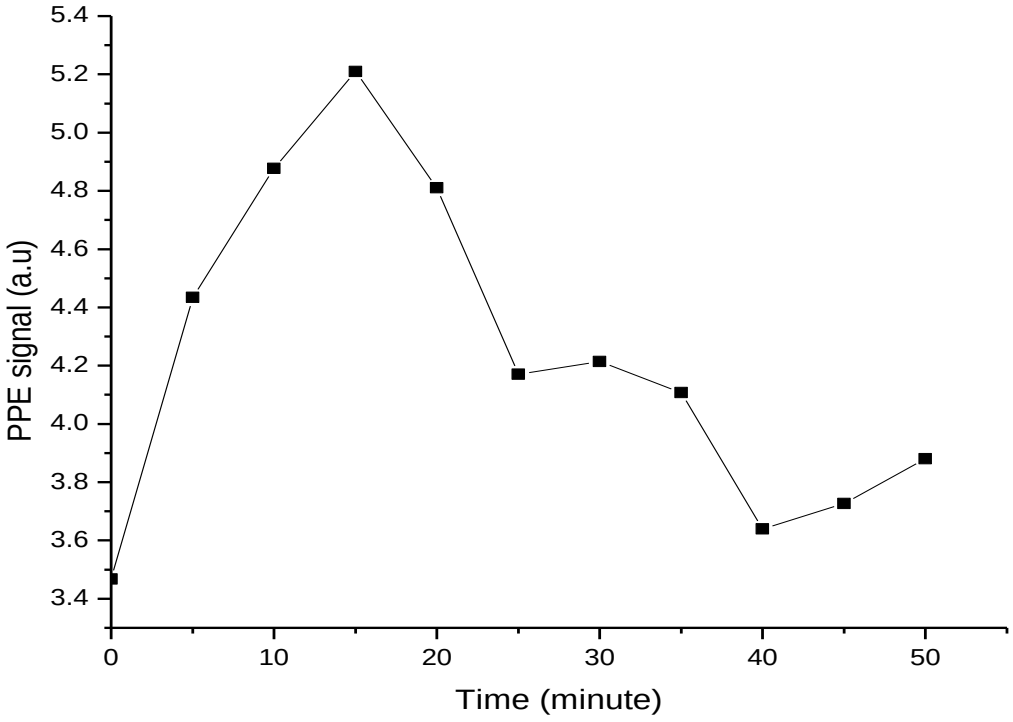

Fig 4.23 PPE signal for pure jasmine oil versus evaporation time

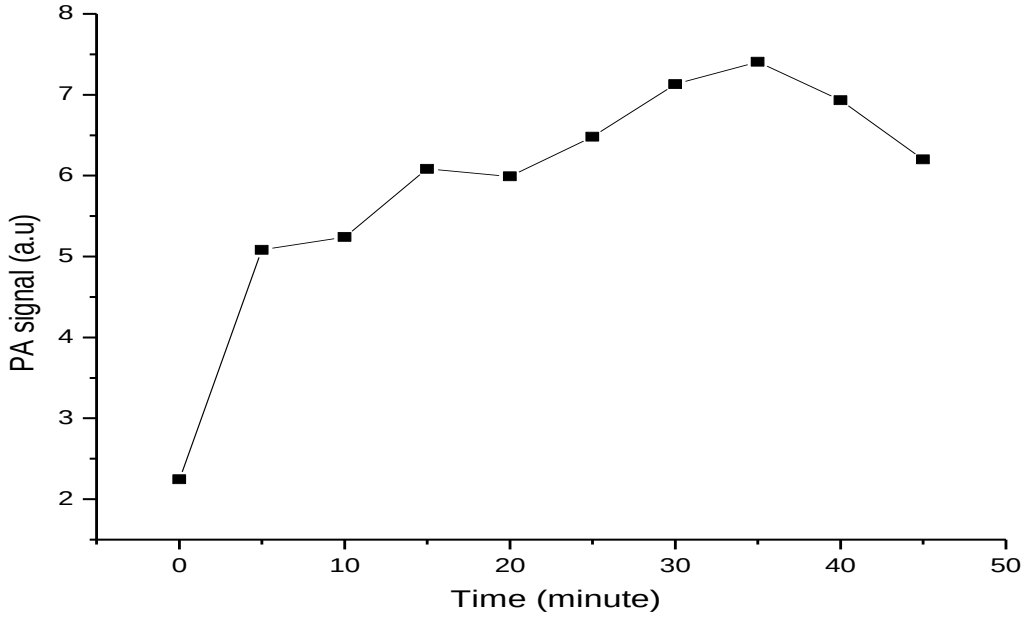

Fig 4.24 PA signal for pure jasmine oil versus evaporation time

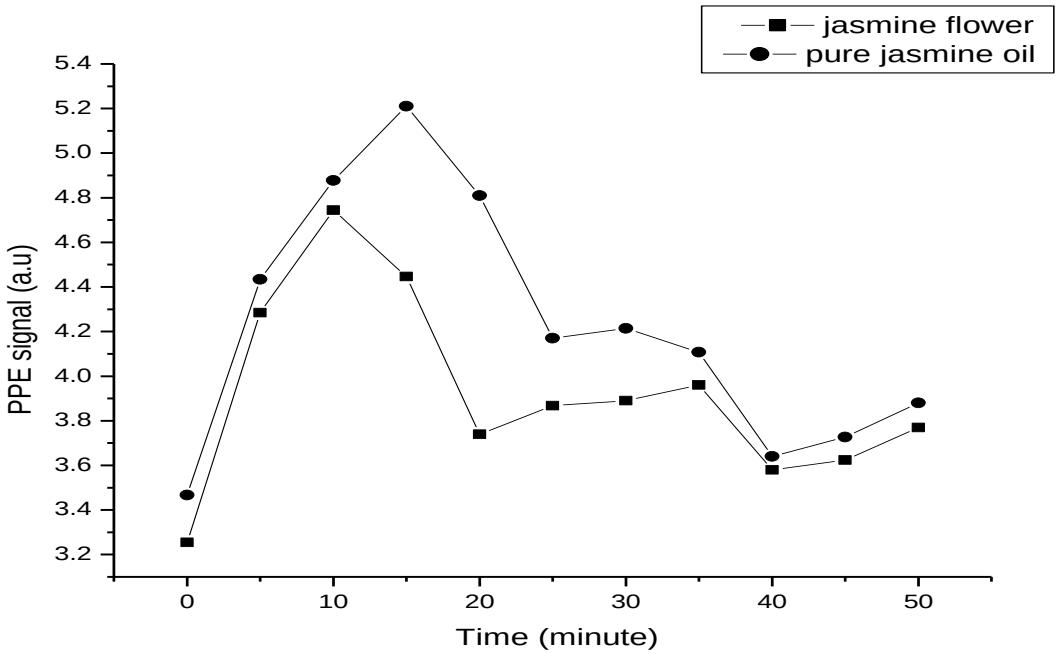

Fig 4.25 PPE signal versus evaporation time for jasmine flower using 0.03g and pure jasmine oil

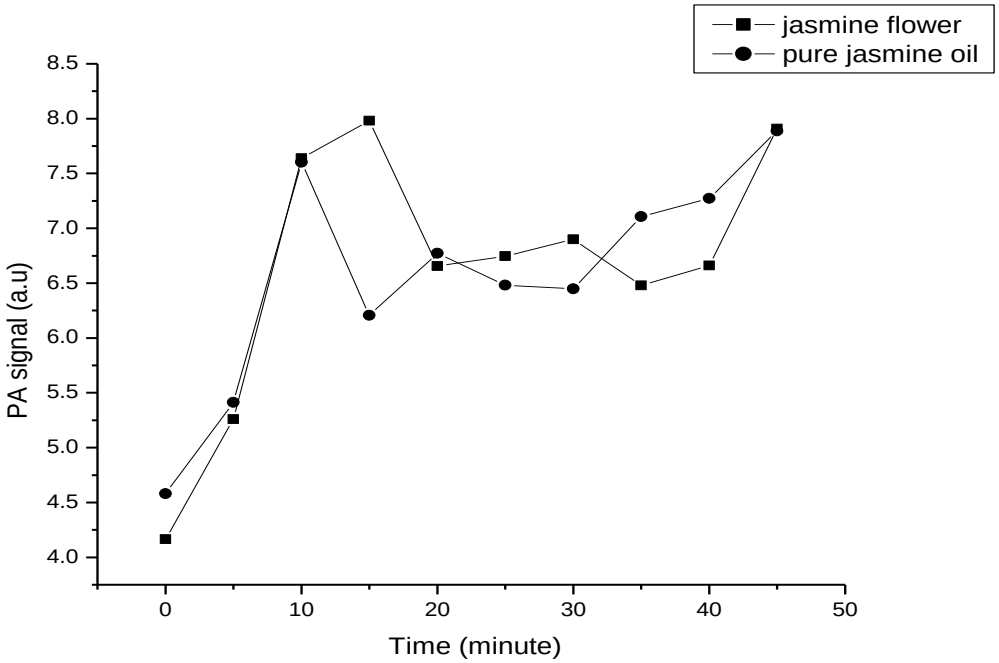

Fig 4.26 PA signal versus evaporation time for jasmine flower using 0.03g and pure jasmine oil

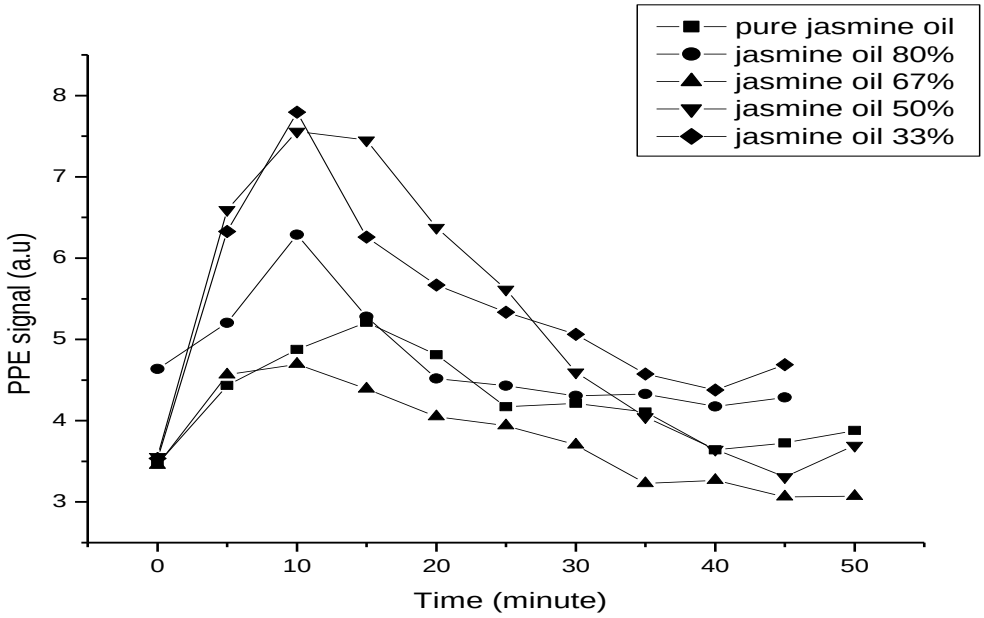

Fig 4.27 PPE signal versus evaporation time for jasmine oil at different purities

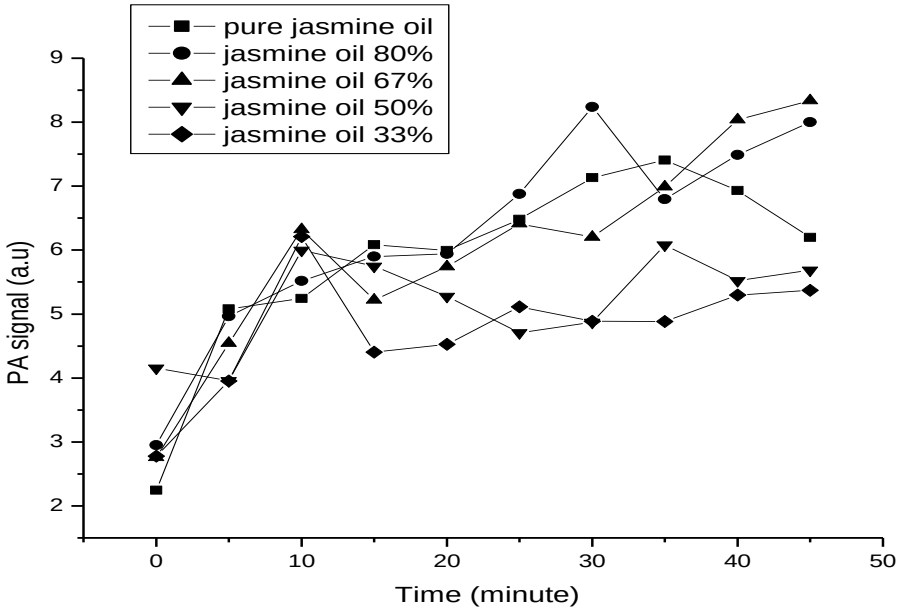

Fig 4.28 PA signal versus evaporation time for jasmine oil at different purities

Using the FTIR spectrometer the investigation was carried out for 5µl from the oil and the result was shown in Fig 4.29.

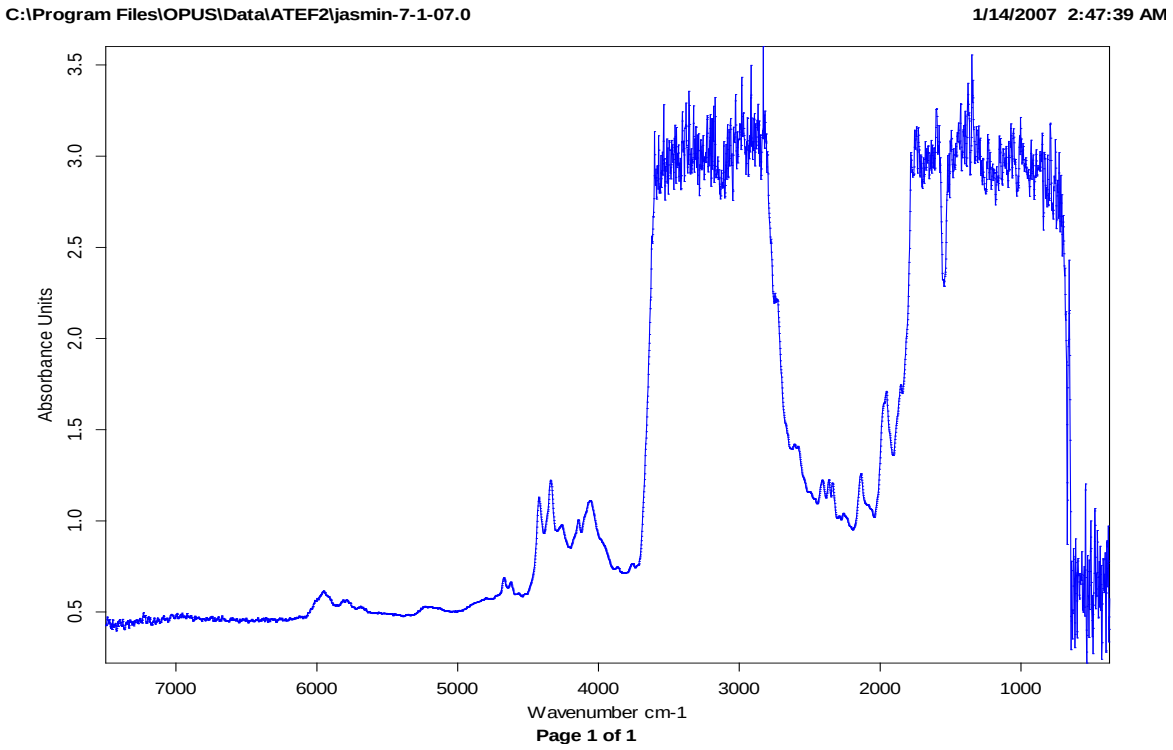

Fig 4.29 FTIR absorption spectrum for pure jasmine oil

4.5.2: Result for Damask rose and oil

In this part of the experiment the rose oil at different purities and rose flower are also investigated in the same manner and the results are in Fig 4.30 – Fig 4.37, with different experimental conditions made clear in the figure captions.

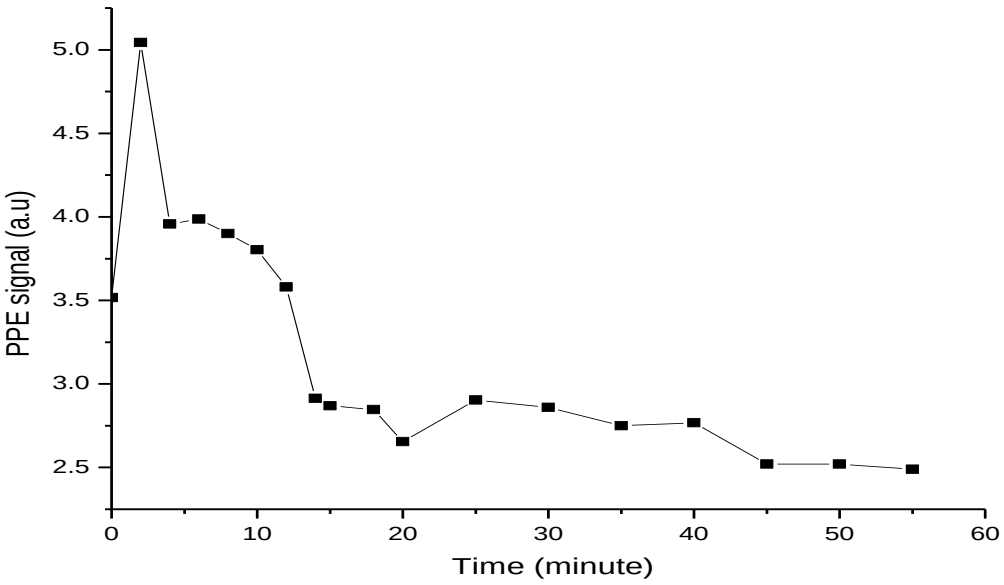

Fig 4.30 PPE signal from 0.03g rose flower versus evaporation time

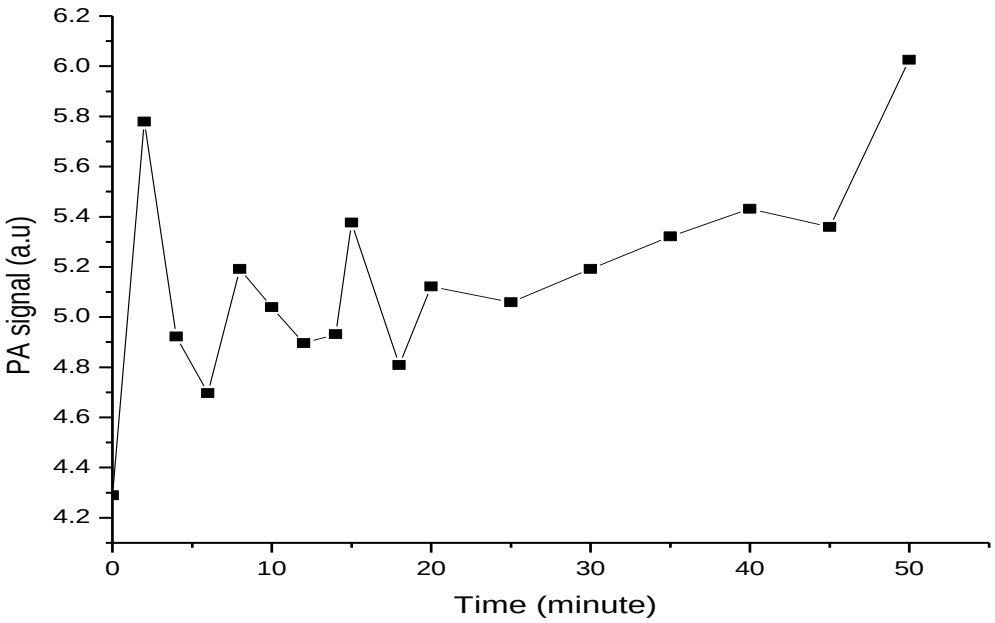

Fig 4.31 PA signal from 0.03g rose flower versus evaporation time

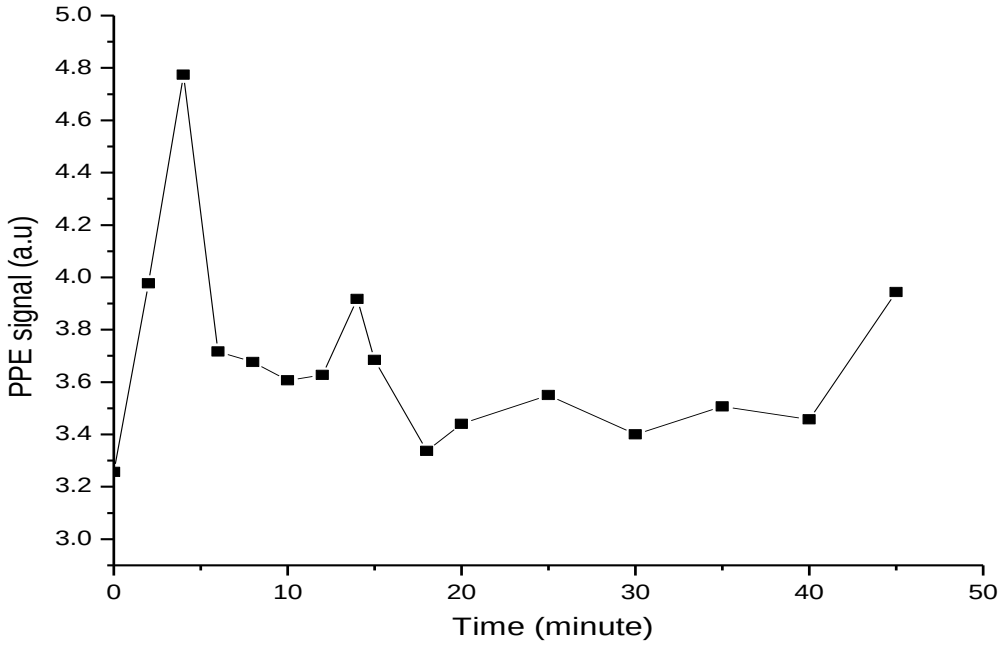

Fig 4.32 PPE signal for pure rose oil versus evaporation time

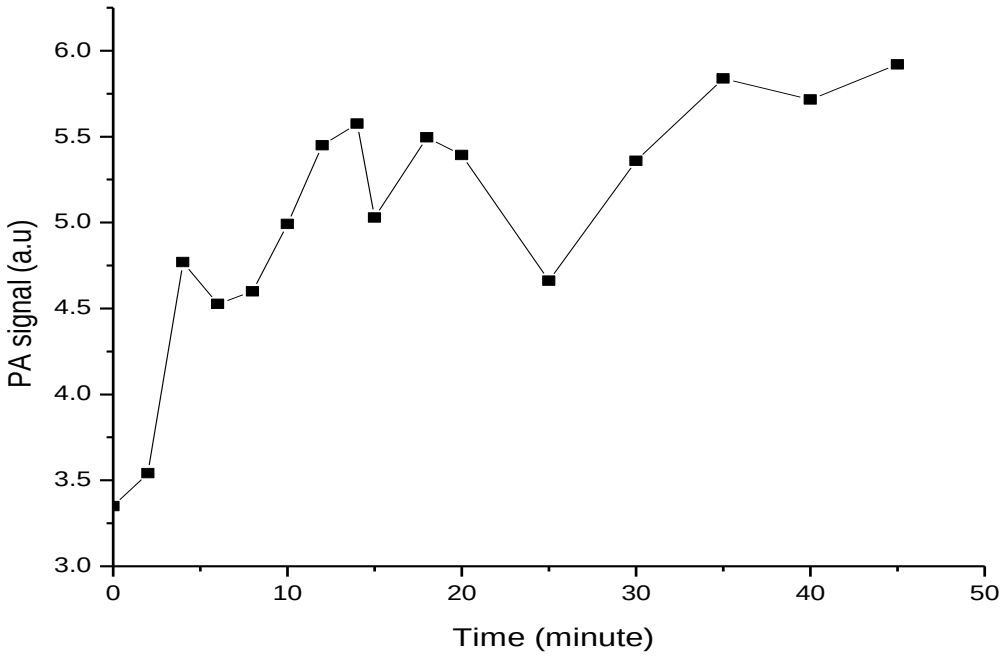

Fig 4.33 PA signal for pure rose oil versus evaporation time

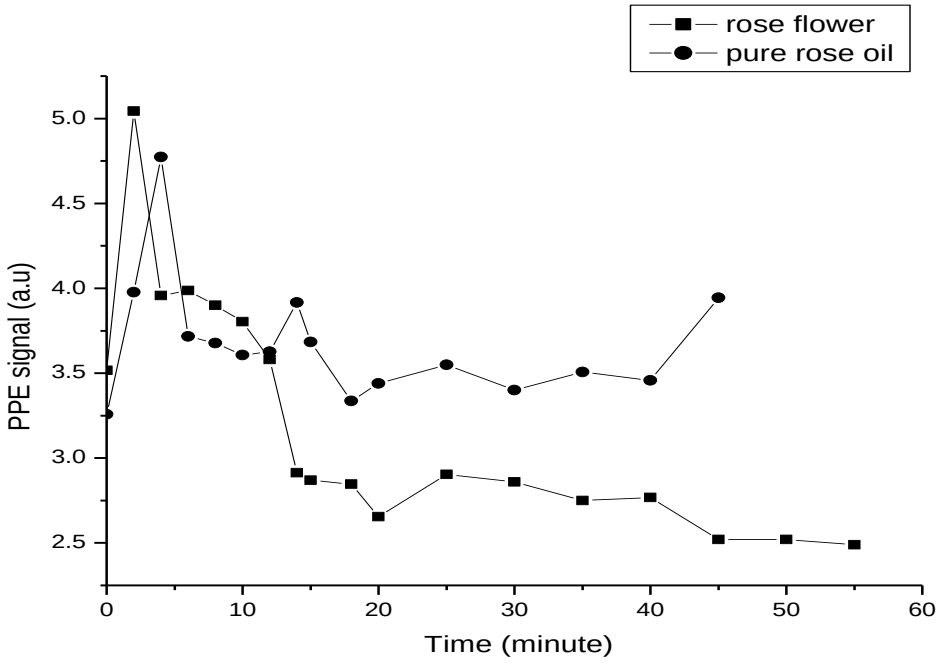

Fig 4.34 PPE signal versus evaporation time for rose flower using 0.03g and pure rose oil

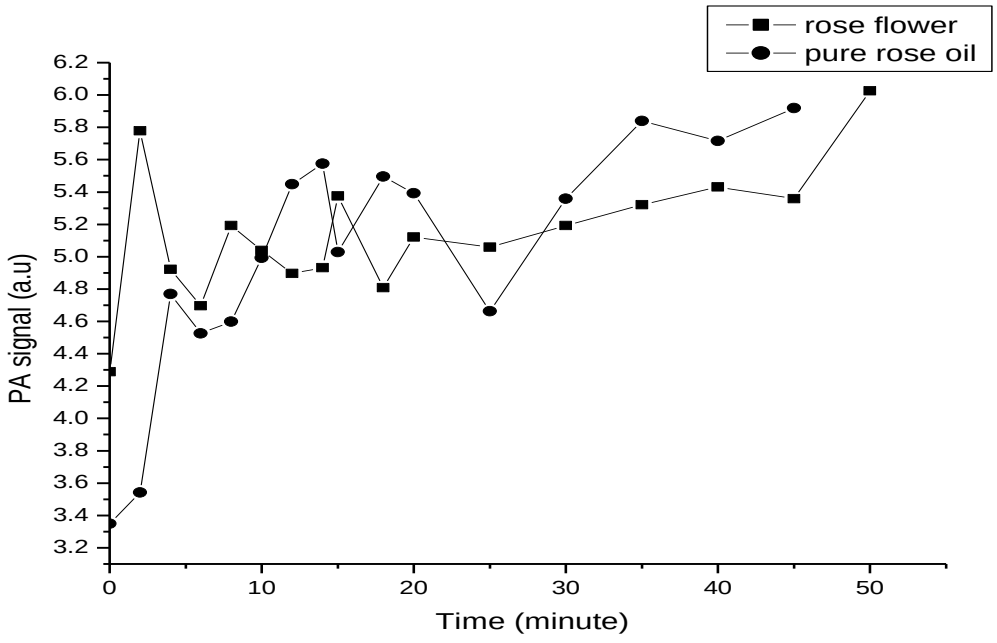

Fig 4.35 PA signal versus evaporation time for rose flower using 0.03g and pure rose oil

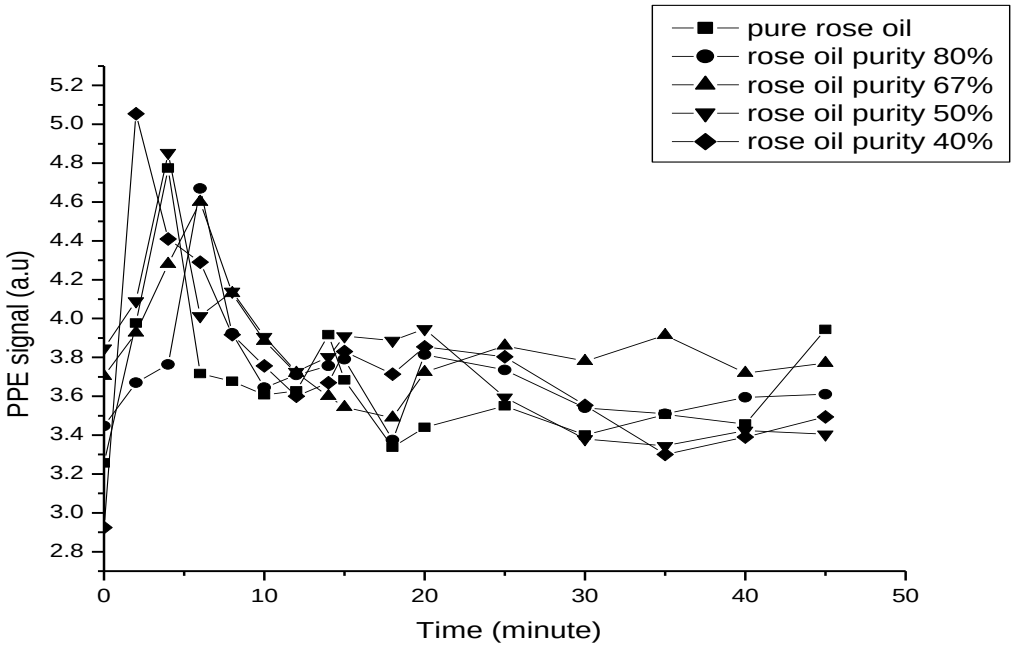

Fig 4.36 PPE signal versus evaporation time for rose oil at different purities

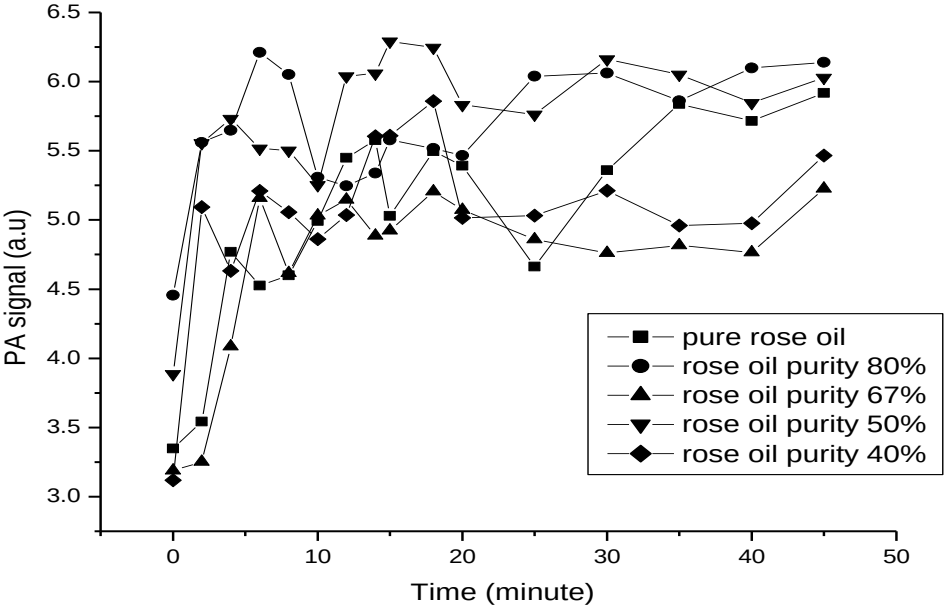

Fig 4.37 PA signal versus evaporation time for rose oil at different purities

FTIR spectrum of rose oil in the liquid phase using 5µl from the sample is shown in Fig 4.38

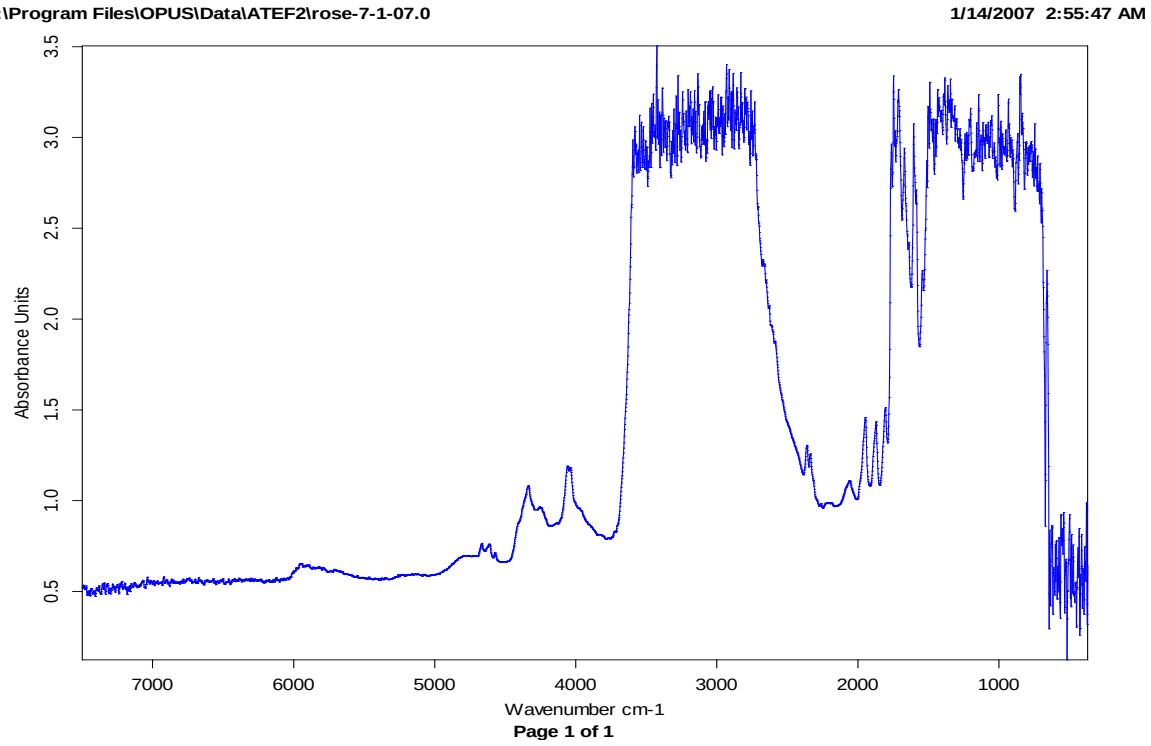

Fig 4.38 FTIR absorption spectrum for pure rose oil

4.5.3: Results for mint's oil and leaves

Finally the same procedure was performed for mint leaves when dried or from the garden, and for it's oil. The obtained results are shown in figures 4.39 and 4.40 with the different experimental conditions are indicated.

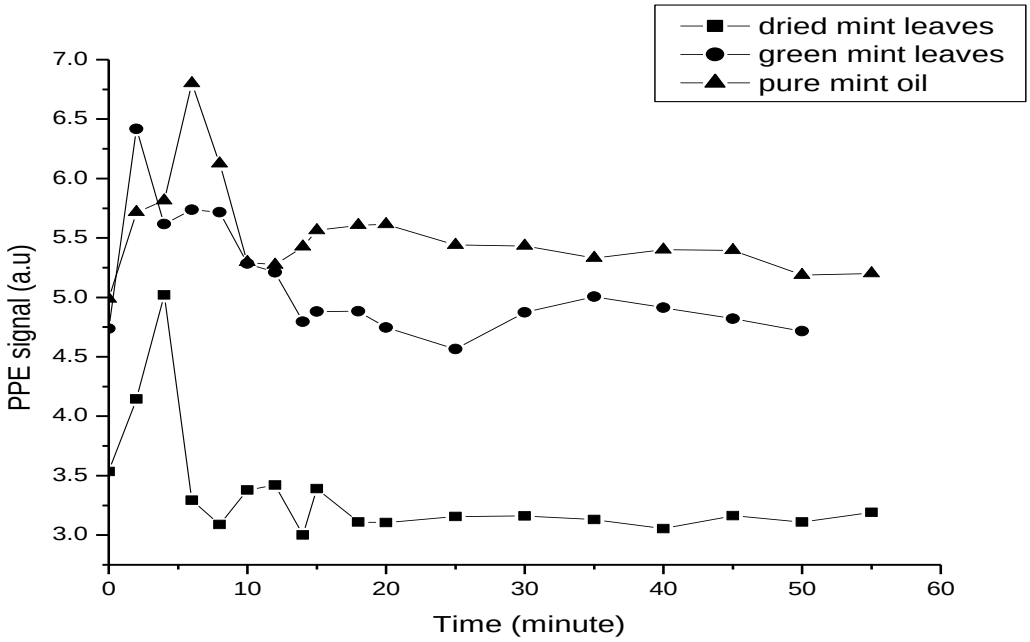

Fig 4.39 PPE signal versus evaporation time for dried and green mint leaves using 0.03g from each and pure mint oil

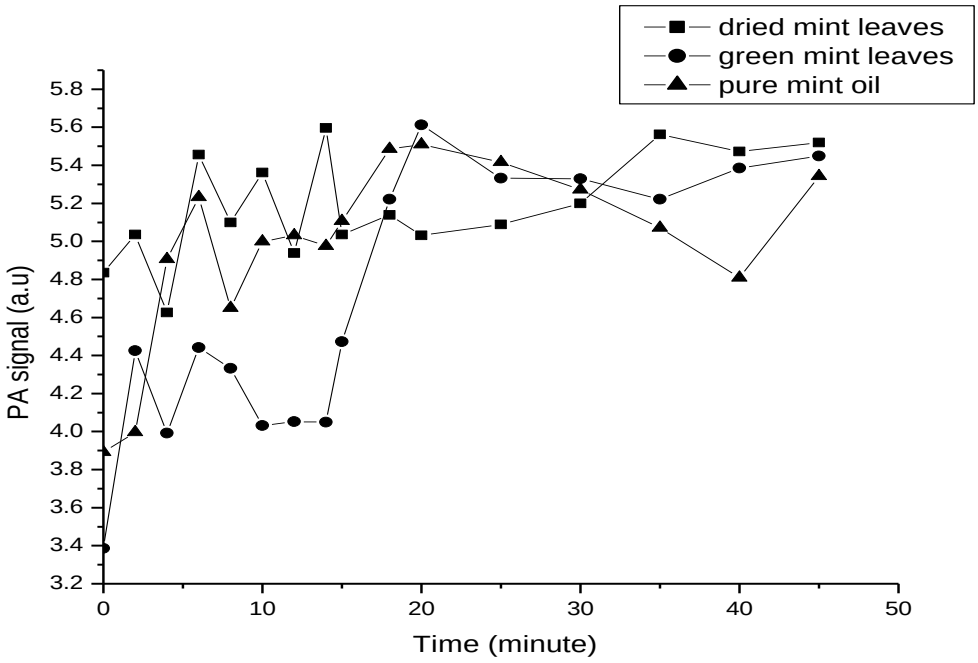

Fig 4.40 PA signal versus evaporation time for dried and green mint leaves using 0.03g from each and pure mint oil

The absorbed signal for mint oil in the liquid phase using 5µl form the sample, by the FTIR spectrometer was shown in Fig 4.41.

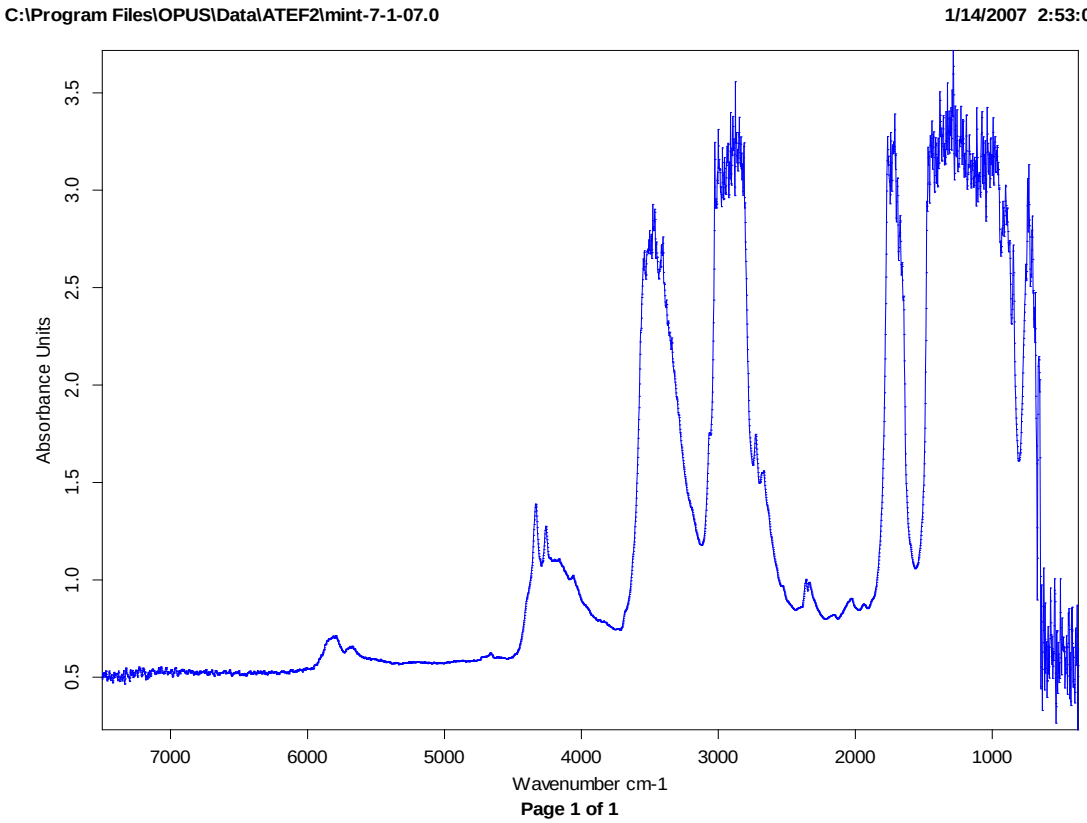

Fig 4.41 FTIR absorbance for pure mint oil

Comparing the PPE and PA signals for rose, jasmine flower and mint leaves and their corresponding oils with time were shown in the Fig 4.42 to Fig 4.45.

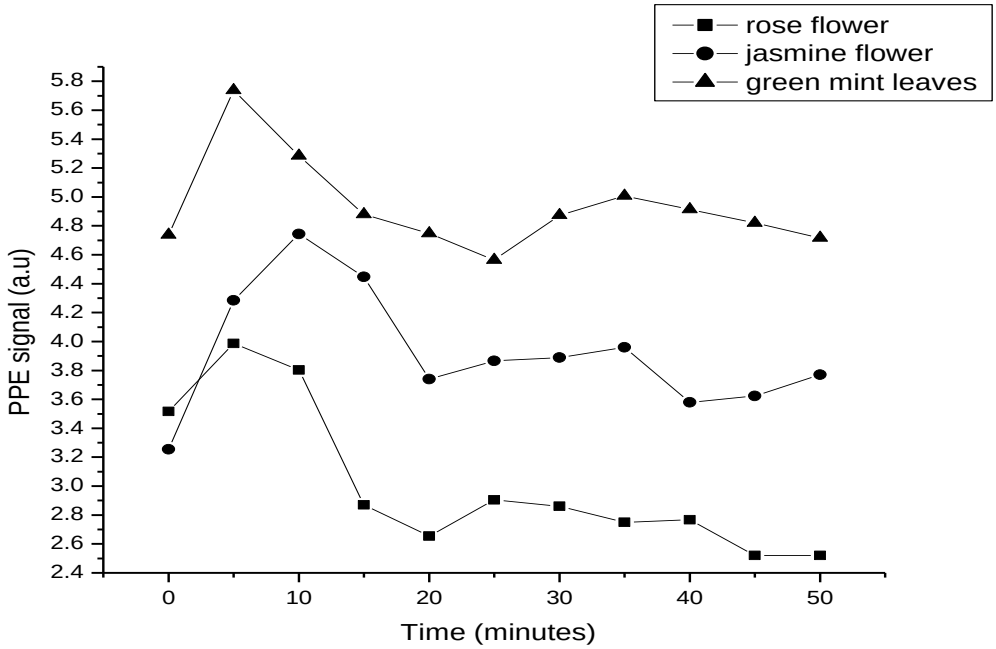

Fig 4.42 PPE signal for jasmine and rose flowers and mint leaves versus evaporation time

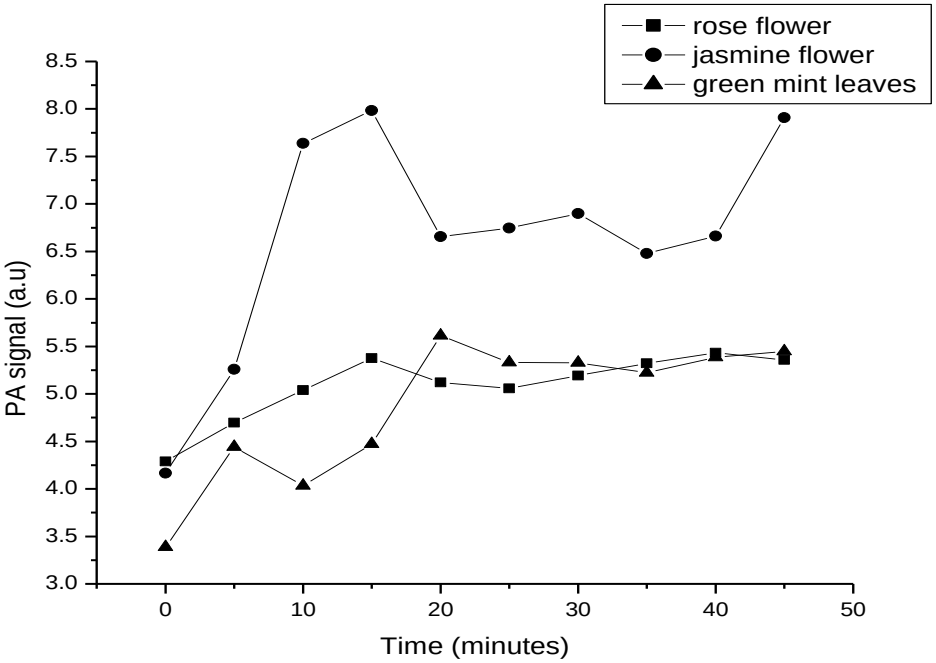

Fig 4.43 PA signal for jasmine and rose flowers and mint leaves versus evaporation time

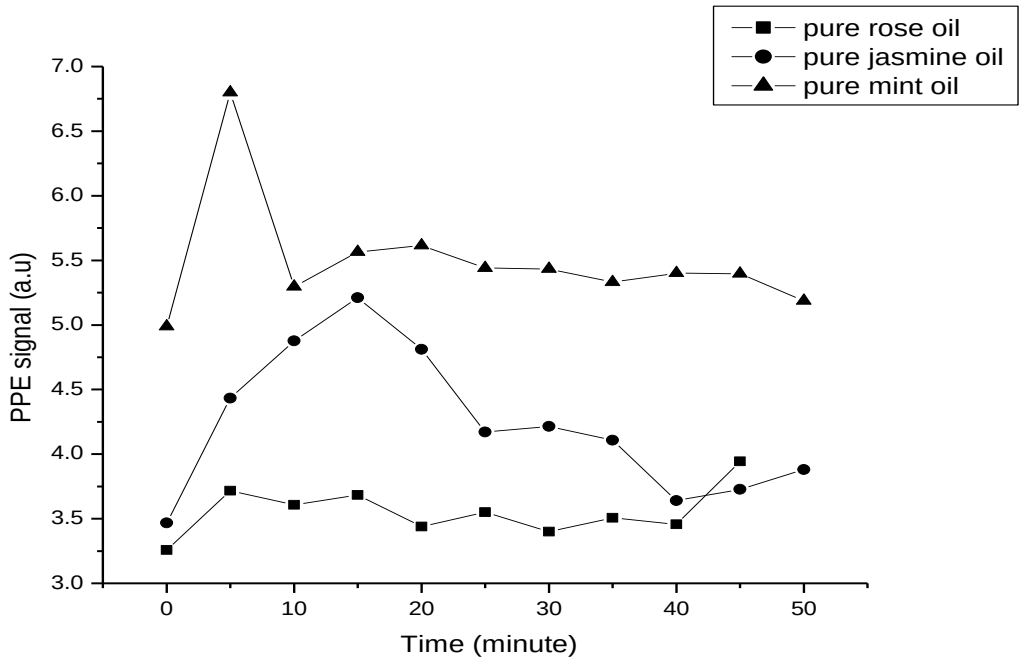

Fig 4.44 PPE signal for pure rose, jasmine and mint oils versus evaporation time

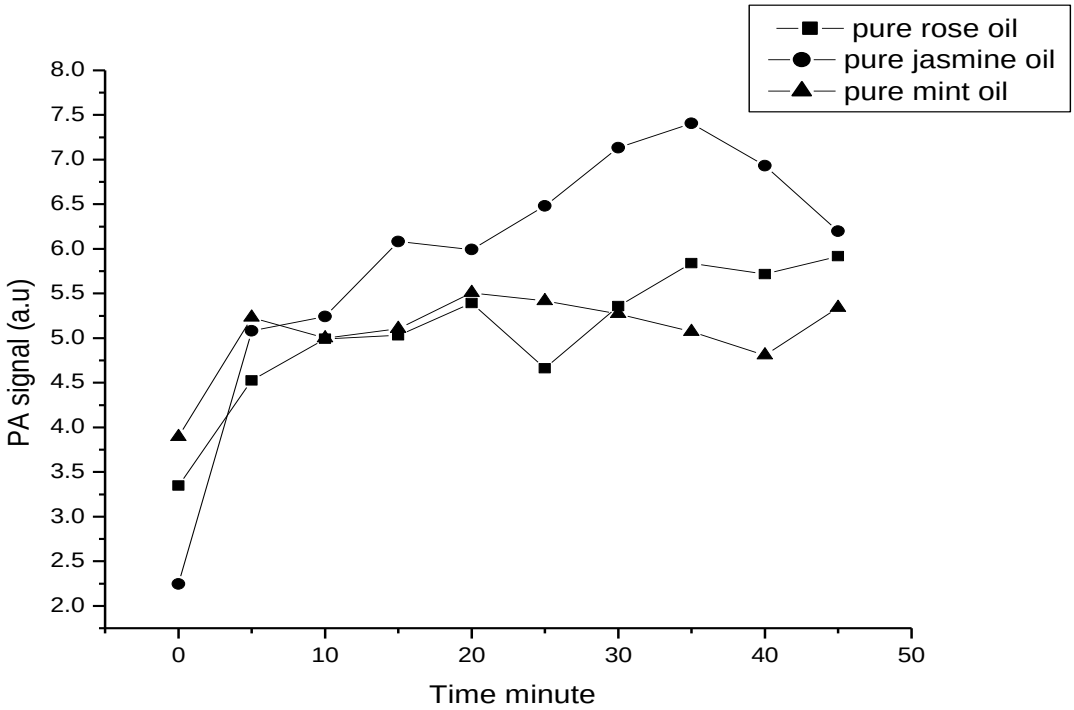

Fig 4.45 PA signal for pure rose, jasmine and mint oils versus evaporation time

Chapter 5

Discussion

5.1 Introduction

In this chapter, the data obtained from the experiment are discussed along two paths: One involves results of DNA samples using PVD sensor to correlate the PPE signal to the structural parameters. The second involves the combined PPE-PA results comparing PA signals with previously known results. PA results were then compared with the PPE signal obtained simultaneously in the combined PPE-PA cell. Both PA and PPE signals were monitored as a function of evaporation time. The samples used are allowed to absorb broadband IR radiation from a pulsed source in two ways: the samples placed on top of the PVD film, absorb radiation in the liquid form. Essential oils and plant part samples absorb radiation by their trace gas emissions. The experiments described here depend on the band absorption in the region 5000-1000 cm^{-1}, and therefore FTIR absorption spectra were also measured for comparison.

Chemical bonds have specific frequencies at which they vibrate. These frequencies and corresponding energy levels are determined by the shape of the molecular potential energy surfaces, the masses of atoms and eventually by the associated vibronic coupling. The vibrational mode in a molecule is associated with changes in the permanent dipole. The resonant frequencies can be related to the strength of the bond and the mass of the atoms at either end of it. Thus, the frequency of vibrations can be associated with a particular bond type (http://www.answers.Com/topic/infrared-spectyroscopy-correlation, October 2006). Infrared radiation causes covalent bonds to vibrate by stretching and contracting. The part of the infrared spectrum absorbed by the molecules depends on the strength of the chemical bond. Therefore for molecules with different kinds of bond (e.g. a C-H and a C=O), one would expect to see at least two different absorption bands. The amount of absorbed radiation is given by the Beer-Lambert law (Nell, Hons, 2000). The appearance of several absorption peaks is common for a high number of double and triple bond systems. The absorption peaks are often solvent dependent, as shown in the FTIR spectra. Vibrational fine structure is most pronounced in vapor phase spectra, but becomes broadened and sometimes obscured in a solution (http://www.cem.msu.edu /UV-Visible Spectroscopy, Visible and Ultraviolet Spectroscopy, October 2006). In the present study, PVDF and/or the combined PPE-PA are aimed at a collective signal that is used as a technique to differentiate between different samples. This strong dependence of spectra on the structure is used to establish a simple spectroscopic technique that reduces cost of using expensive optical components and laser sources.

5.2 Combined PPE-PA detection

The new technique combining PA and PPE measurement is used to carry out simultaneous detection by a PVD sensor and microphone. Liquid samples are left for some time to evaporate in the cell before radiation is allowed in, to insure that the resulting signals are determined by trace gas.

5.2.1: Methanol results

Methanol absorbs in the range "5000 to 667" cm^{-1} (Earle, Plyler, 1952). The bands appear to have been attributed to the O —H, C —H, C —O, and C —C vibrations within the molecules. Several weak bands have been observed in Fig 4.7, which can be classified as fundamentals and combinations. The intense absorptions of methanol occur near 3704, 2941,1346, 1333, and 1042 cm^{-1} which are attributed to the O - H and C - H stretching, O – H and C - H bending and C —O stretching vibrations, respectively. A further general confirmation results in many weak peaks between "1667 to 1000" cm^{-1}. Combinations of the O—H twisting with the C—O stretching and the CH_3 rocking vibrations might well give rise to the complicated structure between 1515 and 1087 cm^{-1} (Earle, Plyler, 1952).

Fig 4.1b shows the signals of the direct IR radiation reaching the PVD film, where there is a decrease in the signal with increasing the methanol vapor in the pipe, since this will reduce direct radiation reaching PVD film, while in Fig 4.1a methanol vapor absorption show an increase in the absorbed radiation by increasing the concentration of trace gases as determined by Beer-Lambert law. Conversely, the PA signal of Fig 4.2 shows two peaks the second is of greater magnitude, due to resonance detection. This is because the mid-infrared radiation used (approx. 4000-400 cm^{-1}) causes fundamental vibrations and associated rotational-vibrational

structure which is expected to increase with concentration, and the resonant frequency occurs depending on the shape of the molecular potential energy surfaces, the masses of the atoms and, eventually by the associated vibronic coupling (Elkan, Melvin, 1948). Comparing the PPE and PA signals shows a good agreement. The nonlinear dependence in Fig 4.1a is attributed to the loss of translational energy with increasing concentration of molecules. Increasing sample vapor concentration increases internal collisions between molecules in the cell, which will increase the heat until the entire drop is evaporated, and the cell pressure reach saturation. It is seen that the PPE signals gradually increase to a certain value, while PA signals involve many peaks depending on the number of double and triple bonds that is increased by increasing the number of molecules, hence the concentration. The PPE signal measure the total resulting heat, and independent of the exact absorbed intensity or emitted radiation frequency.

Investigation of the effects of increasing radiation power is achieved by changing the current driving the pulsed IR source that will increase the emitted source power as shown in Fig 4.3 and Fig 4.4 for PPE and PA signals respectively. As expected, when the incident energy increases, the PPE signal is increased, and the relation is linear because the absorbed energy is distributed equally to all chemical bonds all the time. PA results of Fig 4.4, is different from that of Fig 4.3, due to the dependence of the PA signal on different parameters, for example cell conditions that result in resonance signal or otherwise a damped signal, a case not noticed in PPE detection.

The final part concerned with investigating methanol while changing the modulation frequency of the IR source at a constant current of 300 mA. Fig 4.5a, PPE signal for methanol molecules, shows resonance absorptions at a modulation frequency of 49 Hz and its approximate duplication at 97 Hz. Since the PPE signal is an accumulated heat signal, then

resonances are not manifested. It seems that there is enhanced absorption at these particular frequencies leading to increased temperature in the cell. This is confirmed by the PA signal, which is frequency dependant, that is made clear by Fig 4.6 which shows a resonance at 90 Hz, while the calculated PA resonances according to equation 2.37 is found to be ~100 Hz without including the damping factor and the change of the speed of sound by the existence of sample vapors in the cell. Including damping, equation 2.39 predicts a lower resonance value. The increase of modulated frequency shows a decrease in absorption, which is discussed by Laine *et al* in 1997 as a decrease in the depth with frequency. The different peaks appeared in Fig 4.6 are due to the existence of double, triple bonds, and different kinds of bond between different atoms. Fig 4.5b shows the direct radiation to the PVD film from the source which shows a great dip at the resonance frequency and that means molecule absorption is enhanced at that frequency. Enhanced absorption blocks direct radiation from PVD film and hence the temperature of the inner side face of the PVD sheet is reduced, and leaving the outer face with higher temperature since it is isolated by a block of Perspex, overlapping the dipole of the sheet and therefore reverse the PPE signal. The final observation is the experimental overload in the signal, regarding a modulated frequency of 50 Hz; according to equation 2.22 when w_j: the natural resonant frequency equal w: modulated frequency, hence the dominator becomes infinite, leading to a good correlation between theory and experiment.

5.2.2: Ethanol Results

The spectra of ethanol have been measured from 5000 to 250 cm^{-1} in the vapor state and from 5000 to 767 cm^{-1} in solutions (Earle, Plyler, 1952). Their findings show it is difficult to untangle the C—H vibrations in the 2941 cm^{-1} region because there are stretching vibrations that occur in the CH_2 and CH_3 groups that give rise to five fundamental modes. The ethanol spectrum should have nine more fundamental modes than methanol, because of the internal vibrations of the CH_2

group, the C—C—O skeletal vibrations that consist of one bending and two stretching vibrations. The band at 427 cm^{-1} is assigned to this bending vibration, and the two bands at 1064 and 877 cm^{-1}, are related to the C—O and C —C stretching vibrations. In the 1250 cm^{-1} region, the ethanol bands are somewhat better defined than those for methanol. There are three intense bands at 1456, 1391 and 1242 cm^{-1}. These are assigned respectively to the asymmetric C—H bending in CH_2 and CH_3, to the O—H bending, and to the bending of the CH_2 symmetrically about the C—C axis (Earle, Plyler, 1952). These bands are shown in Fig 4.10. System shown in figure 3.7 was used to investigate the evaporated molecules of ethanol and the results shown in Fig 4.8 and Fig 4.9. The PPE signal shown in Fig 4.8 followed a usual evaporation trace, until it reaches a maximum value at 20 minutes then the signal decreased until it leveled off after 28 minutes. As the time go on the intensity of radiation reaching PVD film decrease according to the increase in the concentration of evaporated molecules, hence an increase in absorption by the vapor in the atmosphere of the cell. When the sample is totally evaporated a saturation pattern occurs as a result of regular transfer of heat to the PVD film generated by the internal collision between molecules. The PA signal in Fig 4.9, shows an increase in absorption by increasing the evaporation time until reaching 20 minutes, and then maxima stays at the same value approximately. This means that the speed of evaporation determines the time needed to reach the constant rate of heat transfer. In ethanol, the number of double and triple bonds are higher than Methanol and, therefore, several absorption peaks appear in the ethanol spectrum.

5.3 The PPE data of DNA

Nucleotides have an IR spectrum in the range 670 to 1443 cm^{-1}. The strong absorptions around 3333 cm^{-1} are probably associated with hydroxyl and amino stretching vibrations. The bands at 1667 cm^{-1} are associated with C=C, C==N, and C=0 stretching modes, and the strong compounds show a band in the region of 1042 to 1087 cm^{-1} (Elkan, Melvin, 1948). Conversely, the DNA samples which contain nucleotides as polymer were investigated in the region (5000-1000 cm^{-1}), in which an expected absorption will occur as mentioned by Elikan and Melvin. In this range, absorption spectra include wave numbers that correspond to the additional double and triple bonds between the nucleotides. Verification of this conclusion was done by investigating the unknown materials indicated in Table 4.2. Results of these samples demonstrate the ability of the system to distinguish different DNA samples, where the PPE signals for these unknown DNA samples show characteristically different result. So the PPE results confirm that this technique is capable of distinguishing different types of DNA structures. Results of Fig 4.11 for the synthetic DNA samples show an increase in the signal with increasing DNA nucleotides, a result confirmed by the increase in the PPE signal with molecular weight as shown in shown in Fig 4.12. Signal levels exhibit a nonlinear behavior due to the presence of hydroxyl and amino acid stretching vibrations which have a strong absorption around 3333 cm^{-1}, and the presence of C=C, C=N, and C=O stretching at 1667 cm^{-1} (Elkan, Melvin, 1948), which appear clear as the number of nucleotide decreased, and an increase in the number of double and triple bond following the increase in the number of nucleotides will decrease the absorption. This conclusion is supported by the results of Fig 4.16, in which the absorbed signal for the PCR and synthetic DNA samples is plotted against the number of nucleotides. FTIR spectra show an increase in the absorbed signal with the number of nucleotide as indicated in the Fig 4.17 - Fig 4.20. These figures show an absorption in the region of 1000 - 5000 cm^{-1}, which lies in the emission range of

the IR source used in this study. Also FTIR results show that absorption occurs at a lower wave number by increasing the number of nucleotide, hence a decrease in the radiated energy is needed for absorption, as mentioned in section 2.7, where the existence of double and triple bonds shift the absorption peak to a lower wave number, which explain the nonlinear relation in Fig 4.16.

In Fig 4.13, 4.14 and 4.15 the resulting signal versus the number of double bonds, triple bonds and the CG ratio respectively, doesn't show any relation between these factors and the corresponding initiated signals.

5.4: Essential oils

Several components of the essential oil provide different absorption peaks. Additional peaks mean additional components in the oil. Components of essential oil are complicated and have several double and triple bonds in addition to sugar rings, which increase the number of FTIR peaks as shown in Fig 4.29, Fig 4.38 and Fig 4.41, where the signal obtained for the three essential oils in liquid state. Investigation of absorbance for the essential oils needs analytical investigation of each component alone, which is a hard task (Rai, 1992). Hence, in this work a band study of absorption is advantageous. Separate studies to the result obtained for the essential oils are:

Jasmine's oil and flower: Fig 4.21- Fig 4.24 shows the PPE and PA signals for Jasmine's oil and flower look similar explanations follow that of ethanol results. In addition the Jasmine flower trace vapor reaches the saturation pattern faster than Jasmine oil vapor and absorption by Jasmine oil vapor is greater than that for Jasmine flower vapor, as a result of the existence of additional components in Jasmine flower vapor such as water, which is the main absorber of the

sunlight and shows strong absorption in the infrared region. In the gas phase water absorbs in the regions 3657, 3755, 1594 cm^{-1}, in the liquid phase the bands occur at 3280, 3490, 1644 cm^{-1}, and in the solid phase they are at 3085, 3220, 1650 cm^{-1}. The vibrations responsible for these bands involve combinations of symmetric stretching, asymmetric stretching and bending of the covalent bonds respectively (http://www.lsbu.ac. uk/water/index2.html,,january 2007).

The amount of volatile oil in the 0.03g whole flowers is less than that in 0.8 µ*l* of volatile oil and the oil itself will take more time to evaporate than water. Comparing the PA and PPE signal for jasmine flower i.e. Fig 4.22 and Fig 4.21 respectively, shows that they have the same shape and maxima approximately, meaning that they have the same origin, except that the PA signal always increased by increasing the evaporation time, while the PPE signal settles to saturated value. A comparison between the PPE and PA signals for jasmine flower and oil is shown in Fig 4.25 and Fig 4.26 respectively, which supports our hypotheses that the signals of flower and oil have the same origin with some additional component while extracting the oil; hence, the two signals support each other. Changing the concentration of the essential oil by diluting it with ethanol increase the rate of evaporation and decrease, the time needed to reach saturation point. The absorption increased by increasing the amount of diluted ethanol, since ethanol itself is sensitive to this range of radiation and absorbed more because it's structure is simpler than that for the essential oil component as shown in Fig 4.27. The PA signals shown in Fig 4.28 support the result obtained by the PVD film, implying that PPE and PA signals have the same origin.

Damask rose's flower and oil: Investigation of rose flower and oil may have in general the same explanation as jasmine, but the existence of different component expected to give different peaks. Fig 4.30 – Fig 4.33 indicate the need for less time to reach saturation for the rose flower and oil at different concentration compared to that for jasmine. Fig 4.34 and Fig 4.35 compare

the PPE and PA signals for rose flower and oil and shows that the time needed for the oil to reach the saturation is greater than that for its flower. Two minutes needed for rose flower and 4 minutes for its oil, and the absorption by the oil vapor is greater than that for the flower vapor. Changing the concentration of the essential oil and comparing the result as shown in Fig 4.36, indicates an increase in the absorption signal by decreasing the oil purity, since increasing the amount of ethanol increase the absorbing molecules and the evaporation rate. The PA signals in Fig 4.37 authenticate the result obtained by the PPE signals.

Mint oil and leaves: In this part, the dried and green mint leaves were investigated in addition to its oil. Fig 4.39 shows that the absorption for green mint leaves is greater than that for the dried leaves since the later lost many kind of evaporated molecules when dried specially water, and the time needed to reach the saturation for green mint leaves is less than that for dried mint leaves which means that the rate of trace gas emission from the green mint leaves is greater than that for dried leaves. The essential oil of the mint shows an increase in absorption, and more time needed to reach the saturation. This can be explained by the fact that the essential oil has fewer amounts of small molecules like water that increases the rate of evaporation. Fig 4.40 for the PA signal shows that the trace gas emission is increased from the essential oil to the dried mint leaves then the green mint leaves. The absorption by the oil vapor is greater than that for dried and green mint leaves, which confirms the results obtained from the PPE signal, and encourage using it as a monitor for the gas traces. More explanation mentioned for rose and jasmine flower and oil can be applied for the mint leaves and oil also.

Fig 4.42 and Fig 4.43 show the PPE and PA signals respectively for the three flowers versus time, and Fig 4.44, Fig 4.45 for their oils. Fig 4.42 and Fig 4.44 compare the PPE signals for the three flowers and their essential oil respectively. Both sets of curves have similar shapes suggesting similar origins. Fig 4.43 and Fig 4.45 show the PA signals and they have similar

shapes also, suggesting that the flower and the oil have similar origins, and conferming the use of PPE technique for gas traces.

Comparisons between results obtained by PPE and or PA techniques with those obtained by FTIR are always useful in authenticating and confirming the absorbance spectrum of samples in either liquid or gas phases. Fig 4.42 and Fig 4.44 show the PPE signal for trace gas emissions from the plant part and their corresponding oils respectively. There is clear resemblance between each oil absorption spectrum and its corresponding spectrum produced using the green plant part. On the other hand, the different oils and their green plant part absorptions are very well distinguishable. Mint oil gave a more pronounced curves and this was clear also from its sharp smell compared to other oils. Fig 4.43 and Fig 4.45 represent the PA results; similar arguments of the previously mentioned PPE also apply. FTIR absorbance spectrum for Jasmine, Rose and Mint oils are shown in Fig 4.29, Fig 4.38 and Fig 4.41 respectively. Their absorbance spectrums show little difference apart from that of mint oil. This is attributed to the great number of molecules having the sugar ring and the double and triple bond, such differences could be distinguished using their vibratinal fine structure that is most pronounced in the vapor phase spectra and is increasingly broadened and obscured in solutions. This explains the better distinguish ability of the PPE and PA absorption curves taken as trace gas emissions.

The estimated sensitivity for CPPC system is ~ 6 part per million (~ 6 ppm) for the case of liquid samples, while for emission from plant parts the sensitivity is expected to be a few part per billion (~ 6 ppb). Since the vapor of the plant part contains small amounts of the oil, ~ 1g of rose, oil needs 10000g from the fresh plant (Gernot, 2003). So the number of particles reduced by ~10^{-3} .

Chapter six.

Conclusion and further work

6.1 Conclusions:

A set of experiments was performed successfully using two simple, inexpensive, easy to handle and yet very accurate systems. Many conclusions can be drawn, and in this chapter concentration is focused on basic ones. One important conclusion can be drawn from the use of PVD method to test liquid samples such as testing DNA samples for the first time. The experiment proved the ability to distinguish different DNA samples assuming band absorption of IR radiation in the region ~ 2-10μm.

Simultaneous detection of PPE and PA in the combined cell opened the door to many important conclusions:

1- It proved good possibilities of using PVDF method to detect trace gases; leading to many important applications.

2- The origins of both PPE and PA are probably the same and the produced temperature increase from both effects lead to the detected signal.

3- As an agricultural region we can benefit from trace gas detection from the green or dried plant part, as it opens a wide area of applications in agriculture. The part of the plant used to produce the corresponding essential oil and the oil itself are found to emit similar gas traces. This is concluded from similarities in the absorbance curves for both essential oil and the plant part from which it is produced.

4- Absorption spectra obtained by FTIR confirm the sensitivity of detection by both PVDF and PA methods, in the low power range of micro watts or lower given by the IR source. This result suggests the use of the designed systems without the costly laser systems usually employed in such studies.

In conclusion, the PVD method has proven successful in studying trace gas detection in the combined cell. The method is rarely used for gases. The experimental result is very encouraging, and sensitivities as low as ppb may be detected. The origin of the signals detected by PA and PVDF are the same although there is some differences in the value of the signals detected by both techniques, specially the dependence of the PA signal on cavity volume, pressure and temperature. The study show that the combined cell of PVD and PA techniques is an interesting way that can lead to complemented result; leading to a deaper understanding of sample under study.

6.2 Further work.

The type of work carried out in the present study opens an era to further applications of the methods used in different directions. For example, the use of PVD method can still be used to test human and other living species DNA samples. Their absorption in a certain range of IR radiation can be studied using a set of discriminating IR filters. The signal obtained from the DNA of a cell infected with certain virus and that obtained from the DNA of the virus can be used to test for possibility of cell infection by the expected virus causing the disease. This is simpler than the conventional method, less expensive and safer, since DNA does not transfer the disease. As for as the PVDF method is concerned new applications for the use of the method for studies involving gas detection for pollution research. The good correlation between the trace gases emitted by the essential oil and the corresponding plant tissue from which it is produced opens a new line of research for agricultural applications geared toward follow up of oil content in the plant part prior to harvest time.

Appendix:

Appendix A

Experimental data for DNA study

Table A: PPE signal from different type of DNA samples

number	Type of DNA	Signal	Number of nucleotide	Molecular weight	Number of double bond	Number of triple bond
1	DNA3	3.72	40	12244	2	18
2	DNA1	4.035	44	13471.8	11	11
3	DNA2	4.890	60	18415	15	15
4	DNA121	5.582	121			
5	DNA216	5.958	216			
6	DNA1036	7.224	1036			

References:

- Agarwal G. P (1995), Semiconductor lasers, AIP Press, Melville, New York. **72**: 219-272.
- Aklonis J. J (1981), Mechanical properties of polymers. T. chem. Ed. PP: 892, 897.
- Andras,Miklos,1996,Optoacoustic detection with near infrared diod lasers,Infrared Physics and Technology,p21,22.
- Anonymous,1996,Essential oil extraction
- Aparicio R, Ferreiro L, Alonso V (1994) Anal. Chem. Acta **292**: 235-241.
- Australia: The Perfect Potion, 1997, 170.
- Baeten V, Meurens M, Morales M, Aparicio R (1996) J Agricultural and Food Chem 44: 2225 – 2230.
- Benz M, William B, Euler W.B (2002) J. Applied Polymer Sci. **89**: 1093-1100.
- Bianchi B, Catalano P (1996) Grasas y Aceites **47**: 136-141.
- Bower D. I, Maddams W. F, (1992), The vibration of spectroscopy of polymer. Cambridge University of press, PP: 15, 24, 27, 29, 36.
- Boyer R.F (1974) Macromolecules. **20**:142.
- Bret W, Ludwig, Marek W, Urban (1996) Polymer. Elsevier Science Ltd **38**: 2077-2091.
- Bret W. Ludwing and Marek W. Urban (1996), Rheo photoacoustic FT : studies of thermal history – strain dependance in poly (vinylidene fluoride); Department of polymers and coating . North Dakola State University, Fargo, ND 58105 , USA

- Bults G, Horwite BA, Malkin S and Gahen D (1982) photoacoustic measurement of photosynthetic activities in whole leaves: photochemistry and gas exchange . Biochim Biophys Acla G79 452-465.
- Bults G. Horwitz BA, Malkins an Cahen D (1981) Frequency dependant photoacoustic Signal from leaves and their relation to photosynthesis FEBS lett 129:44-46.
- Burns J, Ciurczak K (1992) In The Chemistry and Technology of Pectin., Walter. Academic Press, London, PP: 158-169.
- Carla , Giuseppe ,2000, Impedance measurements to study the antimicrobial activity of essential oils from Lamiaceae and Compositae, International Journal of Food Microbiology 67 2001 187–195.
- Carson,Riley,antimicropal activity of the major component of the essential oil Melaleuca alterifolia.JAppl Bacteriol,1995,78
- Chao, Pai, 2006, reconstruction of optical energy for back ward optoacoustc imaging,Optical and quantum Electronics 2005DOI p 1339-1341
- Cheong W.F S.A. Prahl and A.J Welch. IEEE Trrans Quantum Electron, 26. 2166. 1990.
- Chirtoc M, Bentefour E, Gloriex C, Thoen J (2001) Thermochimica Acta **377**: 105-112.
- Chirtoc M, Bicanic D, Dadarlat D, Chirtoc I (1985) Isotopic and Molecular Technology. **700**:57.
- Chirtoc M, Mihailescu G (1989) Phys. Rev. B **40**: 606-608
- Colthup W (1990), Introduction to infrared and Ramman spectroscopy. Academic .Press, San Diego, P: 99.

- Constantinos,Andreas,1990,solid state sensor for trace hydrogen gas detection American Institute of Physics, pR5-R20
- Corliss J. 1992 " Researchers Mind the Mint".Agricultural Research . 40: 15-17.
- Coufal H (1984) Appl Phys Lett **44**: 59.
- Dadarlat D, Gibkes J, Bicanic D, Pasca A (1996) J. Food Eng.**30**:155- 162.
- Dadarlat D. Bicanic D, Visser, H Mercuri,F and Frandas A (1995a) photopyroelectric method for determination of thermophysical parameters and detection of phase transition in fatty acids and triglycerides, Part I: Principles, theory and instrumentational concepts.J. Amer. Oil chem.. Soc, 72,273.
- Dadarlat D. Bicanic D, Visser, H Mercuri,F and Frandas A (1995b) photopyroelectric method for determination of thermophysical parameters and detection of phase transition in fatty acids and triglycerides, Part II: Temperature dependance of thermophysical parameters. .J. Amer. Oil chem.. Soc, 72,273.
- Dadarlet D and Frandas A.(1993). Inverse photopyroelectric detection methode. Appl. Phys. A56 . 235.
- Earle, Plyler, 1952, Infrared Spectra of Methanol, Ethanol, and rz-Propanol,pp281-286.
- Elkan, Melvin, 1948, ABSORPTION SPECTRA* VII. THE INFRA-RED SPECTRA OF SOME NUCLEIC ACIDS, NUCLEO-TIDES, AND NUCLEOSIDES,pp335-343 .

- Ernesto Reverchon,andGiovanna Della Porta,1994,Supercritical CO2 Fractionation Of Jasmine Concrete, The Journal of Supercritical Fluids,1995,8,60-65.
- Eugenio,Roberto,Jorge,Fernando,2001,characterization of two photon processesby photoacoustic spectroscopy,Analytical sciences The Japan Society for analytical chemistry,p17
- Feinstein (1990) Meas. Sci. Technol **2**: 412.
- Frandas A, Bicanic D (1999) J Sci Food Agric **79**:1361-1366.
- Frandas A, Paris D, Bissieux C, Chirtoc M, Antoniow J and Egee M (2000) Appl. Phys. B **71**: 69-75.
- Fried R. J (1995), Polymer science and technology. Ann Sullivan. PP:141, 271, 320, 350.
- Gernot,2003, Report problems and suggestions ,Spice Pages: Damask Rose (Rosa damascena Miller),1-13
- Harrick (1995) IEE Proc. Optoelectron **140**: 63-67.
- Hay and Waterman 1993, Volatile oil crops:there Biology, Biochemistry and Production Longman Scientific & Technical ,New York NY.
- Hiroshi,Nobuo,Fumiya,2001Carrier concentration dependence of photoacoustic spectra Analytical sciences The Japan Society for analytical chemistry,p13
- Hollas J (1996), Modern spectroscopy. P: 84, 127, 128.
- Ivanov V. S, Migunova I. I, Mikhailov (1988) Radiat. Phys. Chem **37**: 119-123.

- Jeffreys A.J, V. Wilson, S.L. Thein, "Hypervariable minisatellite regions in human DNA**,**" Nature, 314(6006):67-73, 1985.
- Joel, Michael, Robert, Peter, Martin, 2005, Combined Ultrasound and optoacoustic system for real-time high contrast vascular imaging in Vivo,IEEE transaction on medical imaging, 436.
- Julia Lawless, The Illustrated Encyclopedia of Essential Oils (Rockport, MA: Element Books, 1995), 57-67.
- krenzer Lioyd.B(13) 1977 (13) optoacoustic spectroscopy and detection)
- Kreuzer .L.B.(1971).J.Appl.phys.42.2934.2943
- Laine' D, Al-Jourani M, Carpenter S, Sedgbeer M(1997) IEE Proc.-Optoelectron **144**: 315-323.
- Lovell (1991) Infrared Physics & Technology **30**: 186-187.
- Ludwing W. B, Marek W. V, Urban M. W (1996) J Polymer **38**:2077 – 2091.
- Mana ,2001, Rose - Rosa damascena 'Trigintipetala' Crop & Food Research [BROAD sheet] Number 29 March 2001
- Mandelis A (1984) Chem. Phys. Lett **108** : 388.
- Mandelis A, Zver M (1985) J appl. Phys. **57**: 4421-4430.
- Marcel Bens, William B. Euler 2002,Determination of the crystalline phase of poly (vinylidene fluoride) Under Different Preparation condition Using Differential Scanning,Calorimetry and Infrared Spectroscopy ; Department of chemistry 51 Lower College Road. University of Rhode Island, Kingston, Rhode Island 02887.
- Marinell (1992) J Agricultural and Food Chem **44**:3516 – 3520.

- Masahiro, Norikazu ,Yoshiko ,Miki , Kazuhito ,2003, Inhibition of elastase activity by essential oils in vitro Faculty of Pharmaceutical Sciences, Setsunan University, Japan 183,184
- McLennan, J.E. (2003) "A0 and A1 studies on the violin using CO_2, He, and air/helium mixtures." Acustica, **89**, 176-180.
- Morales M, Aparicio R and Rios J (1994) J Chromatography A 668: 455 – 462.
- Morawetz (1985) J of Applied Polymer Science **57**: 239-246.
- Morse P.M (1948) Vibrational and Sound .Mc. Graw Hill New York.
- Morse P.M and Ingard K. (1961) Encyclopedia of physics Vo XI/1, s, Flugge (Ed) Springer Verlag, Bertin and New York.
- Nell, Hons, 2000, monitoring oil degradation with infrared spectroscopy, pp 1-8.
- Potter, N. N. 1986. Food Science. 4^{th} ed. Van Nostrand Reinhold, Inc., NY.
- Rai, 1992, Nonradiative state in essential oil from aromatic plants, International center for theoretical physics, Triest, Italy, pp 1-2.
- Rajeswara , Kaul , Syamasundar ,2003, Chemical profiles of primary and secondary essential oils of palmarosa (Cymbopogon martinii (Roxb.) Wats var. motia Burk. Industrial Crops and Products 21 (2005) 121–127)
- Rhea,2005, Perfumed Inspiration: The Damask Rose, Welcome to the American Rose Society,1-3.
- Richard B. Hallick.(1995), Introduction to DNA structure; Molecular Grahics companion to an Introductory Cours in Biology or Biochemistry.
- Robert H, Randall, 1951,an introduction to acoustic , Addison- Wesley press,INC Cambridge 42, mass ,106-110

- Robert Tisserand, Essential Oil Safety (United Kingdom: Churchill Livingstone, 1995), 207.
- Rockport, M. A. : Element Books, 1995), 57-67.
- Rosencwaig A., photoacoustic and photoacoustic spectroscopy, (John Wiley and Sons.N.Y 1980).
- Siegel – Maier , K. 1998 " Peppermint: More Than Just Another Pretty Flavor." Better Nutrition 60:24 .
- Simon, J.E., A.F. Chadwick and L.E. Craker. 1984. Herbs: An Indexed Bibliography.
- Smith P. Appl. Phys. Lett, H, 132-134, 535, (1971).
- Stephen,Tao,Thomas,2000,New application of photoacoustic to study of photosynthese,2001 Kluwer Academic Oublishers.Printed in Netherland
- Tassou ,Koutsoumanis , Nychas,2000, Inhibition of Salmonella enteritidis and Staphylococcus aurous in nutrient broth by mint essential oil , National Agricultural Research Foundation, Institute of Technology of Agricultural Products, S. Venizelou 1, Lycovrisi 14123, Athens, Greece,273,274.
- Tuchin, V. Tissue Optics, SPIE Press, Washington, 2000.
- Viengerov M.L.1938 Dokl. Akad, Nauk, SSSR 19;687.
- Watson, J.D., and Crick, F.H.C. 1953. "Molecular Structure of Nucleic Acids. A Structure for Deoxyribose Nucleic Acid." Nature 171:737-738. This short paper is the original presentation of Watson and Crick's hypothesis regarding the double helical structure of the DNA molecule.
- Weidmann D, Courtois D (2000) Infrared Physics & Technology **41**: 361-371.

- Winstanley, Inst,1955, textbook on sound ,Longmans, green, and co London . New York . Toronto ,p 134 – 139
- Yoh-Han Pao, 1977, ophtoacoustic spectroscopy and detection,Academic press New York San rancisco
- Zott H, Heusinger H (1978) Eur. Poly J **14**: 1025.

Internet Sites

- http:// en.wikipedia.org/wiki/Methanol_fuel , October 2006.
- http://dl.clackamas.cc.or.us/ch106-09/linking.htm, October, 2006.
- http://dl.clackamas.cc.or.us/ch106-09/nucleoti1.htm,October, 2006.
- http://en.wikipedia.Org/wiki /DNA_sequencing, October, 2006.
- http://en.wikipedia.org/wiki/Ethanol, October 2006.
- http://en.wikipedia.org/wiki/Methanol" , October 2006.
- http://en.wikipedia.org/wiki/Methanol_fuel, October 2006.
- http://w w w .pueblo.gsa.gov/cic_text/health/sun_uv/sun-uv-you.htm, October 2006.
- http://www.worthpublishers.com/lehninger3d/index.html, October, 2006.
- http://www.answers.com/topic/infrared-spectyroscopy-correlation-table, October, 2006.
- http://www.cem.msu.edu/UV-Visible Spectroscopy, Visible and Ultraviolet Spectroscopy, October 2006.
- http://www.daytonnursery.com/Encyclopedia/Encyclopedia.htm, October 2006.

- http://www.frontierherb.com/aromatherapy/esso.extr.html. 1996. Frontier Cooperative Herb, October 2006.
- http://www.metax.co.uk/infrared_source.htm, October 2006.
- http://en.wikipedia.org/wiki/Piezoelectricity, may 2007
- www .factbites.com/topics/Ethyl-alcohol, October 2006.
- www.airpower.maxwell.af.mil/airchronicles/apj/apj04/spr04/spr04.pdf, October 2006.
- www.arlingtoninstitute.org/library/A%20Strategy%20-%20Moving%20America%20Away%20from%20Oil.pdf, October 2006.
- www.phys.unsw.edu.au/~jw/guitarintro.html, October 2006.